SIMULATION OPTIMIZATION SYSTEMS
Research Laboratory

GENERALIZED SENSITIVITY EVALUATION OF ELECTRICAL POWER SYSTEMS

H.K. Grewal

SOS-86-7-T

July 1986

McMASTER UNIVERSITY
Hamilton, Canada L8S 4L7
Department of Electrical and Computer Engineering

GENERALIZED SENSITIVITY EVALUATION OF ELECTRICAL POWER SYSTEMS

H.K. Grewal

SOS-86-7-T

July 1986

GENERALIZED SENSITIVITY EVALUATION OF ELECTRICAL POWER SYSTEMS

GENERALIZED SENSITIVITY EVALUATION OF ELECTRICAL POWER SYSTEMS

By

HARKIRAT KAUR GREWAL

A Thesis

Submitted to the School of Graduate Studies

in Partial Fulfilment of the Requirements

for the Degree

Doctor of Philosophy

McMaster University

July 1986

DOCTOR OF PHILOSOPHY (1986)
(Electrical and Computer Engineering)

McMASTER UNIVERSITY
Hamilton, Ontario

TITLE: GENERALIZED SENSITIVITY EVALUATION OF ELECTRICAL POWER SYSTEMS

AUTHOR: Harkirat Kaur Grewal
B.Sc.Eng. (Elect. Eng.) (Panjab University)
M.Eng. (Electronics and Comm. Eng.) (Univ. of Roorkee)
M.Eng. (Elect. and Computer Eng.) (McMaster University)
Member, I.E.E.E.
Associate Member, Institution of Engineers, India

SUPERVISORS: J.W. Bandler, Professor,
Department of Electrical and Computer Engineering
B.Sc. (Eng.), Ph.D., D.Sc. (Eng.) (University of London)
D.I.C. (Imperial College)
P.Eng. (Province of Ontario)
C.Eng., F.I.E.E. (United Kingdom)
Fellow, I.E.E.E.
Fellow, Royal Society of Canada

M.A. El-Kady, Associate Professor (part-time),
Department of Electrical and Computer Engineering
Resource Utilization Development Manager,
Ontario Hydro-Power System Operations
B.Sc. (E.E.), M.Sc. (Cairo University)
Ph.D. (McMaster University)
P.Eng. (Province of Ontario)
Senior Member, I.E.E.E.

NUMBER OF PAGES: xii, 151.

ABSTRACT

The material presented in this thesis is a logical extension of and addition to previous work on network sensitivities as applied to power system analysis and planning. The continuing tendency of supplementing the existing extra-high voltage a.c. transmission systems with high-voltage d.c.(HVDC) lines has been taken into consideration, and various relevant component models have been investigated using a new hybrid network formulation based on the methodology developed by Bandler and El-Kady. The load buses, frequently modelled as PQ-buses at which both the real and reactive injected powers are known, and the generator buses characterized by a constant voltage magnitude and constant real injected power, have been dealt with by exploiting a special complex conjugate notation. In addition, the current, voltage and/or power relationships associated with the transmission network branches have been investigated. A hybrid formulation for generalized power system component models has been developed. This novel formulation not only encompasses the work established on the basis of one-port theory, but it is also capable of manipulating multiport, nonreciprocal, a.c. as well as integrated a.c.-d.c. bulk transmission networks. The attractive features of adjoint modeling have been retained, and consequently, exact sensitivity formulas associated with various control variables have been derived, tabulated and verified. Applications of the novel sensitivity formulation to both, the HVDC link and phase-shifting transformer modeling, are presented. In the first application, a two-port model of an HVDC link connecting two a.c. networks has been used. The terminal relations of the converters have been utilized ingeniously to develop an adjoint converter model. Both firing angle and commutation reactance have been considered as the control variables of interest, and their respective sensitivity formulas have been numerically verified on a test power system. In the second application, a cascaded phase-shifting transformer model comprising an ideal transformer in series with a transformer equivalent impedance has been considered. Exact sensitivity formulas for the control variables representing transformer turns ratio magnitude, phase angle, equivalent resistance and reactance have been derived elegantly and compactly.

The theoretical results achieved have been extensively verified using a 2-bus and a 6-bus sample power systems. The functions encountered in steady-state security assessment have been considered, and investigated in applications to two practical IEEE (30-bus and 118-bus) test systems.

ACKNOWLEDGEMENTS

The author gratefully thanks Dr. J.W. Bandler and Dr. M.A. El-Kady for their expert guidance, encouragement, continued assistance and supervision during the course of this work. She also thanks Dr. F.A. Mirza and Dr. A.A. Smith of Civil Engineering, members of her supervisory committee, for their understanding and friendly interest.

The author acknowledges many stimulating discussions with her former colleagues Drs. A.E. Salama, M. El-Sobki and W. Kellermann, as well as her present colleagues S. Daijavad, Q.J. Zhang, S.H. Chen, M. El-Naga and J. Affolter. She expresses her sincere appreciation for the patience and support from her husband, Paramjit Singh.

The financial assistance provided by the Natural Sciences and Engineering Research Council of Canada through Grants A7239 and A1708, and the Department of Electrical and Computer Engineering through a Teaching Assistantship, is gratefully acknowledged.

Thanks are also due to the Faculty of Engineering Word Processing Centre for its diligent efforts in typing this thesis.

Last, but not least, the author is indebted to her employer at her parental institution, Guru Nanak Engineering College, Ludhiana, India, for granting an uninterrupted study leave.

TABLE OF CONTENTS

TABLE OF CONTENTS (continued)

TABLE OF CONTENTS (continued)

CHAPTER 1

INTRODUCTION

1.1 BACKGROUND

Sensitivity considerations enter into power system planning and operation problems in many distinguished ways. One of the pertinent problems is concerned with area load forecasts and planned generation additions which usually requires an estimate of necessary transmission reinforcements so that the area demands can be met economically, reliably, and in an environmentally acceptable manner. Various automated transmission tools have been developed and well-established, based on sensitivity evaluation methods as incorporated in the studies requiring subsequent optimization. However, due to the inherently large size of power transmission networks, some of the attractive features of an effective sensitivity evaluation method, namely, the simplicity of derivation and formulation, flexibility in component modeling, and computational efficiency, are always given fundamental importance.

Some of the techniques addressed in the literature tend to satisfy the requirements for efficient sensitivity evaluation by approximating the steady-state model of a given power system. In other methods, an exact a.c. load flow model is exploited utilizing the elements of the Jacobian matrix available at the power flow solution. The so-called Lagrangian method has recently been established in the complex mode as well, where the power flow equations are retained in their original complex form and treated by using a special conjugate notation. Furthermore, a considerable amount of flexibility in modeling various network components has also been gained with the implementation of an augmented Tellegen's theorem developed by Bandler and El-Kady.

The Tellegen theorem-based method utilizes the advantageous properties of the well-known adjoint network formulation, leading to fairly simple adjoint models pertaining to both source as well as transmission branches. The derivation, formulation, and any subsequent manipulation of the original and adjoint power network equations are largely simplified owing to the state variable notation commonly used in control theory. The power flow equations and other equality constraints associated with advanced component models can readily be dealt with by using a hybrid vector/matrix notation developed in this thesis. The hybrid treatment not only encompasses the previous work done on the basis of one-port theory, but it is also capable of handling multiport, nonreciprocal, a.c. as well as a.c.-d.c. power transmission networks.

1.2 CONTENTS OF THE THESIS

This thesis employs a compact complex notation together with appropriate techniques to define, extend, establish and provide a qualitative comparison of the sensitivity evaluation methods in the context of long-range planning studies. Chapter 2 contains a brief, and systematically documented description of the single-phase a.c. modeling pertaining to the load and generator buses, and transmission branches including control transformers. Essential information concerning the a.c.-d.c. conversion and inversion is also provided starting from the basic principles involved therein. Special care is exercised to maintain conceptual clarity of the diverse material, and adequate references as well as background for the high-voltage d.c. transmission (HVDC) are included. The simplified models reported in the literature are emphasized. Additionally, typical installations of the HVDC links together with phase-shifting transformers are included to make this chapter interesting, self-contained and more useful.

Chapter 3 basically reviews the existing practices and options available for solving the ubiquitous power flow problem. It also elaborates on some new terminology to be used in the subsequent chapters, and provides an overall perspective of the thesis. In addition, the preliminaries required to help understand the implications of a successful sensitivity evaluation method are addressed. The problem of optimal power flow, which concurrently involves an optimization routine to extremize certain performance index for a specified set of control variables, is also highlighted.

In Chapter 4, the sensitivity evaluation methods commonly used in power system analysis are presented pragmatically. The powerful features, complemented by intricacies of the Tellegen theorem-based method are discussed. A generalized adjoint network formulation is developed by exploiting the complex conjugate notation in conjunction with a hybrid vector/matrix notation. Further, the sensitivity of a general network function of interest with respect to a generic control variable is compactly derived, and verified with the help of previously established results for the source branches and the a.c. transmission lines.

Chapter 5 includes a brief description of the other types of transmission branches frequently encountered in a modern power system. Different types of transformers used for specific purposes (including the a.c.-d.c. converters) are introduced. Based on the two-port theory, the terminal behaviour of an elementary HVDC link is modelled as a cascade connection containing a voltage-controlled voltage source in series with an equivalent commutation reactance. A phase-shifting transformer model involving an ideal transformer with a complex turns ratio is investigated. Further, the validity of the sensitivity formulas derived in Chapter 4 is demonstrated by considering simple test power systems.

The material presented in Chapter 6 deals with the simulation, power flow solution, and sensitivity evaluation of some approved test systems. Firstly, a 6-bus sample system containing a phase-shifting transformer with large phase angle is considered. The unsymmetric nodal admittance matrix associated with this system is conveniently handled, and the corresponding power flow solution is reported in a systematic manner. The network sensitivities associated with a customer (load) bus with respect to several different control variables are calculated, verified, and tabulated. Secondly, the IEEE 30-bus power system is simulated. The sparsity structure of its nodal admittance matrix is exploited using the sparsity-oriented software developed in the Simulation Optimization Systems Research Laborartory at McMaster University. The functions reflecting overload alleviation of the transmission lines are taken into considerations, and the sensitivities with respect to various control variables are mentioned. Finally, the network configuration of the IEEE 118-bus power system is described with the help of its optimally structured one-line diagram. The sensitivities of the slack bus real power are obtained at the base-case.

The last chapter of the thesis provides an overall conclusion of the research undergone in the present area of specialization. Both, the contribution and utilization of the adjoint modeling in electrical power systems studies, are systematically presented and summarized. The flexibility offered by this modeling technique is enhanced via the hybrid vector/matrix notation, which encompasses the analysis of multiport, nonreciprocal, a.c. as well as a.c.–d.c. integrated power networks. The treatment of converters and phase shifting transformers is emphasized. Some new directions for further research efforts are also discussed.

CHAPTER 2

COMPUTER MODELING OF POWER SYSTEM COMPONENTS

2.1 Introduction

In parallel with the development of larger and faster computers, significant progress in modeling the gross behaviour of different power system components has accrued from the need to have *a priori* knowledge of the performance of viable control strategies (Arrillaga et al. 1983; Chen and Dillon 1974; Singh 1983). The mathematical models pertaining to most of the components have often been simplified, or idealized intentionally, in order to simplify the power system problems and/or to make it solvable at all.

Loads are considered as components, even though, their exact composition and characteristics are not known with complete certainty (Powel 1955; Weedy 1979; Wildi 1981). For most of the modern generators, the output voltage is controlled by automatic devices so as to register a constant prearranged value (Elgerd 1982; Wildi 1981). The real generated power of these generators is continuously monitored by exploiting the variations of system load frequency. The load centres are connected to the generating stations through transmission lines. In addition, control transformers are installed in the lines for specific purposes (Grewal 1983; Han 1982; Lyman 1930).

This chapter is solely devoted to the modeling in the context of steady-state power system analysis using the bus frame of reference. In the cases of three-phase generators, motors and transformers, phase symmetry is assured by design; whereas for single-phase loads, the phase symmetry is assumed to be achieved by balanced distribution between the three phases. Further, the transmission lines are assumed to exhibit phase-symmetric characteristics, either by placing the identical phase conductors in a symmetric geometrical configuration, or by transposing the conductors at regular intervals (Elgerd 1982; Stagg and El-Abiad 1968). Under these assumptions throughout a given power system, the analytical efforts are substantially reduced. Consequently, the so-called per-phase or single-phase analysis is used as an appropriate point of departure for the material to follow.

The re-emergence of high-voltage d.c. (HVDC) lines as an adjunct to existing a.c. lines (Zorpette 1985) is given adequate attention in this chapter. The d.c. transmission, that is discussed today, is a constant-potential system with high-voltage rectifiers at the sending end, and inverters at the receiving end (Kimbark 1971).

At the heart of an HVDC converter station are the so-called thyristor valves that alternately block and conduct the current flow in a particular line (Adamson and Hingorani 1960; Uhlmann 1975). A fairly simple converter model, containing a voltage-controlled voltage source, is discussed in this chapter. Any new terminology involved in the subsequent chapters is also defined.

2.2 Basic Single-phase Modeling

Modern electrical power systems are invariably three-phase systems. The design of various subsystems and the associated networks is such that the normal operation of a power system is reasonably close to a balanced three-phase (Elgerd 1982). Often a study of the electrical conditions in one phase is sufficient to furnish a complete analysis. Equal loading on all the three phases of a network is ensured by allowing as far as possible equal domestic loads to each phase of the low-voltage distribution feeders. The industrial loads usually take three-phase supplies; whereas large customers are directly served from the subtransmission level as shown in Fig. 2.1.

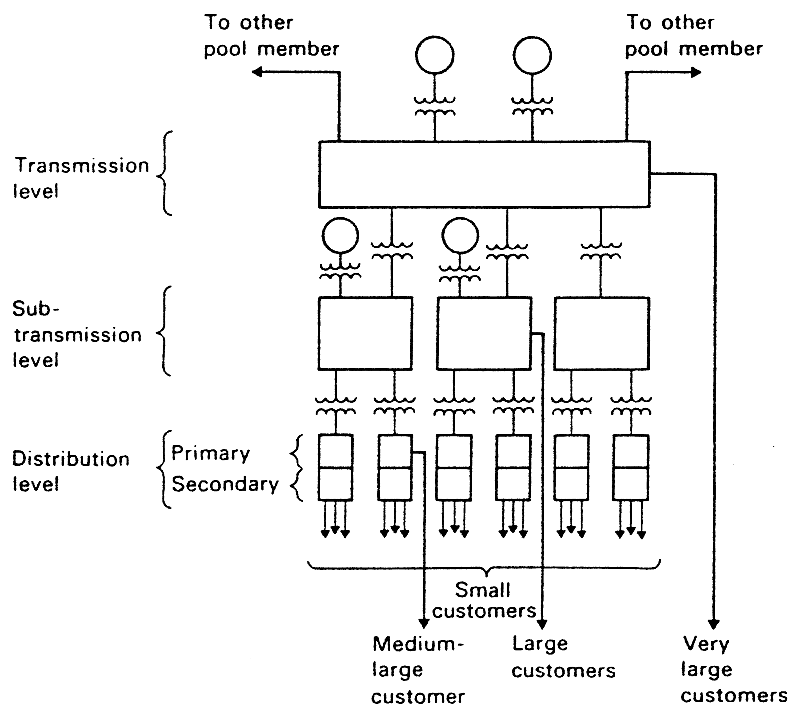

Fig. 2.1 A typical power system structure (Elgerd 1982, p. 6).

For economical and technological reasons, most of the power systems are electrically interconnected into vast power grids which are subdivided into regional operating groups, called power pools (Happ 1973; Happ and Nour 1975). The operating voltage at the transmission level is kept extra-high (e.g., 345 kV, 500 kV or 765 kV). The generating stations as well as the major loading points in a nation-wide system are interconnected at this transmission level. The electrical energy is conveniently routed in any desired direction on the various links of the transmission system in a manner that corresponds to best overall operating economy (Han 1982; Lyman 1930; Lyman and North 1938). Fig. 2.2 illustrates the usage of phase-shifting transformers to interconnect three Canadian provincial power systems (Dandeno 1982).

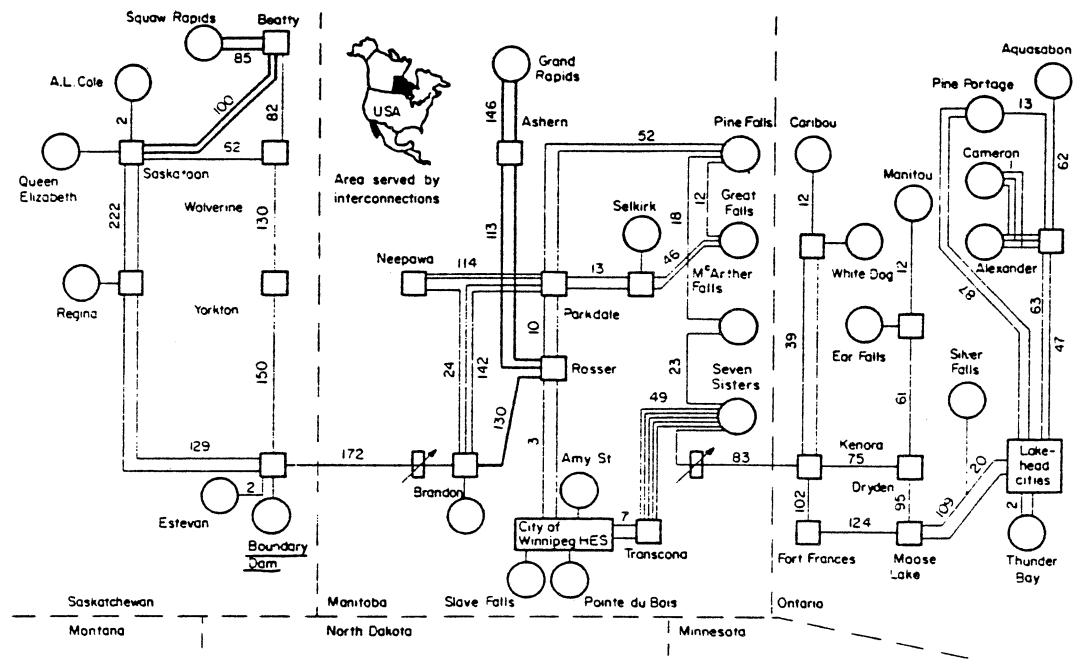

Fig. 2.2 An interconnection of three provincial power systems (Dandeno 1982, p. 256).

The fundamental difference in the purpose of a transmission system as compared with its subtransmission and distribution systems shows up in the network structure. The latter two, in general, are of radial structure; whereas the former tends to obtain a loop structure (Dhar 1982; Elgerd 1982). A radial-type network is an obvious solution in case the energy flow has a predominant direction. Contrarily, the loop structure evidently lends more path combinations, and therefore, better suits the purpose of the transmission level (Weedy 1979; Wildi 1981).

Among the many alternative possibilities of describing a modern transmission system to comply with the Kirchhoff's laws, the two most commonly used methods involve the mesh and nodal analyses. The latter has been found to be particularly suitable for digital computer usage, and is almost exclusively used for routine network calculations. The advantages of the nodal method are summarized as (Arrillaga et al. 1983; Elgerd 1982; Stagg and El-Abiad 1968):

- The numbering of nodes, performed directly from a system diagram, is very simple and easy.
- Data preparation is conveniently achieved.
- The number of variables and equations is usually less than as with the mesh methods.
- Network crossover branches present no difficulty.
- Parallel branches do not increase the number of equations.
- Node voltages are directly available from the solution, and consequently, branch currents or powers can be computed in a straightforward manner.
- Off-nominal transformers can readily be represented.

Under perfectly balanced conditions, the power system components are invariably represented by their single-phase models. The nodal equations of an n-node system are compactly expressed in the matrix form (El-Kady 1980; Grewal 1983)

$$\mathbf{I_M} = \mathbf{Y_T}\,\mathbf{V_M}\,, \tag{2.1}$$

where $\mathbf{Y_T}$ represents the nodal admittance matrix, $\mathbf{V_M}$ is a vector of complex bus voltages, and $\mathbf{I_M}$ contains the bus injected currents in a corresponding order.

2.2.1 Load Bus Model

Generally, the term load is used to indicate a device or a group of devices that tap electrical energy from a power network (Powel 1955; Elgerd 1982). In a practical situation, the load devices may range from a few-watt night lamp to a multi-megawatt induction motor.

However, a well-developed and properly designed power system is assumed to be capable of supplying the customer demand at all times.

The three-phase motors exhibit considerable load constancy and very predictable duty cycle. Nevertheless, the domestic load may consist mostly of single-phase apparatus operated in quasi-random manner. In such situations the laws of statistics are utilized, and a certain average pattern is recognizable at the distribution level (Elgerd 1982; Singh 1983). This averaging effect is still more pronounced at the subtransmission level, and finally an almost predictable situation is arrived at the transmission level. The major consumption groups are industrial, residential (domestic), and commercial. They are routinely represented as a composite load on a particular substation. A typical composition of such a load is as follows (Weedy 1979):

Induction motors	50-70%,
Lighting and heating	20-25%,
Synchronous motors	10%,
(Transmission losses	10-12%).

Most of the industrialized countries have the induction motors as a significant load. Consequently, it is customary to model an ℓth load bus as a nonvoltage controlled bus for the power flow studies (Stagg and El-Abiad 1968). Both the real power P_ℓ and reactive power Q_ℓ are known at this bus. These quantities are assumed to be unaffected by small variations in the system bus voltages, and in practice, are estimated with the help of megawatt- and megavar-meters installed at the relevant substation.

Using the per-unit system (Appendix A), the complex power S_ℓ at the ℓth load bus is expressed as

$$S_\ell \triangleq P_\ell + j\,Q_\ell = V_\ell I_\ell^*, \tag{2.2}$$

where V_ℓ and I_ℓ are the unknown voltage and unknown injected current, respectively. The symbol * stands for the complex conjugation (Ahlfors 1966).

2.2.2 Generator Bus Model

The three-phase synchronous generators are largely used to produce the electrical power in bulk (Elgerd 1982; Weedy 1979), and therefore, dominate the operating features of a power system. Based on the magnitude and direction of the real and reactive powers pertaining to the synchronous machines, there are six important practical operating combinations. As a generator, driven by a prime mover, the machine is usually operated either as a producer or consumer of the reactive power. Two similar cases exist when the machine is being used as a motor, delivering torque to a mechanical load. When operated with zero real power and overexcited, the machine is referred to as a synchronous capacitor (or condenser). Its sole purpose in this mode of operation is to generate the reactive power. If underexcited, the machine consumes reactive power, and the mode is used especially when there is a need in a network to dispose of the surplus reactive power. For example, during night hours the real load is light, but the high-voltage lines still must be energized.

The basic role of the synchronous generators, however, is to produce megawatts at a fairly constant voltage. There are continuous closed-loop control actions provided by automatic voltage regulator (AVR) and automatic load frequency control (ALFC), rendering a simple model for the generator buses. The AVR loop associated with a gth generator bus controls the magnitude of voltage, $|V_g|$. The voltage magnitude is continuously sensed, rectified, smoothed and compared with a d.c. reference. Any resulting error voltage, after amplification and signal shaping, is used as the input to the exciter which finally delivers the voltage to the generator field windings. Furthermore, the ALFC loop regulates the megawatt output P_g, and frequency (speed) of the generators by two distinct closed circuits (Elgerd

1982). The primary loop indirectly performs a coarse speed or frequency control, and a slower secondary loop maintains a fine adjustment of the system frequency.

The governing equation corresponding to a generator bus, thence, is

$$\tilde{S}_g \triangleq P_g + j|V_g|$$
$$= 0.5(V_g I_g^* + V_g^* I_g) + j(V_g V_g^*)^{1/2}, \tag{2.3}$$

where $\tilde{S}_g$ represents a quasi-complex power at the gth bus. This power is specified prior to the power flow solution (El-Kady 1980; Grewal 1983). The generator buses are also called the voltage-controlled buses, or the PV-buses. In a typical power system, the load buses always dominate. Normally 80 to 90 percent of all buses fall in this category (Talukdar and Wu 1981). The rest are voltage-controlled buses plus one reference (slack) bus, which is given other names as floating or swing bus.

2.2.3 Slack Bus Model

As the transmission losses in a given power network are not known precisely in advance until the calculation of the currents actually flowing in the transmission lines (Dhar 1982; Elgerd 1982; Gross 1979), it is customary to relax the power constraints at one of the generator buses. The so-called slack bus has its voltage phase angle δ_n specified instead of the real power P_n. The phase angle δ_n is usually taken as zero, thereby, in effect designating the slack bus voltage V_n as the reference phasor. The slack bus voltage V_n, associated with the n-node power system is

$$V_n \triangleq V_{n1} + j V_{n2} = |V_n| \angle \delta_n, \tag{2.4}$$

where, the slack bus is always set as the last numbered bus of a given network (Bandler and El-Kady 1982b; El-Kady 1980; Grewal 1983).

The three types of the power system components discussed so far are, basically, one-port elements. These components are referred to as the source branches in this text and in the previous related work (Bandler and El-Kady 1982b; El-Kady 1980; Grewal 1983). The various quantities associated with these branches are routinely grouped into two categories; viz., independent and dependent variables. These branch variables are given the names control and state variables, respectively, in the control theory. The variables which are physically used to control certain performance indices of a system fall in the former category. Table 2.1 provides a summary of the state and control variables pertaining to the power network source branches.

TABLE 2.1

BUS CLASSIFICATION ON THE BASIS OF SPECIFICATION

Bus Type	Symbol	A priori known variables (**u**)				Unknowns obtained from the power flow solution (**x**)			
		P_i	Q_i	$\lvert V_i \rvert$	δ_i	P_i	Q_i	$\lvert V_i \rvert$	δ_i
Load bus $i = \ell$		o	o					o	o
Generator bus $i = g$		o		o			o		o
Slack bus $i = n$	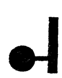			o	o	o	o		

2.2.4 Transmission Line Model

The bulk power transmission is accomplished by high-voltage transmission lines falling in any one of the categories: aerial lines, underground cables and compressed-gas insulated lines. Because, the vast majority of the existing power lines are of three-phase aerial design with bare conductors and the surrounding air serving as the insulating medium, the dominance of aerial lines has received main attention as per line modeling is concerned.

The electrical performance characteristics of a transmission line are expressed in terms of its parameters, namely, line inductance, shunt capacitance, line resistance and shunt conductance. The line inductance is by far the most important line parameter from a power system engineer's viewpoint (Dhar 1982; Elgerd 1982; Gross 1979). For normal design purposes, the corresponding inductive reactance is the dominating impedance element owing to its effect upon transmission capacity and voltage drop. The resistance of a transmission line is relatively unimportant because it does not affect the transmission capacity; nevertheless, it cannot be ignored when considering the real transmission losses of a given system. Both, the line resistance and line inductance, constitute the element that contributes as the series impedance of a transmission line.

The capacitance and conductance form the shunt (or parallel) admittance of the line. The series elements, with dominating inductance, set a limit to the current that can flow through the line, and therefore, physically determine the corresponding power transmittability. Whereas the shunt elements, with capacitance dominating, represent a source of the reactive power. The generated megavars are proportional to the square of the line voltage. The importance of the shunt elements increases with the magnitude of the operating voltage (Dhar 1982; Wildi 1981). In a high-voltage cable, for example, the close proximity of the conductors results in a very large shunt capacitance. The shunt conductance, on the other hand, accounts for the resistive leakage current between the phases and ground.

This current mainly flows along the insulator strings for the aerial lines. It strongly depends on the vagaries of weather, atmospheric humidity, pollution, as well as salt content (Elgerd 1982).

The manner, in which the transmission lines are to be represented, depends considerably on their physical length and the accuracy required in a particular analysis. The three broad classes are – short, medium and long lines. The actual line is a distributed-parameter circuit (Stagg and El-Abiad 1968; Weedy 1979; Wildi 1981); that is, it is characterized by resistance, inductance, capacitance and leakage resistance, distributed uniformly along its entire length. Except for electrically long lines (lines roughly above 240 km), the total resistance, inductance, shunt capacitance and conductance of the line are concentrated to give a lumped-parameter circuit. The equivalent π and T networks are quite common representations for the lines. However, the π-model is more popular in the power flow studies (Arrillaga et al. 1983; Dhar 1982; Wildi 1981).

The short-circuit admittance matrix for the π-equivalent of a t-th element, connecting buses p and q, is given by

$$\mathbf{y} = \begin{bmatrix} y_{pp} & y_{pq} \\ y_{qp} & y_{qq} \end{bmatrix}, \tag{2.5}$$

where the y-parameters of (2.5) represent the short-circuit admittance parameters of the line under considerations (Stagg and El-Abiad 1968; Grewal 1983).

The transmission lines are reciprocal, bilateral power network elements, and their main role is to transport electrical power from one end to the other. For acquiring a manipulative action over the power flow in the lines, control transformers (Gross 1979, Wildi 1981) are installed as discussed in the following section.

2.2.5 Control Transformer Model

In the operation of a power system involving various kinds of electrical networks, a fundamental necessity is that each transforming as well as transmitting unit must handle a reasonable share of the total customer demand (load). The problem of load division has not, in general, been troublesome for a single system that has been developed and expanded in a coordinated manner. The problem has been solved successfully by judicious selection of parallel circuits, use of reactors and/or proper system set-up. Further, with the advent of inter-company connections, systems of diverse characteristics have been brought together to help operate the overall system in unison and equilibrium (Happ 1973; Happ and Nour 1975).

The inter-company contracts are guided by load exchanges which have to be regulated within rather definite limits. In some cases, conditions have arisen where maintenance of adequate load division has been very difficult, if not impossible. A practical method of dealing with this problem has been facilitated by the concept of voltage-phase relations (Lyman 1930; Lyman and North 1938; Gross 1979). A quadrature voltage at any place within the loop is introduced to cancel the inherent displacement produced by a particular circuit loading (Dandeno 1982). The device employed to provide the required angular displacements is called phase-shifting transformer.

A phase-shifting transformer consists of a delta-connected primary with two secondary configurations (Grewal 1983; Han 1982), ganged together in such a manner to lend independent control over the magnitude as well as phase of the transformer turns ratio. As the effective turns ratio is considered to be a complex quantity, the component is also referred to as a nonreciprocal power network element (Bandler, El-Kady and Grewal 1985a, and 1985b).

The transformer control actions may be manual or automatic, complete with output sensors and feedback methods. The transformers are employed to delay the future transmission reinforcements in the expansion plans of existing power systems (Ershovich et al. 1982; Han 1982).

The transformer model, shown in Fig. 2.3, comprises an ideal transformer, having a complex turns ratio $a_t = |a_t| \angle \phi_t$, in series with an equivalent impedance Z_t. The short-circuit admittance matrix, pertaining to this model (Dhar 1982; Grewal 1983; Han 1982; Stagg and El-Abiad 1968), is written in a convenient form

$$y_t = \frac{1}{Z_t} \begin{bmatrix} \frac{1}{a_t^*} \\ -1 \end{bmatrix} \begin{bmatrix} \frac{1}{a_t} & -1 \end{bmatrix} . \tag{2.6}$$

The off-diagonal elements of the y-matrix of (2.6) are unequal for $\phi_t \neq 0$. The transformers with real turns ratio (i.e., $a_t = a^*_t$) are called tap-changing-under-load transformers (Elgerd 1982; Grewal 1983; Weedy 1979). As far as their modeling is concerned, the cascaded model shown in Fig. 2.3 is equally valid.

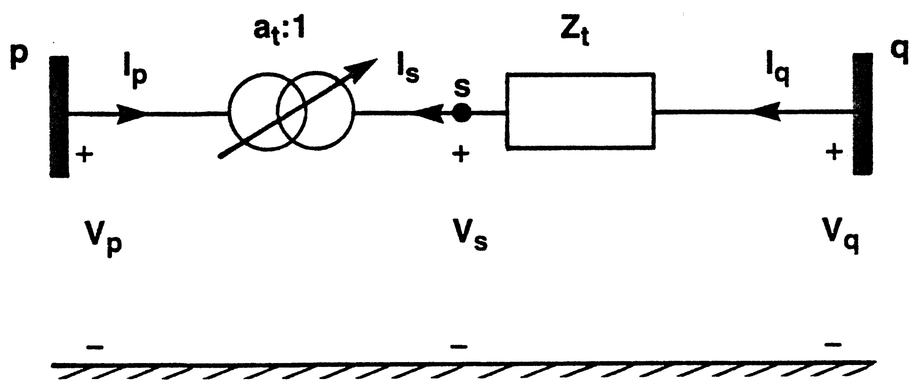

Fig. 2.3 A phase-shifting transformer model (Bandler, El-Kady and Grewal 1985b, p. 1293).

An alternative way of expressing the transformer primary/secondary relations is to consider the ideal transformer of Fig. 2.3 as a separate branch (Bandler, El-Kady and Grewal 1985b). It is useful to designate the primary current and secondary voltage conjugate as the transformer state variables of interest. The corresponding relations are compactly written as

$$\begin{bmatrix} -V_p \\ I_s^* \end{bmatrix} = -a_t \begin{bmatrix} 0 & 1 \\ 1 & 0 \end{bmatrix} \begin{bmatrix} I_p \\ V_s^* \end{bmatrix}^* . \tag{2.7}$$

The reason for involving the complex conjugation as well as hybrid variables is clarified later in Chapter 4.

The control transformers discussed in this section are used to interconnect two a.c. networks having the same frequency. However, in some cases it is required to tie systems with different frequencies (Ellert and Hingorani 1976). The HVDC links are used instead, and are discussed in the following section.

2.3 Modeling of Static AC-DC Converters

The concept of direct current transmission has been around for a long time (Adamson and Hingorani 1960; Powel 1955; Uhlmann 1975). Being inherently stable, the d.c. transmission requires smaller conductors, less insulation, and narrower rights-of-way at any power level. The high-voltage d.c. (HVDC) transmission is a proven alternative under conditions, where long distances from the generation to load center exist, where asynchronous ties are mandatory; or where underground/underwater cables of considerable length are necessary.

The essential parts of an HVDC system are a d.c. transmission line, a rectifier to convert a.c. to d.c., and an inverter to reconvert d.c. to a.c. (Ellert and Hingorani 1976; Kimbark 1971; Uhlmann 1975). Although, this type of the power device is basically a switch, it is only explicitly represented as such in dynamic studies. The periodicity of the switching sequences can be used in the steady-state studies to model the real as well as the reactive power loading conditions of the a.c.-d.c. converters at the relevant buses. The so-called quasi-steady state modeling is discussed here, with reference to the most commonly used configuration. The rectifier operation is discussed first.

2.3.1 Rectification

A three-phase bridge rectifier (Kimbark 1971) is shown in Fig. 2.4. For brevity purposes, a simple diode rectifier with various waveforms at the specific points is considered.

Let the time frame of reference be the instant at which the phase-to-neutral voltage in phase b is maximum. Then the commutating voltage of valve 3 is expressed as

$$e_b - e_a = \sqrt{2}\, a_p V_p \sin\left(\omega t + \frac{\pi}{3}\right), \tag{2.8}$$

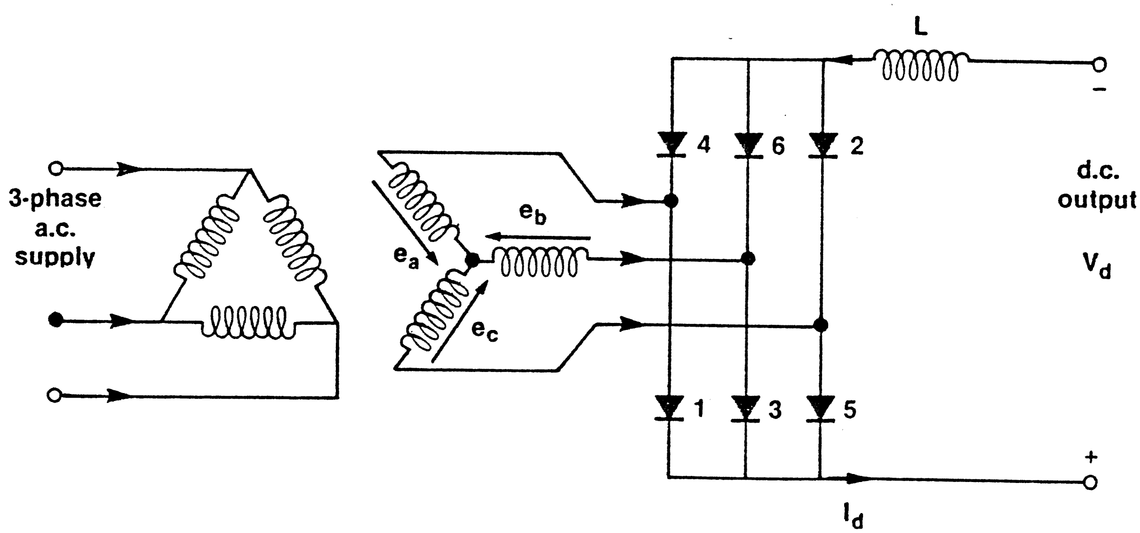

Fig. 2.4 Basic three-phase rectifier bridge.

where a_p is the converter transformer ratio. The shaded area in Fig. 2.5(b) indicates the potential difference between the common cathode cc, and common anode ca bridge poles for the case of uncontrolled rectification. The maximum average rectified voltage is given by

$$V_o = \frac{1}{\pi/3} \int_o^{\pi/3} \sqrt{2}\, a_p V_p \sin\left(\omega t + \frac{\pi}{3}\right) d(\omega t) = \frac{3\sqrt{2}}{\pi} a_p V_p . \tag{2.9}$$

The uncontrolled rectification, however, is rarely used in large power conversions (Kimbark 1971; Uhlmann 1975). The controlled rectification is achieved by phase-shifting the valve conducting periods w.r.t. their corresponding phase voltage waveforms.

With precalculated delay angle control, the average rectified voltage is

$$V_d = \frac{1}{\pi/3} \int_\alpha^{\pi/3+\alpha} \sqrt{2}\, a_p V_p \sin\left(\omega t + \frac{\pi}{3}\right) d(\omega t) = V_o \cos\alpha . \tag{2.10}$$

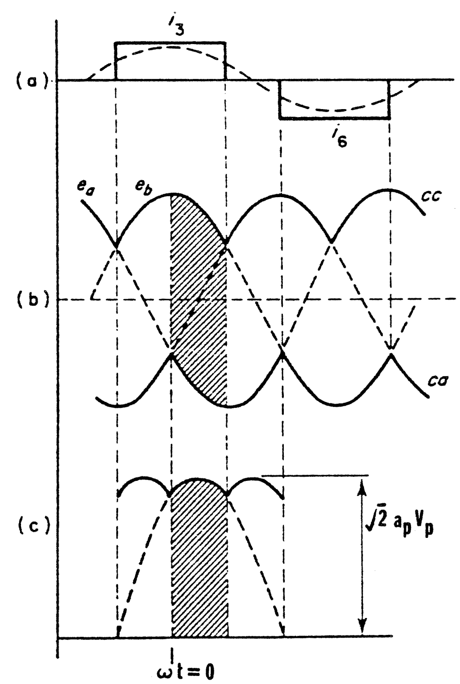

Fig. 2.5 Diode rectifier waveforms.

In practice, the voltage waveform is of a sinusoidal shape. However, some area is lost due to the inherent reactance of the system as observed from the converter. This reactance is called commutation reactance, and is denoted by X_c. The final a.c.-d.c. relationship is given by

$$V_d = V_o \cos a - \frac{\pi}{6} X_c I_d \,. \tag{2.11}$$

Using the nomenclature consistent with the input/output quantities of a conventional two-port connecting nodes p and q, the rectifier equations associated with Fig. 2.6 are expressed in a matrix form as

$$\begin{bmatrix} -\bar{V}_q \\ |I_p| \end{bmatrix} = -\begin{bmatrix} \frac{\pi}{6} X_c & \cos a \\ 1 & 0 \end{bmatrix} \begin{bmatrix} \bar{I}_q \\ |V_p| \end{bmatrix} . \tag{2.12}$$

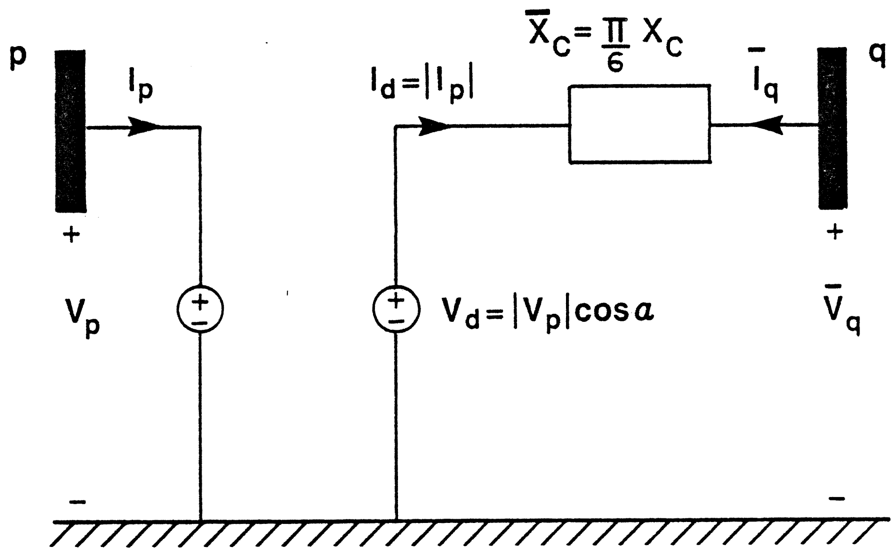

Fig. 2.6 A two-port rectifier model.

2.3.2 Inversion

Owing to the unidirectional nature of the current flow through the converter valves, the power reversal requires direct voltage polarity reversal (Ellert and Hingorani 1976; Kimbark 1971; Uhlmann 1975). This is achieved by incorporating the delay angle control. The inverter voltage, although of opposite polarity with respect to the rectifier, is usually positive when considered alone. Typically, the inverter operation requires the existence of the following three conditions (Adamson and Hingorani 1960):

(i) An active a.c. system to provide the commutating voltages.

(ii) A d.c. power supply of opposite polarity to provide continuity for the unidirectional current flow, that is, from anode to cathode through the switching devices.

(iii) Fully controlled rectification to provide firing delays beyond 90°.

When these conditions are satisfied, the inverter equations are conveniently written in a form similar to the rectifier equations (2.12).

2.3.3 High Voltage DC Transmission

The advantages of transmitting electrical power by d.c. rather than by a.c. can be summarized as (Kimbark 1971; Weedy 1979; Wildi 1981):

- The d.c. power can be controlled much more quickly. Prompt power control facilitated by the d.c. lines also means that d.c. short-circuit currents can be limited to much smaller values than those encountered in the a.c. networks.
- The d.c. power can be transmitted in cables over great distances, and under large bodies of water where the use of a.c. cables is forbidden. Furthermore, underground d.c. cables may be used to deliver power into large urban centers.

- The d.c. intertie provides a big advantage of linking two a.c. systems having different frequencies.
- Overhead d.c. transmission lines have proved to be economically competitive with their counter parts. This is one of the reasons for the d.c. transmission being used to carry the electrical power directly from a mine-mouth, nuclear, or waterfall generating station to the distant load centers.

2.3.4 Typical Installations

The HVDC transmission is no more a new subject. Its versatility has been adequately realized (Zorpette 1985). Following are some of the important HVDC installations:

Schenectady Project. This installation is of historic importance (1936). It is a 17-mile line connecting Mechanicville and Schenectady, New York. The operating voltage of this line is 30 kV. It transports 5.25 MW, and ties together a 40 Hz and 60 Hz systems.

Gotland Installation. This is the first commercial d.c. transmission line, installed in Sweden (1954). It is a 96-kilometer, 30 MW line under the Baltic Sea between the Island of Gotland and the Swedish mailand. The single-conductor cable operates at 100 kV, and transmits 100 GW-hours of energy to the island each year.

English Channel Project. This is a bipolar submarine link laid in the English Channel between England and France. Two cables, one operating at +100 kV and the other at −100 kV, laid side by side, together carry 160 MW of power in one direction or the other.

Vancouver Island Project. The Vancouver Island-Mainland HVDC link connects the island to the province of British Columbia via a 32 km submarine cable and a

41 km overhead line. The first pole carries 312 MW at 260 kV. An additional pole with thyristor valves started commissioning in 1979. Its transmitting capability is 470 MW.

NW-SW Pacific Intertie. A bipolar link, shown in Fig. 2.7 (Ellert and Hingorani 1976), was installed in 1970 between Dalles, Oregon, and Los Angles, California. A total of 1440 MW is transmitted over a distance of 1370 km. The d.c. link helps stabilize the three-phase a.c. transmission system connecting the Northwest and Southwest regions.

Nelson River Installation. The hydropower generated by the Nelson River, situated 890 km north of Winnipeg, Canada, is being transmitted by means of two bipolar lines operating at $\pm$450 kV. Each bipolar line carries 1620 MW, which is converted and fed into the a.c. system near Winnipeg. According to the studies undertaken, it was slightly more economical to transmit power by d.c. rather by a.c. over this considerable distance.

Eel River Project. The converter station at the Eel River, Canada (1972), provides an asynchronous intertie between the 230 kV electrical systems of Quebec and New Brunswick. Although both systems operate at a nominal frequency of 60 Hz, it was not feasible to interconnect them directly owing to the stability considerations. In this case, the d.c. line is merely a few metres long, representing the length of the conductors needed to connect the converter components. Power may flow in either direction, up to a maximum of 320 MW.

CU Project. The power output of a generating station situated next to the lignite coal mines near Underwood, North Dakota, is converted to d.c. and transmitted 436 miles eastwards to a terminal near Minneapolis, Minnesota, where it is reconverted to a.c. The bipolar line transmits 1 GW at $\pm$ 400 kV.

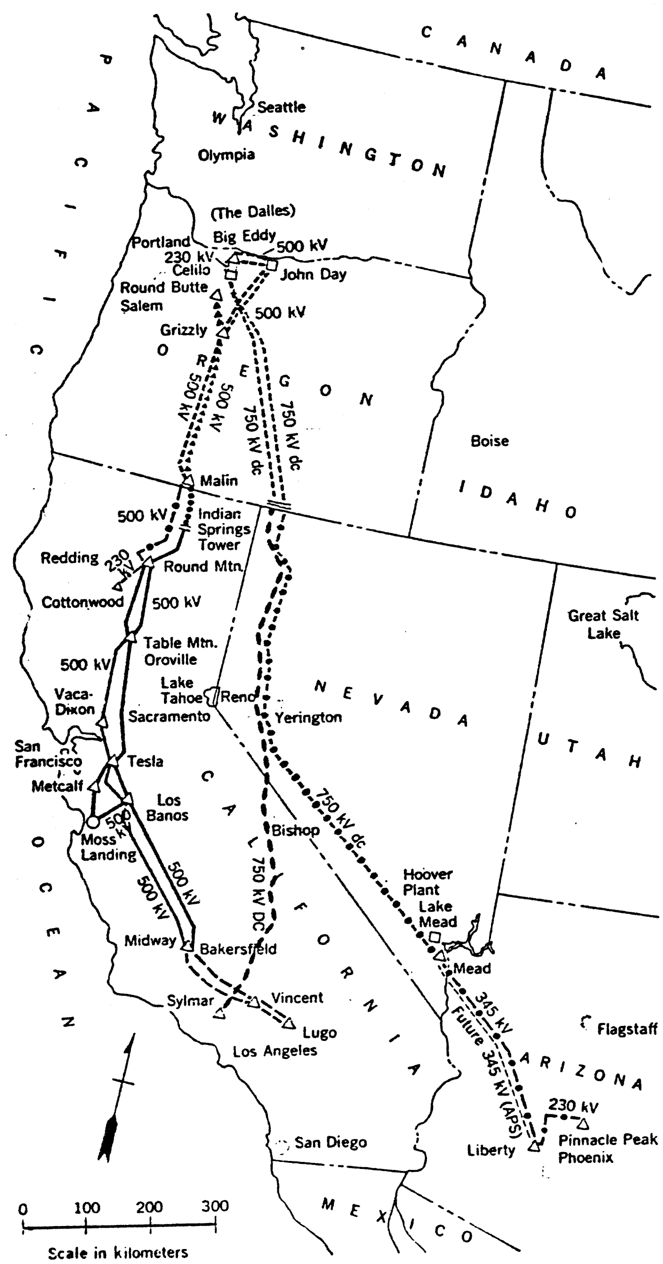

Fig. 2.7 A symbolic map of the NorthWest-SouthWest Pacific Intertie.

EPRI Compact Substation. This project aims at compacting HVDC converter stations so that they may be installed in thickly populated metropolitan areas where land costs are very high. All components are gas-insulated, and the thyristors are cooled with liquid freon. This Electric Power Research Institute development project is located in Queen's, New York. It provides a bipolar link with a capacity of 100 MW at ± 50 kV, and interconnects two large Consolidated Edison substations about 700 m apart.

2.4 Summary

This chapter has dealt with the mathematical models pertaining to major components of a modern power system in order to serve as a sound point of departure for the following text.

The important and useful assumptions involved in the single-phase modeling have been briefly discussed. The nodal method of analysis has been emphasized, owing to its inherent advantages and suitability for the computer usage. A representation of the composite load has been considered. Both the real and reactive powers at the load buses of a given power system have been assumed to be specified. The generator buses, incorporated with sophisticated closed-loop control accessories, have been modelled as the voltage-controlled buses. Additionally, the concept of the slack bus has been discussed.

Further, the electrical properties of extra high-voltage (EHV) a.c. transmission lines have been adequately represented with the help of their equivalent π model. A two-port cascade transformer model has been investigated using the short-circuit admittance matrix as well as a hybrid description.

The essential features of high-voltage d.c. (HVDC) transmission have been highlighted. A fairly simple converter model has been illustrated, and some typical examples of the HVDC installations are appended.

CHAPTER 3

POWER FLOW AND RELATED TOPICS – A REVIEW

3.1 Introduction

The electrical power transmission systems, under normal conditions, operate in their steady-state mode. The basic calculation required to determine the characteristics of this state is termed power flow or load flow. The main objective of power flow calculations is to evaluate the complex bus voltages for a given set of customer demand. Active (real) power generation is normally specified in accordance with economic-dispatch (Carpentier 1979; Dommel and Tinney 1968; El-Hawary and Christensen 1979). The voltage magnitude at all the generator buses is maintained at a specified level by automatic control devices, mentioned in Section 2.2.2.

The power flow problem of a given system is frequently formulated using the nodal admittance matrix (Y-matrix) description (Arrillaga et al. 1983; Elgerd 1982; Singh 1983). Although, the transmission network is represented by linear lumped parameters; the power and voltage constraints of the system make the problem inherently nonlinear. Consequently, the numerical solution of the power flow problem involves iterative methods. For an efficient power flow solution method, the fundamental requirements are high computation speed, low computer storage, reliability of the solution, and versatility as well as simplicity of the algorithm. The first practical digital solution methods were Y-matrix iterative methods, but they were found unsuitable owing to their slow convergence. Subsequently, impedance matrix (Z-matrix) methods were developed which did overcome the reliability problems, but a sacrifice of both the storage and speed was deemed objectionable in the case of large systems (Stott 1974; Talukdar and Wu 1981).

The well-known Newton-Raphson method (Tinney and Hart 1967) was also in progress at that time, and it exhibited strong convergence properties when applied to the power flow equations (Elgerd 1982). Nevertheless, the method was not declared competitive until the sparsity-oriented programming in conjunction with optimally ordered Gaussian elimination was introduced (Tinney and Walker 1967). Later on, other methods involving nonlinear programming and hybridized formulation, were also developed (Sasson 1969; Sasson and Merrill 1974). In power industry, the Newton-Raphson method and algorithms derived from its variants are gradually replacing the previously used techniques.

This chapter basically concerns itself with the ordinary load flow problem formulation and various aspects involved in the Newton-Raphson (N-R) method. The three modes – complex, rectangular and polar, are briefly described. Furthermore, the polar mode of formulation is extended to include the development of the well-known fast decoupled load flow method (Stott 1972; Stott and Alsac 1974).

Additionally, an application of the Tellegen's theorem accomplished by Bandler and El-Kady (1982b) is considered. A rather new methodology for solving the load flow problem is discussed. For the sake of brevity, only the exact version of the Tellegen theorem method is included to help understand generalized adjoint network formulation presented in the subsequent chapters. A qualitative comparison of the exact and fast decoupled load flow solution methods is concisely illustrated using the results of a 6-bus system and a 26-bus Saskatchewan Power Corporation system. Some of the ingenious features, pertaining to the software developed in Simulation Optimization Systems Research Laboratory at McMaster University, are also mentioned.

Finally, the intricacies involved in an optimal power flow problem (Dhar 1982; El-Hawary and Christensen 1979; Elgerd 1982) are discussed. The optimal power flow equations are solved in a manner quite similar to the ordinary power flow equations, except that the generator real powers are not specified as such. Instead, both upper and lower bounds associated with each of the generator power are included realistically in the problem.

3.2 Basic Nodal Admittance Equations

In the power transmission networks, the nodal method deals with the complex bus voltages, injected currents, and the slack bus concept (El-Kady 1980; Grewal 1983). The slack bus provides the reference voltage phase angle, which is usually taken as zero (Section 2.2.3). For an n-node system having n_L load buses, the ith bus injected current I_i is the net current entering the network from the ith source branch. Accordingly, the load bus current I_ℓ for $\ell = 1,2,\dots,n_L$ is taken as negative. The generator bus current I_g for $g = n_L+1,\dots,n_L+n_G$ is positive. Note that the last numbered bus of a given system is assumed as the slack bus in this text.

Using the vector/matrix notation, the basic expression for the power flow equations is written in a compact form (Bandler, El-Kady and Grewal 1986) as

$$\mathbf{S}_M^* - \mathbf{E}_M^* \mathbf{Y}_T \mathbf{V}_M = \mathbf{0}\,, \tag{3.1}$$

where $\mathbf{S}_M$ is a vector of the complex bus powers, $\mathbf{V}_M$ is the complex bus voltage vector, i.e., $[\mathbf{V}_L^T\ \mathbf{V}_G^T\ V_n]^T$, $\mathbf{Y}_T$ is the bus admittance matrix, and $\mathbf{E}_M$ is an n-dimensional diagonal matrix of complex voltages in the corresponding order.

The bus admittance matrix $\mathbf{Y}_T$ of a power system, usually has a well-defined structure (Alvarado 1978; Wildi 1981). For routine calculations, it is automatically constructed from the given data. The matrix is square, and structurally symmetrical with complex elements. Each of the off-diagonal element, Y_{ki} for $k \neq i$, is equal to negative of the branch admittance between the pertinent nodes. For large systems, with every node connected to at the most four or five other nodes, the corresponding $\mathbf{Y}_T$ is highly sparse. The kth diagonal element Y_{kk} of Y_T is obtained by summing up the admittances of those branches which terminate on the kth node.

Consider a 6-bus sample system shown in Fig. 3.1. The system contains three load buses ($n_L = 3$), two generator buses ($n_G = 2$) and a slack bus declared as the last bus ($n = 6$). The transmission branches are mainly lines. One branch has a phase-shifting transformer in series with the line connecting buses 1 and 4. The turns ratio phase angle of this transformer is deliberately taken large; that is, $\phi_7 = 36.8°$ (Table 3.1). The total number of interconnections in this system is equal to 8. The unsymmetrical nodal admittance matrix of the system is provided in Table 3.2a.

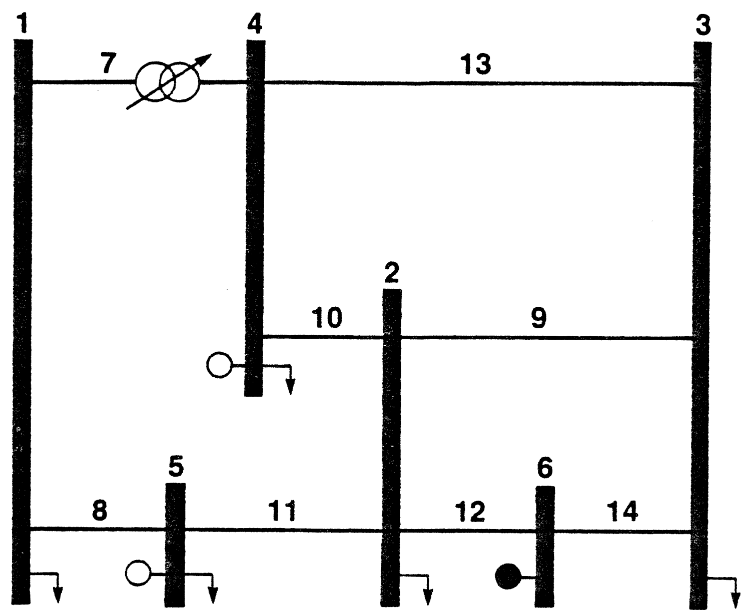

Fig. 3.1 One line diagram of a 6-bus sample system.
(Bandler, El-Kady and Grewal 1985b, p. 1294)

TABLE 3.1

TRANSMISSION NETWORK DATA FOR THE 6-BUS SAMPLE SYSTEM

Branch Index, t	Terminal Buses	Resistance R_t (p.u.)	Reactance X_t (p.u.)	Complex Turns Ratio $a_t \triangleq a_{t1} + j\, a_{t2}$ (p.u.)
7	1,4	0.05000	0.200	0.8 + j0.6
8	1,5	0.02500	0.100	1.0
9	2,3	0.10000	0.400	1.0
10	2,4	0.10000	0.400	1.0
11	2,5	0.05000	0.200	1.0
12	2,6	0.01875	0.075	1.0
13	3,4	0.15000	0.600	1.0
14	3,6	0.03750	0.150	1.0

TABLE 3.2a

NODAL ADMITTANCE MATRIX OF THE 6-BUS SYSTEM

The sequence in each row is: Column Index, Real(YT), and Imaginary(YT)

Bus No. 1						
	1:	3.529412	−14.117647	4:	−3.764706	3.058824
	5:	−2.352941	9.411765			
Bus No. 2						
	2:	5.490196	−21.960784	3:	−0.588235	2.352941
	4:	−0.588235	2.352941	5:	−1.176471	4.705882
	6:	−3.137255	12.549020			
Bus No. 3						
	3:	2.549020	−10.196078	2:	−0.588235	2.352941
	4:	−0.392157	1.568627	6:	−1.568627	6.274510
Bus No. 4						
	4:	2.156863	−8.627451	1:	1.882353	4.470588
	2:	−0.588235	2.352941	3:	−0.392157	1.568627
Bus No. 5						
	5:	3.529412	−14.117647	1:	−2.352941	9.411765
	2:	−1.176471	4.705882			
Bus No. 6						
	6:	4.705882	−18.823529	2:	−3.137255	12.549020
	3:	−1.568627	6.274510			

The nonzero entries of the nodal admittance matrix are stored efficiently using three vectors JRYT, ICYT, and YT (Bandler, El-Kady and Wojciechowski 1983). The dimensions of the integer vectors JRYT and ICYT, associated with the 6-bus system, are 7 and 22, respectively. The vector YT contains the complex values of the admittance matrix in a corresponding manner. Its dimension is also 22. As the zero elements of the admittance matrix are not stored, lot of effort is saved, especially for large systems. The three vectors, pertaining to the 6-bus system, are shown in Table 3.2b.

TABLE 3.2b

STORAGE OF THE 6-BUS NODAL ADMITTANCE MATRIX

I	JRYT(I)	ICYT(I)	YT(I)
1	1	1	3.529412−j 14.117647
2	4	4	−3.764706+j 3.058824
3	9	5	−2.352941+j 9.411765
4	13	2	5.490196−j 21.960784
5	17	3	−0.588235+j 2.352941
6	20	4	−0.588235+j 2.352941
7	23	5	−1.176471+j 4.705882
8	–	6	−3.137255+j 12.549020
9	–	3	2.549020−j 10.196078
10	–	2	−0.588235+j 2.352941
11	–	4	−0.392157+j 1.568627
12	–	6	−1.568627+j 6.274510
13	–	4	2.156863−j 8.627451
14	–	1	1.882353+j 4.470588
15	–	2	−0.588235+j 2.352941
16	–	3	−0.392157+j 1.568627
17	–	5	3.529412−j 14.117647
18	–	1	−2.352941+j 9.411765
19	–	2	−1.176471+j 4.705882
20	–	6	4.705882−j 18.823529
21	–	2	−3.137255+j 12.549020
22	–	3	−1.568627+j 6.274510

3.3 Power Flow Solution using Newton-Raphson Method

The power flow calculations, performed in system planning and operational planning, require a strategic choice of a solution method for practical applications (Carpentier and Merlin 1982; Meliopoulos et al. 1982; Sachdev and Ibrahim 1974, 1975). A careful analysis of the comparative merits and demerits of the many available methods has to be made in such respects as storage, speed and convergence characteristics. Insofar as the specific application and computing facilities are concerned, it is quite difficult to relate the performance of the most efficient method (Stott 1974; Talukdar and Wu 1981). For routine calculations, however, the Newton-Raphson method (also called Newton's method) has gained widespread popularity (Tinney and Hart 1967). Different versions as well as variants of the Newton's method are briefly discussed in the following sections.

3.3.1 Complex Mode Formulation

The power flow equations, expressed in (3.1), involve the complex bus voltage vector $\mathbf{V}_M$ together with its conjugate $\mathbf{V}_M^*$. Using the complex conjugate notation (Bandler and El-Kady 1982c; El-Kady 1980; Grewal 1983), it is quite straightforward to write (3.1) in its perturbed form as

$$\mathbf{K}^S \delta\mathbf{V}_M + \overline{\mathbf{K}}^S \delta\mathbf{V}_M^* = \mathbf{d}^S, \tag{3.2}$$

where

$$\mathbf{d}^S = \delta\mathbf{S}_M^* - \mathbf{E}_M^* \delta\mathbf{Y}_T \mathbf{V}_M . \tag{3.3}$$

The coefficient matrices $\mathbf{K}^S$ and $\overline{\mathbf{K}}^S$ of (3.2) are obtained from different source branch equations (Bandler, El-Kady and Grewal 1986).

For the 6-bus system, shown in Fig. 3.1, the bus loading equations associated with the load buses ($\ell = 1,2,$ and 3) are

$$S_1^* = Y_{11} V_1 V_1^* + Y_{14} V_4 V_1^* + Y_{15} V_5 V_1^*$$

$$S_2^* = Y_{22} V_2 V_2^* + Y_{23} V_3 V_2^* + Y_{24} V_4 V_2^* + Y_{25} V_5 V_2^* + Y_{26} V_6 V_2^*$$

$$S_3^* = Y_{33} V_3 V_3^* + Y_{32} V_2 V_3^* + Y_{34} V_4 V_3^* + Y_{36} V_6 V_3^* \ ,$$

respectively.

The generator bus equations are obtained by exploiting the quasi-complex power ($\tilde{S}_g \triangleq P_g + j\,|V_g|$) for g = 4 and 5. The expressions for the perturbed real power and voltage magnitude associated with the gth generator bus are

$$2\delta P_g = V_g \delta I_g^* + I_g^* \delta V_g + V_g^* \delta I_g + I_g \delta V_g^*, \tag{3.4}$$

and

$$\delta |V_g| = (V_g \delta V_g^* + V_g^* \delta V_g) / (2|V_g|), \tag{3.5}$$

respectively. The generator injected current I_g is given by

$$I_g = \mathbf{y}_g^T \mathbf{V}_M, \tag{3.6}$$

where $\mathbf{y}_g{}^T$ represents the corresponding row of the nodal admittance matrix $\mathbf{Y}_T$. The perturbed form of (3.6) is

$$\delta I_g = \mathbf{y}_g^T \delta \mathbf{V}_M + \mathbf{V}_M^T \delta \mathbf{y}_g. \tag{3.7}$$

Using equations (3.4)-(3.7), the perturbed quasi-complex power pertaining to the gth bus, is obtained as

$$\delta \tilde{S}_g^* = \mathbf{k}_g^T \delta \mathbf{V}_M + \bar{\mathbf{k}}_g^T \delta \mathbf{V}_M^* + V_g^* \mathbf{V}_M^T \delta \mathbf{y}_g /2 + V_g \mathbf{V}_M^{*T} \delta \mathbf{y}_g^* /2, \tag{3.8}$$

where

$$\mathbf{k}_g \triangleq (V_g^*/2)\, \mathbf{y}_g + [\mathbf{y}_g^{*T} \mathbf{V}_M^* /2 - j\, V_g^*/(2|V_g|)]\, \boldsymbol{\mu}_g, \tag{3.9}$$

and

$$\bar{\mathbf{k}}_g \triangleq (V_g/2)\, \mathbf{y}_g^* + [\mathbf{y}_g^T \mathbf{V}_M /2 - j\, V_g/(2|V_g|)]\, \boldsymbol{\mu}_g. \tag{3.10}$$

Alternatively, (3.8) is written as

$$\mathbf{k}_g^T \delta \mathbf{V}_M + \bar{\mathbf{k}}_g^T \delta \mathbf{V}_M^* = d_g, \tag{3.11}$$

where

$$d_g \triangleq \delta \tilde{S}_g^* - V_g^* \mathbf{V}_M^T \delta \mathbf{y}_g /2 - V_g \mathbf{V}_M^{*T} \delta \mathbf{y}_g^* /2. \tag{3.12}$$

Further, the nth perturbed equation associated with the slack bus is written in the form

$$\mathbf{k}_n^T \delta \mathbf{V}_M + \bar{\mathbf{k}}_n^T \delta \mathbf{V}_M^* = \delta V_n^*, \tag{3.13}$$

where $\mathbf{k}_n$ is a null vector, and

$$\bar{\mathbf{k}}_n = \boldsymbol{\mu}_n \triangleq [0 \;\; 0 \;\; \dots \;\; 1]^T . \tag{3.14}$$

The linearized power flow equations of the n-node system are collectively expressed as (El-Kady 1980; Grewal 1983)

$$\begin{bmatrix} \mathbf{K} & \bar{\mathbf{K}} \\ \bar{\mathbf{K}}^* & \mathbf{K}^* \end{bmatrix} \begin{bmatrix} \delta \mathbf{V}_M \\ \delta \mathbf{V}_M^* \end{bmatrix} = \begin{bmatrix} \mathbf{d} \\ \mathbf{d}^* \end{bmatrix} . \tag{3.15}$$

The coefficient matrix involved in (3.15) is called the Jacobian matrix. It is composed of four square submatrices. The sparsity structure of the 6-bus Jacobian matrix is as shown in Fig. 3.2.

X			X	X	X				
	X	X	X	X		X			
	X	X	X				X		
X	X	X	X					X	
X	X			X					X
X					X			X	X
	X					X	X	X	X
		X				X	X	X	
			X		X	X	X	X	
				X	X	X			X

Fig. 3.2 Sparsity structure of the 6-bus complex Jacobian matrix.

3.3.2 Rectangular Mode Formulation

The mathematical formulation of the power flow problem in the rectangular mode deals with real equations involving real system variables (Dhar 1982; Stagg and El-Abiad 1968; Stott 1974). The ik-th admittance is separated into its conductance G_{ik}, and susceptance B_{ik}. Additionally, the complex bus voltages V_i for i = 1,2,...,n, are separated into their real parts V_{i1} and imaginary parts V_{i2}. The equations pertaining to the 6-bus system, shown in Fig. 3.1, are

$$\left.\begin{aligned} P_1 &= \mathrm{Re}\{S_1^*\} = f_1(G_{1i}, B_{1i}, V_{i1}, V_{i2}) \\ Q_1 &= -\mathrm{Im}\{S_1^*\} = \bar{f}_1(G_{1i}, B_{1i}, V_{i1}, V_{i2}) \end{aligned}\right\} \text{for } i = 1, 4 \text{ and } 5,$$

$$\begin{matrix} \cdot & \cdot & \cdot \\ \cdot & \cdot & \cdot \\ \cdot & \cdot & \cdot \end{matrix}$$

$$P_5 = \mathrm{Re}\{S_5^*\} = f_5(G_{5i}, B_{5i}, V_{i1}, V_{i2}) \qquad \text{for } i = 1, 2, \text{and } 5,$$

$$V_4 = (V_{41}^2 + V_{42}^2)^{1/2} \ ,$$

$$V_5 = (V_{51}^2 + V_{52}^2)^{1/2} \ ,$$

and

$$V_6 = V_{61} \, .$$

The voltage controlled buses of a given system are assumed to exhibit constant voltage magnitude. Both the real and imaginary components V_{g1} and V_{g2} at these buses are unknowns.

Using the conventional perturbed form (El-Kady 1980; Grewal 1983), the linearized power flow equations in the rectangular mode are

$$\begin{bmatrix} (K_1 + \overline{K}_1) & (-K_2 + \overline{K}_2) \\ -(K_2 + \overline{K}_2) & (-K_1 + \overline{K}_1) \end{bmatrix} \begin{bmatrix} \delta V_{M1} \\ \delta V_{M2} \end{bmatrix} = \begin{bmatrix} d_1 \\ -d_2 \end{bmatrix}, \tag{3.16}$$

where the real subvectors/submatrices are related to their respective complex counterparts as follows:

$$\mathbf{d} = \mathbf{d}_1 + j\,\mathbf{d}_2, \tag{3.17}$$

$$\mathbf{K} = \mathbf{K}_1 + \mathbf{K}_2, \tag{3.18}$$

$$\overline{\mathbf{K}} = \overline{\mathbf{K}}_1 + j\,\overline{\mathbf{K}}_2. \tag{3.19}$$

3.3.3 Polar Mode Formulation

In the polar mode formulation as well, the power flow equations are expressed in terms of the real system variables (Arrillaga et al. 1983; Stagg and El-Abiad 1968; Stott 1974). The complex bus voltages are expressed in their polar coordinates; that is, in terms of the voltage magnitude and voltage angle.

The polar coordinate representation appears to have a computational advantage over the rectangular coordinates (Arrillaga et al. 1983; Dhar 1982; Elgerd 1982). The real power mismatch equations are considered for all buses except the slack bus, while the reactive power mismatch equations are formulated only for the load buses. In order to avoid any notational confusion arising between the first-order change and the voltage phase angle, capital delta Δ is used to denote the former in this section. The variable voltage vector in the polar mode contains $\Delta\delta_i$ and $\Delta|V_i|/|V_i|$. This choice enhances the computational efficiency of the solution method (Stott 1974). The increments $\Delta\delta_i$ as well as $\Delta|V_i|/|V_i|$ are both dimensionless. For further improvement, the reactive power residual ΔQ_i is replaced by $\Delta Q_i/|V_i|$. The resulting linearized matrix equation is

$$\begin{bmatrix} \Delta P / |V| \\ \Delta Q / |V| \end{bmatrix} = \begin{bmatrix} H & N \\ J & L \end{bmatrix} \begin{bmatrix} \Delta\delta \\ \Delta|V| \end{bmatrix}. \tag{3.20}$$

A flow diagram of the basic Newton-Raphson algorithm (Arrillaga et al. 1983) is depicted in Fig. 3.3. The initial values of various unknowns, pertaining to a particular system, are obtained by utilizing a flat voltage profile. Any previously stored solution of the system of interest, if available, is preferred to serve as the starting values. Another reliable alternative is to use a d.c. power flow solution of the system in which both the transmission losses as well as the reactive power constraints are neglected (Stagg and El-Abiad 1968; Stott 1974).

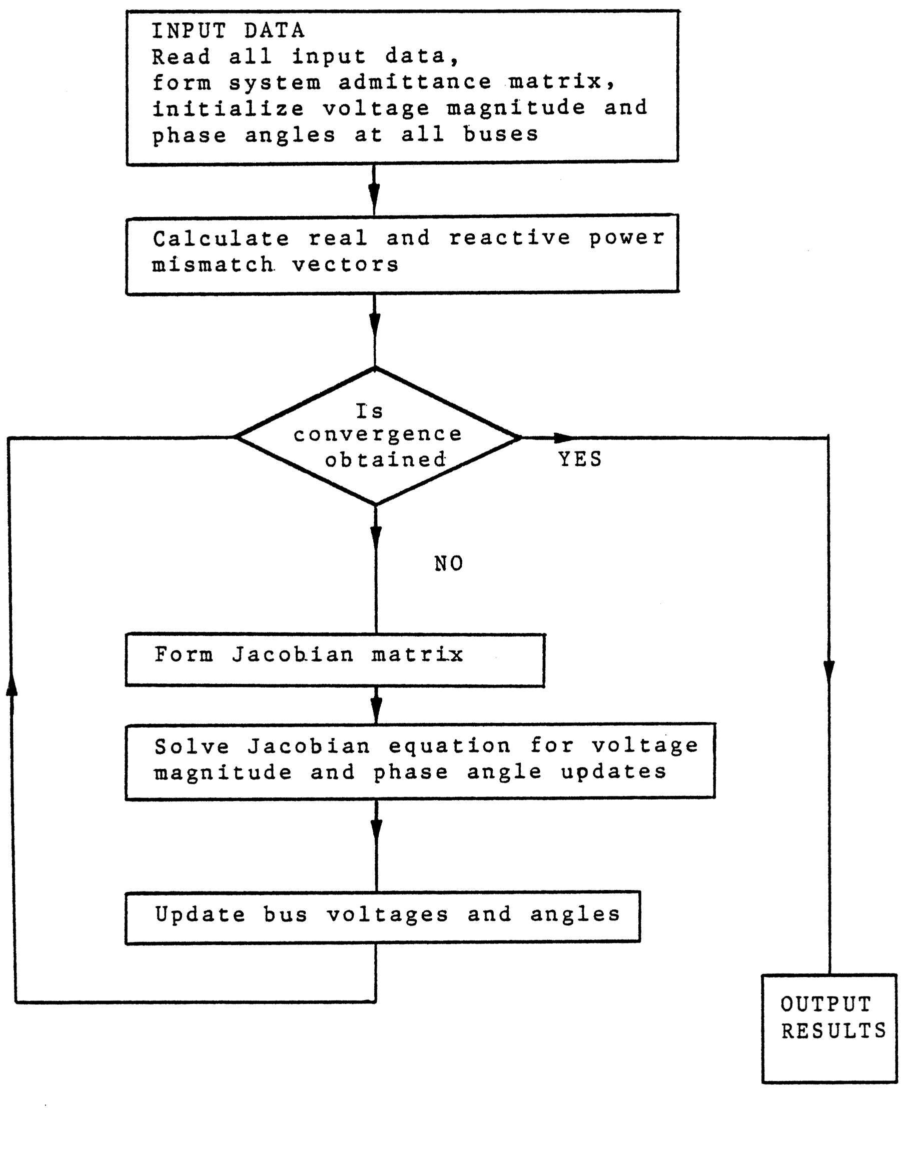

Fig.3.3 Flow diagram of the Newton-Raphson algorithm.

The Newton-Raphson method is very reliable in solving the power flow problem. The number of iterations required to arrive at an acceptable solution is virtually independent of the system size. Most of the well-designed systems, with flat voltage profile, are solved in less than five or six iterations (Bandler, El-Kady and Wojciechowski 1983). The time per iteration rises linearly with the increase in the system size. However, the method readily handles heavily loaded transmission lines with large phase shifts. The performance of the solution method is not hampered by the presence of ill-conditioning, or the location of the slack bus (Arrillaga et al. 1983).

The elements of the Jacobian matrix, involved in (3.15), (3.16), or (3.20), are not constant because they are voltage dependent. These elements vary at every Newton iteration, however, they tend to approach their final numerical values after first two or three iterations (Elgerd 1982; Wildi 1981). Furthermore, there is strong interdependence between the real powers and bus voltage angles, and between the reactive powers and voltage magnitudes. Correspondingly, the submatrices **N** and **J** of (3.20) exhibit relatively weak coupling between the P-δ and Q-$|V|$ equations. Many algorithms ingeniously adopt this decoupling principle (Dhar 1983; Elgerd 1982; Stott 1972).

3.3.4 Some Variants of the Newton-Raphson Method

The voltage vector method uses a series approximation for the sine terms appearing in the power flow equations. Consequently, two decoupled equations are obtained by setting **N** and **J** of (3.20) to null matrices. The corresponding method of solution is called decoupled Newton method. Further approximations are implied by assuming unity voltage magnitude at all the system buses (Arrillaga et al. 1983).

The decoupled Newton method compares very favourably with the formal Newton-Raphson method. While reliability is just as high for ill-conditioned problems, the decoupled version is simple and computationally efficient. The storage of the Jacobian together with the matrix triangulation is saved by a factor of 4. The computation time per iteration is also reduced in the decoupled case, however, it requires more iterations for the same accuracy.

The physical properties of the practical power systems lend further simplification to the equations of concern. The coefficient matrix of the power flow equations is made constant in value (Talukdar and Wu 1981; Stott and Alsac 1974). The approximation leads to the so-called fast decoupled power flow equations, expressed as

$$\Delta \mathbf{P} / |\mathbf{V}| = \mathbf{B}' \Delta \boldsymbol{\delta} \tag{3.21}$$

$$\Delta \mathbf{Q} / |\mathbf{V}| = \mathbf{B}'' \Delta |\mathbf{V}| \tag{3.22}$$

where

$$B'_{km} = -\frac{1}{X_{km}} \qquad \text{for } m \neq k \tag{3.23a}$$

$$B'_{kk} = \sum_{m \omega k} \frac{1}{X_{km}} \tag{3.23b}$$

$$B''_{km} = -B_{km} \qquad \text{for } m \neq k \tag{3.23c}$$

and

$$B''_{kk} = \sum_{m \omega k} B_{km} . \tag{3.23d}$$

The equations (3.21) and (3.22) are solved alternatively using the most recent values of the voltage variables. The square matrices $\mathbf{B}'$ and $\mathbf{B}''$ are both real, having an order $n-1$ and $n-n_G$, respectively. Basically, these matrices are fixed approximations to the tangents of the respective functions defining $\Delta\mathbf{P}/|\mathbf{V}|$ and $\Delta\mathbf{Q}/|\mathbf{V}|$.

3.4 Tellegen's Theorem Method of the Power Flow Solution

The concept of adjoint network simulation (Bandler 1973; Director 1975; Director and Rohrer 1969) using a generalized Tellegen's theorem (Penfield et al. 1970) was first utilized by Fischl and Puntel (1972) to investigate the power flow equations. Based on the d.c.

model, the approach found applications only in cases where sufficient accuracy was not desired. The assumptions concerning the transmission losses, reactive power flow and flat voltage profile, rendered the approach unsuitable from system engineer's point of view. The technique was declared inadequate for the planning studies. These studies anticipated better modeling, and required more sophisticated information (El-Hawary and Christensen 1979).

The a.c. power flow model was recognized (Wu and Sullivan 1976), but it still involved some approximations. Puttgen and Sullivan (1978) used the Tellegen theorem in a suitably extended form, and obtained the gradient information in a straightforward manner. However, the generator modeling was not completely accomplished, owing to the difficulties encountered in handling the generator state and control variables.

Bandler and El-Kady (1981) developed an augmented Tellegen theorem (El-Kady 1980), which readily accommodated the power system equations in the complex domain. Consequently, an exact a.c. model was accomplished, and the first-order sensitivities of properly defined network state (dependent) variables were obtained via one adjoint simulation.

Using the control theory notation (Frank 1978; Tomovic and Vukobratovic 1972), let $\mathbf{x}$ represent the system state vector of interest. The power flow equations of (3.1), when rearranged for the unknowns in an appropriate manner, are expressed in their general form as (Bandler and El-Kady 1982b)

$$\mathbf{f}(\mathbf{x}) = \mathbf{u}\,, \tag{3.24}$$

where $\mathbf{u}$ contains the control variables of a given system. The perturbed form of (3.24), about the nominal point $\mathbf{x}^k$ at the kth iteration, involves the first-order change $\delta\mathbf{x}^k = \mathbf{x}^{k+1} - \mathbf{x}^k$, a mismatch vector $\delta\mathbf{u} = \mathbf{u}_{\text{specified}} - \mathbf{u}^k$, and is written as

$$\mathbf{R}^k\,\delta\mathbf{x}^k = \delta\mathbf{u}^k\,, \tag{3.25}$$

where the coefficient matrix $\mathbf{R}^k$ is

$$\mathbf{R}^k = \begin{bmatrix} \mathbf{H}^k & \mathbf{N}^k \\ \mathbf{J}^k & \mathbf{L}^k \end{bmatrix} . \tag{3.26}$$

The sensitivities of $\mathbf{x}^k$ w.r.t. $\mathbf{u}^k$, as obtained from the adjoint simulation, are essentially the elements of the inverse of matrix $\mathbf{R}^k$. Therefore, $\delta\mathbf{x}^k$ is calculated directly from the mismatch vector $\delta\mathbf{u}^k$.

The adjoint network simulation involves the formulation of the linear equations

$$\mathbf{T}^k \, \hat{\mathbf{x}}_i^k = \hat{\mathbf{b}}_i^k \, , \tag{3.27}$$

where $\hat{\mathbf{b}}_i^k$ is a vector typified by at most two nonzero entries, $\mathbf{T}^k$ is the adjoint matrix of coefficients, and $\hat{\mathbf{x}}_i^k$ is the ith adjoint solution vector (Bandler and El-Kady 1982b). The equation (3.27) is cast into its general form

$$\begin{bmatrix} (\hat{\mathbf{G}}_{LL} + \mathbf{\Psi}_{L1}) & \hat{\mathbf{G}}_{LG} & (-\hat{\mathbf{B}}_{LL} + \mathbf{\Psi}_{L2}) & -\hat{\mathbf{B}}_{LG} \\ \hat{\bar{\mathbf{B}}}_{GL} & (\hat{\bar{\mathbf{B}}}_{GG} - \mathbf{\Psi}_{G2}) & \hat{\bar{\mathbf{G}}}_{GL} & (\hat{\bar{\mathbf{G}}}_{GG} + \mathbf{\Psi}_{G1}) \\ (\hat{\mathbf{B}}_{LL} + \mathbf{\Psi}_{L2}) & \hat{\mathbf{B}}_{LG} & (\hat{\mathbf{G}}_{LL} - \mathbf{\Psi}_{L1}) & \hat{\mathbf{G}}_{LG} \\ \mathbf{0} & \mathrm{diag}\{V_{g2}\} & \mathbf{0} & \mathrm{diag}\{V_{g1}\} \end{bmatrix} \begin{bmatrix} \hat{\mathbf{V}}_{L1} \\ \hat{\mathbf{V}}_{G1} \\ \hat{\mathbf{V}}_{L2} \\ \hat{\mathbf{V}}_{G2} \end{bmatrix} = \begin{bmatrix} \hat{\mathbf{I}}_{L1} \\ \hat{\mathbf{I}}_{G1} \\ \hat{\mathbf{I}}_{L2} \\ \hat{\mathbf{I}}_{G2} \end{bmatrix} , \tag{3.28}$$

where subscripts L and G correspond to the load and generator bus quantities, respectively. Majority of the elements of the coefficient matrix of (3.28) are line conductances and susceptances representing the basic data of a particular system. The subscripts 1 and 2 denote the real and imaginary parts of the various complex quantities. Other square matrices are given by

$$\mathbf{\Psi}_L = \mathrm{diag}\{-S_\ell / V_\ell^2\} \tag{3.29a}$$

and

$$\mathbf{\Psi}_G = \mathrm{diag}\{S_g / V_g\} , \tag{3.29b}$$

respectively. Furthermore, the bus admittance matrix $\hat{\mathbf{Y}}_T \triangleq \hat{\mathbf{G}}_T + j\,\hat{\mathbf{B}}_T$ of the adjoint power network is systematically partitioned as

$$\hat{\mathbf{Y}}_T = \begin{bmatrix} \hat{\mathbf{Y}}_{LL} & \hat{\mathbf{Y}}_{LG} \\ \hat{\mathbf{Y}}_{GL} & \hat{\mathbf{Y}}_{GG} \end{bmatrix} . \tag{3.30}$$

The admittance matrix $\hat{\mathbf{Y}}_T$ is obtained by transposing the original matrix $\mathbf{Y}_T$. The matrices associated with the generator buses are related to the generator bus voltages and adjoint submatrices $\hat{\mathbf{Y}}_{GL}$ as well as $\hat{\mathbf{Y}}_{GG}$ in the following manner:

$$\hat{\bar{\mathbf{G}}}_{GL} + j\,\hat{\bar{\mathbf{B}}}_{GL} = \mathrm{diag}\{V_g\}\,\hat{\mathbf{Y}}_{GL} \tag{3.31a}$$

and

$$\hat{\bar{\mathbf{G}}}_{GG} + j\,\hat{\bar{\mathbf{B}}}_{GG} = \mathrm{diag}\{V_g\}\,\hat{\mathbf{Y}}_{GG} \tag{3.31b}$$

Equation (3.28) represents an exact version of the linear set of equations using the Tellegen theorem method (TTM), and has been successfully implemented in a package called TTM1 (Bandler et al. 1983). The TTM1 package is capable of supplying sensitivities of power network functions with respect to several system control variables. The structural details of this package are illustrated in Figs. 3.4a and 3.4b.

In addition, the package has been designed to solve the power flow equations using the fast decoupled method. Some numerical results (Bandler and El-Kady 1982b), pertaining to the 6-bus system (Fig. 3.1) and 26-bus system (Fig. 3.5), are presented in Tables 3.3 and 3.4, respectively.

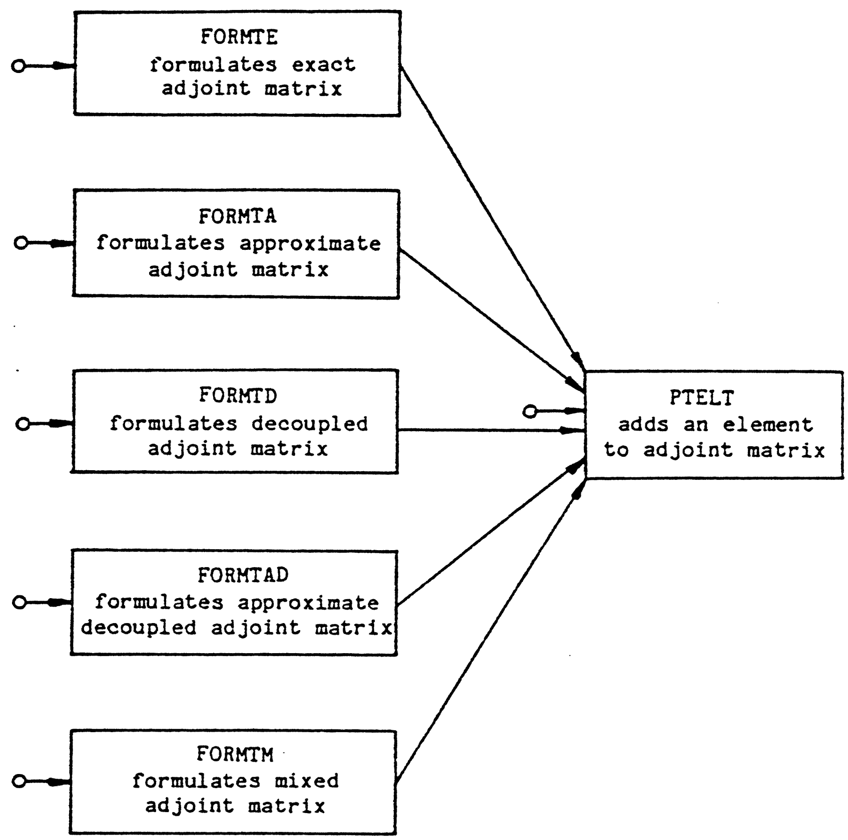

Fig. 3.4a FORMT – a group of subroutines for the formulation of the adjoint coefficient matrix. (Bandler, El-Kady and Wojciechowski 1983, p. 7)

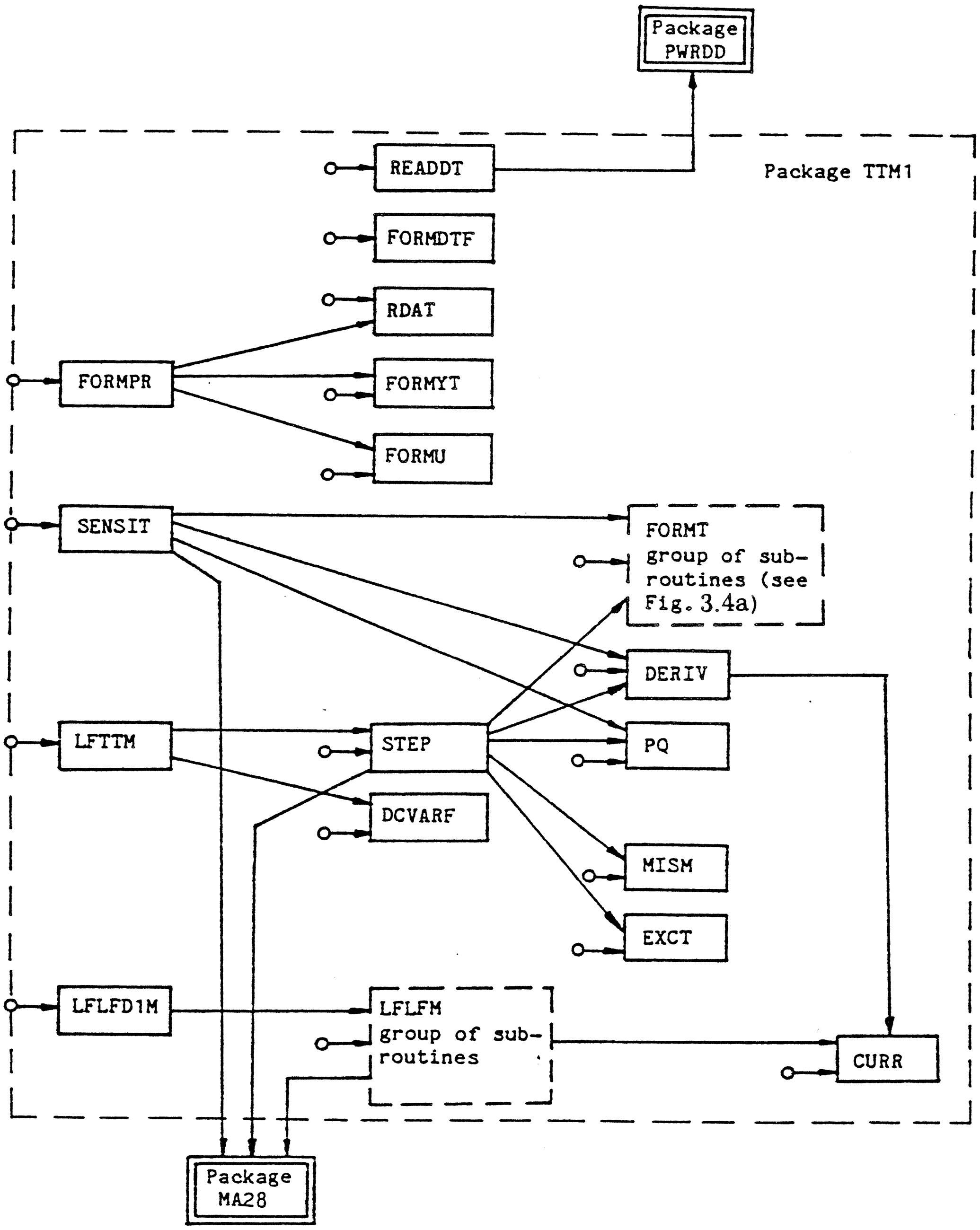

Fig. 3.4b Overall structure of the TTM1 package.
(Bandler, El-Kady and Wojciechowski 1983, p. 6)

TABLE 3.3

POWER FLOW RESULTS FOR THE 6-BUS SYSTEM

		Iteration No. 1	2	3	4
MAX	A	0.167	0.127×10^{-1}	0.948×10^{-4}	0.463×10^{-8}
$\lvert\delta P\rvert$	B	0.205	0.167	0.116×10^{-1}	0.251×10^{-2}
MAX	A	0.554	0.295×10^{-1}	0.166×10^{-3}	0.663×10^{-8}
$\lvert\delta Q\rvert$	B	1.221	0.843×10^{-1}	0.287×10^{-1}	0.133×10^{-1}
MAX	A	0.463×10^{-1}	0.367×10^{-1}	0.244×10^{-4}	0.109×10^{-8}
$\lvert e_v\rvert$	B	0.836×10^{-1}	0.583×10^{-2}	0.233×10^{-2}	0.835×10^{-3}
MAX	A	0.698×10^{-1}	0.649×10^{-2}	0.434×10^{-4}	0.185×10^{-8}
$\lvert e_\theta\rvert$	B	0.118×10^{-1}	0.413×10^{-1}	0.480×10^{-2}	0.140×10^{-2}

Method Code

A Exact Tellegen theorem method (TTM) $e_v = \delta|V|$

B Fast decoupled version $e_\theta = \delta\theta$

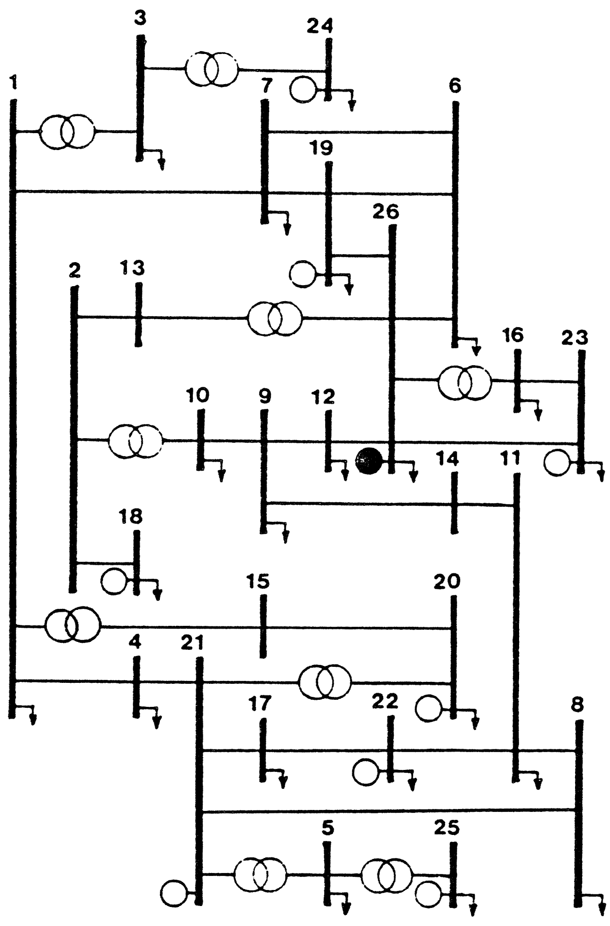

Fig. 3.5 One-line diagram of Saskatchewan Power Corporation 26-bus system (Grewal 1983, p. 53).

TABLE 3.4

POWER FLOW RESULTS FOR THE 26-BUS SYSTEM

		Iteration No. 1	2	3	4
MAX	A	0.271	0.116×10^{-1}	0.591×10^{-4}	0.106×10^{-8}
$\lvert\delta P\rvert$	B	0.546	0.584	0.554×10^{-1}	0.673×10^{-2}
MAX	A	0.837	0.389×10^{-1}	0.106×10^{-3}	0.985×10^{-9}
$\lvert\delta Q\rvert$	B	0.548	0.657×10^{-1}	0.500×10^{-1}	0.828×10^{-2}
MAX	A	0.528×10^{-1}	0.272×10^{-2}	0.818×10^{-5}	0.103×10^{-4}
$\lvert e_v\rvert$	B	0.931×10^{-1}	0.340×10^{-2}	0.112×10^{-1}	0.653×10^{-3}
MAX	A	0.596×10^{-1}	0.462×10^{-2}	0.181×10^{-4}	0.256×10^{-9}
$\lvert e_\theta\rvert$	B	0.615×10^{-1}	0.216×10^{-1}	0.915×10^{-2}	0.512×10^{-2}

Method Code

A Exact Tellegen theorem method (TTM) $e_v = \delta|V|$

B Fast decoupled version $e_\theta = \delta\theta$

3.5 Sensitivity Analysis and Optimal Power Flow

The sensitivity calculations (Najaf-Zadeh and Anderson 1978; Peschon et al. 1968) are performed to evaluate the gradients of network functions of interest subject to equality constraints relating the state and control variables of a particular system. These gradients can be supplied to optimization routines employed in various power system design problems (Carpentier 1979; Carpentier and Merlin 1982). In practice, the power flow problem considers some functional inequality constraints together with upper and lower equipment limits (Sasson 1969; Sasson and Merrill 1974; Talukdar and Wu 1981). The so-called optimal power flow is mathematically expressed as

$$\underset{\mathbf{u}}{\text{Minimize}}\ f(\mathbf{x}, \mathbf{u}) \tag{3.32}$$

subject to

$$\mathbf{h}(\mathbf{x}, \mathbf{u}) = \mathbf{0}\ , \tag{3.33}$$

and

$$\mathbf{g}(\mathbf{x}, \mathbf{u}) > \mathbf{0}\ . \tag{3.34}$$

The objective function $f(\mathbf{x},\mathbf{u})$ of the optimal power flow problems, usually, reflects the total load dispatch of a particular system, and/or total transmission losses in the EHV lines (El-Hawary and Christensen 1979).

The operating limitations arise from the fact that the generating units, transmission lines, and other regulating equipment including phase-shifting transformers, must not be loaded beyond their capacity. In addition, the voltage magnitude at various system buses are expected to be maintained within an allowable range conforming with the statutory act. These inequality constraints are expressed as (Dhar 1982; Elgerd 1982),

$$P_g^{min} < P_g < P_g^{max}$$

$$Q_g^{min} < Q_g < Q_g^{max}$$

$$|a_t|^{min} < |a_t| < |a_t|^{max}$$

$$\Phi_t^{min} < \Phi_t < \Phi_t^{max}$$

$$|V_g|^{min} < |V_g| < |V_g|^{max}$$

and are readily accommodated in (3.34).

Historically, the optimal power flow algorithms started appearing in the literature when Dommel and Tinney (1968) were successful in introducing the reduced gradient steepest-descent algorithm with simple exterior penalty functions (El-Hawary and Christensen 1979). The approach was computationally well-suited for large systems, but it suffered from two basic drawbacks. The algorithm showed slow convergence, and prohibitive ill-conditioning resulted from the penalty functions (Carpentier and Merlin 1982; Sasson 1969; Sasson and Merrill 1974).

Burchett, Happ and Wirgau (1982) accomplished a mathematical structure of the nonlinear power flow equations using a generalized simplex-type iteration. They extended the scope of basic solutions to the nonlinear objective functions of power systems. Their algorithm involves a sequence of nonlinear subproblems, and the progressive solution exhibits quadratic convergence.

3.6 Concluding Remarks

The inherently nonlinear power flow problem has been solved in several different ways. The direct solution methods employ the solution of a related linear system of equations in an iterative fashion; whereas the iterative methods use a scheme of successive displacements. It is quite difficult to make equitable comparisons between these methods based on the available computers, programming methods and test problems. The direct methods show better convergence properties in few iterations. The memory requirements and computing time with the direct methods increase as some power of the problem size.

The iterative methods exihibit slow convergence, and their memory requirements are minimal. The memory requirements with these methods are directly proportional to the problem size. The main disadvantage with these methods is that the number of iterations for an admissible solution increases very rapidly with the size of the problem. With the advent of optimal ordering together with sparsity-oriented techniques, it has been recognized that the Newton-Raphson (N-R) method is one of the immediate solution method for the power flow problems. Further improvements in the N-R method with regard to computational speed and exploitation of the usage of constant Jacobian have been shown by investigating the physical properties of the linearized power flow model. The decoupled Newton method compares very favourably with the formal N-R method. Typically, the voltage magnitudes converge within 0.3 percent of the final solution on the first iteration, and are frequently used as a check for the algorithmic instability. The voltage phase angles converge more slowly than the voltage magnitudes. Adjusted solutions (inclusion of transformer taps, phase angles, interarea power transfers, Q and V limits) take many more iterations.

Based on the physical properties of a practical power system, further simplification with realistic assumptions have culminated in the fast decoupled power flow algorithm. The coefficient matrix involved in this algorithm is triangulated only once per solution for a particular network. The presence of nonreciprocal power elements is duly taken care of. The overall solution time is low for both unadjusted as well as adjusted solution. The method has gained substantial popularilty in the power flow studies, particularly in contingency evaluation with multiple-outages.

Aside from the aforementioned power flow solution methods, a novel method based on the Tellegen theorem has also been discussed. The existing two-port analytical measures, concerning the adjoint formulation, have been extended to include the generalized multiport analyses. Indeed, admittance as well as hybrid parameters of various power network components are easily definable. Furthermore, the hybrid representation conveniently leads to more useful generalization of the relevant adjoint networks, and expedites the computation involved in the subsequent sensitivity evaluation, mentioned in the following chapter.

CHAPTER 4

SENSITIVITY EVALUATION IN POWER SYSTEMS

4.1 General Formulation

The utilization of the first-order sensitivities of certain objective functions, subject to the power flow equations, has been mentioned in the previous chapter. Due to inherently large size of the modern power networks, there are some basic requirements for a successful and practically acceptable sensitivity evaluation method (El-Kady 1980; Grewal 1983).

The sensitivity evaluation techniques, involving approximate power flow models (Fischl and Puntel 1972; Irisarri et al. 1978; Puttegen and Sullivan 1978; Wu and Sullivan 1976), are subjected to many restrictive assumptions. Other methods employ exact a.c. models (Bandler and El-Kady 1981, 1982), however, in some applications both exact as well as inexact models are investigated, depending on the purpose of the study (Ejebe and Wollenberg 1979;Fischl and Wasley 1978).

The well-known method of Lagrange multipliers is quite popular in the power system planning studies (Alvarado 1978; Bandler and El-Kady 1982c, 1984; Rashed and Kelly 1974). It is advantageous to manipulate the already factorized Jacobian matrix at the base-case solution of a particular system. On the other hand, the flexibility offered by using suitable electrical network theorems is equally appreciated when dealing with several different types of the system components (Bandler and El-Kady 1982a; El-Kady 1980; Puttgen and Sullivan 1978). The power network elements ranging from a load bus to a phase-shifting transformer (Bandler, El-Kady and Grewal 1985; Grewal 1983) have been successfully handled by exploiting the Tellegen's theorem.

Using the state variable notation (Branin 1973; Frank 1978), the first-order changes of the equality constraints of (3.33) are given by

$$\delta h_j = \sum_{i=1}^{n_x} \left(\frac{\partial h_j}{\partial x_i} \delta x_i \right) + \sum_{k=1}^{n_u} \left(\frac{\partial h_j}{\partial u_k} \delta u_k \right) = 0 , \qquad j = 1, 2, \ldots, n_x , \tag{4.1}$$

where n_x and n_u are the respective dimensions of the state vector $\mathbf{x}$ and the control vector $\mathbf{u}$ (El-Kady 1980). Similarly, the first-order change of a continuous function f is given by the expansion

$$\delta f = \sum_{i=1}^{n_x} \left(\frac{\partial f}{\partial x_i} \delta x_i \right) + \sum_{k=1}^{n_u} \left(\frac{\partial f}{\partial u_k} \delta u_k \right) . \tag{4.2}$$

Equations (4.1) and (4.2) are the basic equations involved in any of the techniques employed to evaluate the total derivatives of a given function with respect to $\mathbf{u}$.

The commonly used methods of eliminating $\delta\mathbf{x}$ from (4.2) are the sensitivity matrix method, the method of Lagrange multipliers, and the method based on the Tellegen's theorem. The sensitivity matrix method (Dommel and Tinney 1968; Peschon et al. 1968), involves a sensitivity matrix $\mathbf{S}$,

$$\mathbf{S} \triangleq -\left[\left(\frac{\partial \mathbf{h}^T}{\partial \mathbf{x}} \right)^T \right]^{-1} \left(\frac{\partial \mathbf{h}^T}{\partial \mathbf{u}} \right), \tag{4.3}$$

where the partial derivatives represent the Jacobian matrices of $\mathbf{h}$ w.r.t. $\mathbf{x}$ and $\mathbf{u}$, respectively. From (4.1) and (4.3), $\delta\mathbf{x}$ is obtained as

$$\delta\mathbf{x} = \mathbf{S}\,\delta\mathbf{u} . \tag{4.4}$$

Substituting (4.4) into (4.2), the expression for δf becomes

$$\delta f = \left[\frac{\partial f}{\partial \mathbf{u}} + \mathbf{S}^T \frac{\partial f}{\partial \mathbf{x}} \right]^T \delta\mathbf{u} . \tag{4.5}$$

Equation (4.5) is solely in terms of $\delta\mathbf{u}$, and leads to the sensitivity relation given by

$$\frac{df}{d\mathbf{u}} = \frac{\partial f}{\partial \mathbf{u}} + \mathbf{S}^T \frac{\partial f}{\partial \mathbf{x}} . \tag{4.6}$$

The sensitivity evaluation, using (4.6), involves n_u repeat solutions of a system of linear equations formulated from (4.3). This makes the method computationally inefficient.

The method is used in the cases requiring complete knowledge of **S** in subsequent analysis (El-Kady 1980).

4.2 The Method of Complex Lagrange Multipliers

The Lagrange multiplier method is very popular in the domain of optimal power flow problems (El-Hawary and Christensen 1979), not only because it requires one additional solution of a set of linear adjoint equations, but also due to the utilization of the factorized Jacobian matrix (El-Kady 1980; Grewal 1983).

The vector $\boldsymbol{\lambda}$, constituting Lagrange multipliers, is defined as

$$\boldsymbol{\lambda} \triangleq \left(\frac{\partial \mathbf{h}^T}{\partial \mathbf{x}}\right)^{-1} \frac{\partial f}{\partial \mathbf{x}} . \tag{4.7}$$

Using (4.1) together with (4.7) in (4.2), δf becomes

$$\delta f = \left[\frac{\partial f}{\partial \mathbf{u}} - \left(\frac{\partial \mathbf{h}^T}{\partial \mathbf{x}}\right)\boldsymbol{\lambda} \right]^T \delta \mathbf{u} . \tag{4.8}$$

Equation (4.8) yields the sensitivity expression of the form

$$\frac{df}{d\mathbf{u}} = \frac{\partial f}{\partial \mathbf{u}} - \frac{\partial \mathbf{h}^T}{\partial \mathbf{x}} \boldsymbol{\lambda} . \tag{4.9}$$

In the complex mode formulation (Section 3.3.1), the vector $\boldsymbol{\lambda}$ is obtained by solving the vector/matrix equation (Bandler and El-Kady 1984; Grewal 1983); that is,

$$\begin{bmatrix} \mathbf{K}^T & \overline{\mathbf{K}}^{*T} \\ \overline{\mathbf{K}}^T & \mathbf{K}^{*T} \end{bmatrix} \boldsymbol{\lambda} = \begin{bmatrix} \dfrac{\partial f}{\partial \mathbf{V}_M} \\ \dfrac{\partial f}{\partial \mathbf{V}_M^*} \end{bmatrix} . \tag{4.10}$$

This method of sensitivity evaluation readily handles the nonreciprocal power networks (Bandler, El-Kady and Grewal 1986). The algorithm for solving the power flow equations, and subsequently, evaluating various sensitivities has been implemented in a package called XLF3 (Bandler, El-Kady, Grewal and Wojciechowski 1983). A user-oriented description of the package is briefly discussed hereafter.

The XLF3 package is modularized into twelve Fortran subroutines, as depicted in Fig. 4.1. It uses a Harwell package called ME28 in order to solve a given set of complex linear equations. There is no one general entry to the XLF3 package. The user is free to orient his/her computer program to call any of the package subroutines, after making the package accessible. The sequence of call statements in the main program should be appropriate to the user's problem. Furthermore, it is user's responsibility to provide the right-hand side of equation (4.10).

Table 4.1 summarizes the subroutines of the XLF3 package. Two sample computer programs, pertaining to different network functions, are provided in Appendices C.1 and C.2. Both transmission-element as well as bus-type control variables are listed in Table 4.2. The sensitivity formulas for several control variables are provided in Table 4.3. These formulas have been verified by considering different test cases (Bandler, El-Kady, Grewal and Wojciechowski 1983; Grewal 1983).

Additionally, the XLF3 package has been successfully used in conjunction with various gradient-type optimization packages. It utilizes a sparsity-oriented representation of the bus admittance matrix (Duff 1981), the perturbed power flow equations, and the Jacobian matrix. The package and its documentation have been prepared for the CDC 170/815 system with NOS 2.1 580/577 operating system, and the Fortran Extended (FTN) version 4.8 compiler. It exists as a permanent group file, named LIBXLF3, under the charge RJWBAND.

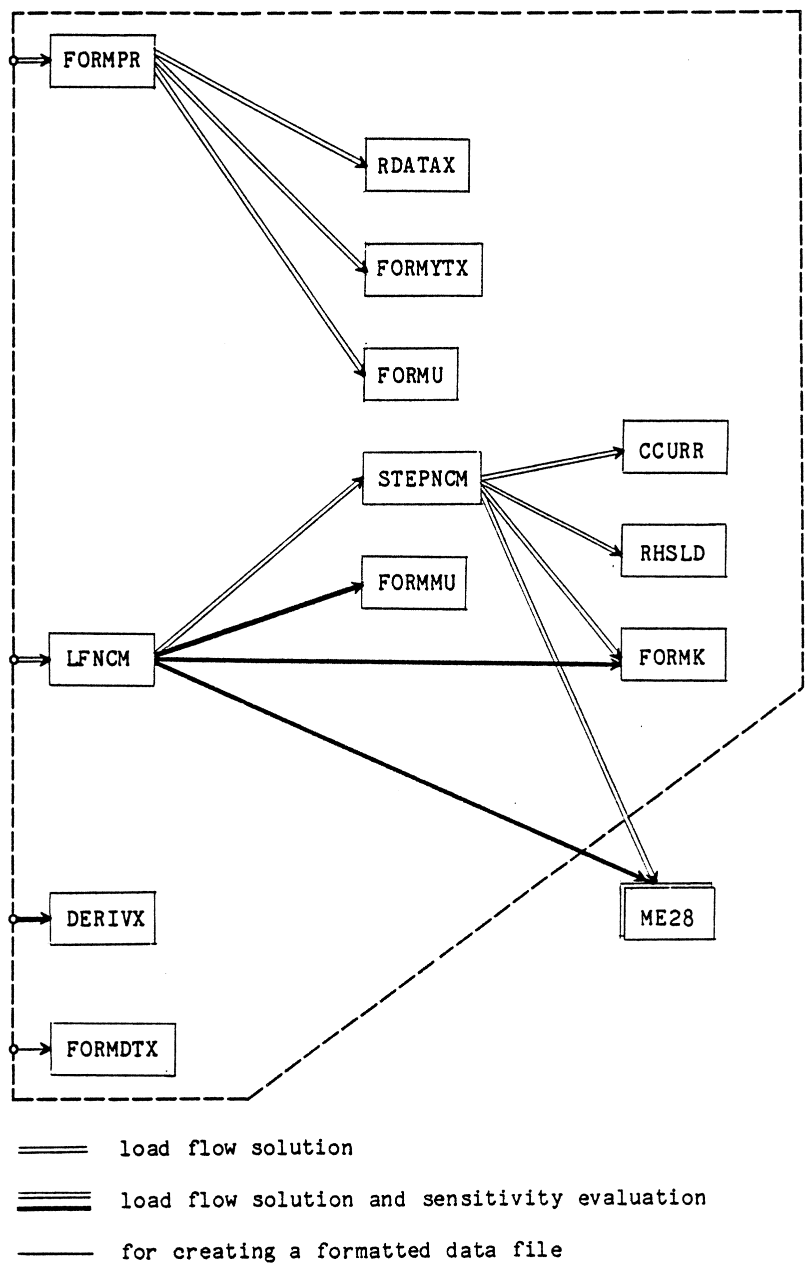

Fig. 4.1 The structural details of XLF3 package (Bandler, El-Kady, Grewal and Wojciechowski 1983, p. 8)

TABLE 4.1

LIST OF SUBROUTINES OF THE XLF3 PACKAGE

Subroutine		Number of lines (source text)	Description (page of *)	Listing (page of **)
1	CCURR	20	13	17
2	DERIVX	80	15	18
3	FORMDTX	39	20	6
4	FORMK	99	23	15
5	FORMMU	18	26	20
6	FORMPR	55	29	4
7	FORMU	45	33	5
8	FORMYTX	61	36	7
9	LFNCM	167	40	10
10	RDATAX	85	45	8
11	RHSLD	38	49	14
12	STEPNCM	47	51	13

* Bandler, El-Kady, Grewal and Wojciechowski 1983, SOS-83-18-U

** Bandler, El-Kady, Grewal and Wojciechowski 1983, SOS-83-18-L.

TABLE 4.2

CODE NUMBER OF CONTROL VARIABLES

Description	A-type variable	B-type variable	Code number
Load bus	P_ℓ	Q_ℓ	1
Generator bus	P_g	$\lvert V_g \rvert$	1
Slack Bus	V_n	–	1
Shunt admittance at a bus	G_{i0}	B_{i0}	2
Line admittance of a transmission line	G_{ij}	B_{ij}	3
Phase-shifting transformer turns ratio			
1. Rectangular coordinates	a_{t1}	a_{t2}	4
2. Polar coordinates	$\lvert a_t \rvert$	Φ_t	5
TCUL* transformer tunrs ratio	a_t	–	6
Transformer internal impedance	R_t	X_t	7

* TCUL stands for tap-changing-under-load.

TABLE 4.3

FORMULAS FOR SENSITIVITY CALCULATIONS

Variable code number	Bus index/indices	Sensitivity formula for DF1 and DF2
1	i	$\hat{V}_i^*$
2	i	† $-\hat{V}_i^R V_i^* V_i$
3	i, j	† $(V_i - V_j)(V_j^* \hat{V}_j^R - V_i^* \hat{V}_i^R)$
4	i, j	† $\frac{V_i}{a_t^2}\left[\frac{2V_i^* \operatorname{Re}\left\{\frac{\hat{V}_i^R}{Z_t}\right\}}{a_t^*} - V_j^*\left(\frac{\hat{V}_i^{*R}}{Z_t^*} + \frac{\hat{V}_j^R}{Z_t}\right)\right]$
5		$\frac{a_{t1}\frac{df}{da_{t1}} + a_{t2}\frac{df}{da_{t2}}}{\lvert a_t \rvert}, -a_{t2}\frac{df}{da_{t1}} + a_{t1}\frac{df}{da_{t2}}$
6		$\frac{df}{da_{t1}}$
7		† $\frac{1}{Z_t^2}\left(\frac{V_i}{a_t} - V_j\right)\left[\frac{\hat{V}_i^R}{a_t^*} - \hat{V}_j^R\right]\left[\begin{matrix} V_i^* \\ V_j^* \end{matrix}\right]$

† $\hat{V}^R = \begin{bmatrix} \hat{V}_L \\ \hat{V}_{G1} \\ 0 \end{bmatrix}$, where superscript R is used to signify that $\hat{V}_g^R = \operatorname{Re}\{\hat{V}_g\}$.

4.3 The Tellegen's Theorem Method

The Tellegen's theorem method (TTM) is based on the concept of adjoint network (Bandler 1973; Chua and Lin 1975; Director 1975). The method has been successfully applied to automated design of networks in the frequency as well as time domain (Director and Rohrer 1969). The Tellegen's theorem (Tellegen 1957; Penfield et al. 1970) depends on the Kirchhoff's laws and the topological constraints of a given network. Mathematically, the theorem states

$$\sum_b \hat{I}_b V_b = 0 \qquad \text{and} \qquad \sum_b \hat{V}_b I_b = 0\,, \tag{4.11}$$

where I_b and V_b represent the respective current and voltage of branch b, and the summation is taken over all the network branches of the system considered.

The equations corresponding to the exact a.c. power flow models are accommodated by including complex power variables in the summation of (4.11). The augmented Tellegen theorem, developed by Bandler and El-Kady (1982a) is expressed in its perturbed form as

$$\ldots + \hat{\mathbf{I}}_b^T \delta \mathbf{V}_b + \hat{\mathbf{I}}_b^{*T} \delta \mathbf{V}_b^* - \hat{\mathbf{V}}_b^T \delta \mathbf{I}_b - \hat{\mathbf{V}}_b^{*T} \delta \mathbf{I}_b^* + \ldots = 0\,. \tag{4.12}$$

4.3.1 Definition of Hybrid Complex Branch Variables

Let a hybrid state vector $\mathbf{x}_b$ represent a vector containing sub-branch quantities ... I_i, I_j^*, V_k, V_ℓ^*, ... of a given power network. The corresponding dual vector $\mathbf{h}_b$ (Bandler, El-Kady and Grewal 1985b), is

$$\mathbf{h}_b \triangleq [\ldots - V_i \quad -V_j^* \quad I_k \quad I_\ell^* \ldots]^T\,. \tag{4.13}$$

The choice of the elements of $\mathbf{x}_b$ is quite flexible. Different current-voltage relations, pertaining to various source branches as well as transmission branches, have been successfully investigated by a judicious selection of $\mathbf{x}_b$.

Using the hybrid vectors $\mathbf{x}_b$ and $\mathbf{h}_b$, the augmented Tellegen's theorem (El-Kady 1980) is rewritten in the form

$$\ldots + \hat{\mathbf{h}}_b^T \delta\mathbf{x}_b + \hat{\mathbf{h}}_b^{*T} \delta\mathbf{x}_b^* - \hat{\mathbf{x}}_b^T \delta\mathbf{h}_b - \hat{\mathbf{x}}_b^{*T} \delta\mathbf{h}_b^* + \ldots = 0 . \tag{4.14}$$

4.3.2 Perturbed Steady-state Component Models

In power networks, the steady-state models of some components involve complex conjugation as discussed in Chapter 2. For example, the ℓth load bus equation (2.1) is expressed in terms of the complex bus voltage V_ℓ and the corresponding bus current conjugate I_ℓ^*. The corresponding perturbed equation is

$$\delta S_\ell = V_\ell \, \delta I_\ell^* + I_\ell^* \, \delta V_\ell = 0 ,$$

or

$$V_\ell \delta I_\ell^* = - I_\ell^* \, \delta V_\ell . \tag{4.15}$$

Similarly, the gth generator bus equation characterized by $\tilde{S}_g \triangleq 2P_g + j|V_g|^2$, yields a perturbed equation given by

$$\delta \tilde{S}_g = V_g \delta I_g^* + V_g^* \delta I_g + (I_g + jV_g) \delta V_g^* + (I_g^* + jV_g^*) \delta V_g . \tag{4.16}$$

Furthermore, the perturbed equation of a transmission network described by $\mathbf{I}_b = \mathbf{Y}_b \mathbf{V}_b$, is

$$\delta \mathbf{I}_b = \mathbf{Y}_b \, \delta \mathbf{V}_b , \tag{4.17}$$

where subscript b distinguishes the branch vectors/matrix. The equations (4.15)-(4.17) are written in a generalized form

$$\delta \mathbf{h}_b = \boldsymbol{\Gamma}_b \, \delta \mathbf{x}_b + \overline{\boldsymbol{\Gamma}}_b \, \delta \mathbf{x}_b^* + \boldsymbol{\kappa}_b \, \delta \mathbf{u}_b , \tag{4.18}$$

where $\boldsymbol{\Gamma}_b$, $\overline{\boldsymbol{\Gamma}}_b$ and $\boldsymbol{\kappa}_b$ denote the formal partial derivatives of $\mathbf{h}_b$ with respect to $\mathbf{x}_b$, $\mathbf{x}_b^*$, and $\mathbf{u}_b$, respectively.

Substituting (4.18) together with its conjugate into (4.14), the equation (4.14) is rearranged as

$$\ldots + (\hat{\mathbf{h}}_b - \boldsymbol{\Gamma}_b^T \hat{\mathbf{x}}_b - \overline{\boldsymbol{\Gamma}}_b^{*T} \hat{\mathbf{x}}_b^*)^T \delta \mathbf{x}_b + (\hat{\mathbf{h}}_b^* - \overline{\boldsymbol{\Gamma}}_b^T \hat{\mathbf{x}}_b - \boldsymbol{\Gamma}_b^{*T} \hat{\mathbf{x}}_b^*)^T \delta \mathbf{x}_b^*$$

$$- (\boldsymbol{\kappa}_b^T \hat{\mathbf{x}}_b + \boldsymbol{\kappa}_b^{*T} \hat{\mathbf{x}}_b^*)^T \delta \mathbf{u}_b + \ldots = 0 . \tag{4.19}$$

The first-order change of a real or complex network function is expressed as (Bandler and El-Kady 1982b)

$$\delta f = \ldots + \left(\frac{\partial f}{\partial \mathbf{x}_b}\right)^T \delta \mathbf{x}_b + \left(\frac{\partial f}{\partial \mathbf{x}_b^*}\right)^T \delta \mathbf{x}_b^* + \left(\frac{\partial f}{\partial \mathbf{u}_b}\right)^T \delta \mathbf{u}_b + \ldots \; . \tag{4.20}$$

Subtracting (4.19) from (4.20), the resulting expression for a real function f is given by

$$\begin{aligned} \delta f \; = \; \ldots + \left(\frac{\partial f}{\partial \mathbf{u}_b} + 2\,\mathrm{Re}\{\boldsymbol{\kappa}_b^T \hat{\mathbf{x}}_b\}\right)^T \delta \mathbf{u}_b - (\hat{\bar{\mathbf{h}}}_b - \boldsymbol{\Gamma}_b^T \hat{\mathbf{x}}_b - \bar{\boldsymbol{\Gamma}}_b^{*T} \hat{\mathbf{x}}_b^*)^T \delta \mathbf{x}_b \\ - (\hat{\bar{\mathbf{h}}}_b^* - \bar{\boldsymbol{\Gamma}}_b^T \hat{\mathbf{x}}_b - \boldsymbol{\Gamma}_b^{*T} \hat{\mathbf{x}}_b^*)^T \delta \mathbf{x}_b^* + \ldots , \end{aligned} \tag{4.21}$$

where

$$\hat{\bar{\mathbf{h}}}_b \triangleq \hat{\mathbf{h}}_b - \frac{\partial f}{\partial \mathbf{x}_b} \; . \tag{4.22}$$

By setting the coefficient of $\delta \mathbf{x}_b$ (or $\delta \mathbf{x}_b^*$) in (4.21) equal to **0**, the adjoint hybrid vector $\hat{\bar{\mathbf{h}}}_b$ is obtained as

$$\hat{\bar{\mathbf{h}}}_b = \boldsymbol{\Gamma}_b^T \hat{\mathbf{x}}_b + \bar{\boldsymbol{\Gamma}}_b^{*T} \hat{\mathbf{x}}_b^* \; . \tag{4.23}$$

The generalized adjoint equation (4.23) is valid for electrical as well as electronic networks. In the electronic networks, $\bar{\boldsymbol{\Gamma}}_b$ turns out to be a null matrix owing to the absence of expressions involving complex conjugation (Choma, Jr. 1985; Chua and Lin 1975).

The electrical power networks, containing one or more phase-shifting transformers, have complex conjugate terms in their branch admittance matrix $\mathbf{Y}_b$. Choosing a state vector $\mathbf{x}_b \triangleq \mathbf{V}_b$, the corresponding dual vector $\mathbf{h}_b$ is $\mathbf{I}_b$. The partial derivatives of $\mathbf{h}_b$ with respect to $\mathbf{x}_b$ and $\mathbf{x}_b^*$ are obtained from (4.17) as

$$\boldsymbol{\Gamma}_b = \mathbf{Y}_b \quad \text{and} \quad \bar{\boldsymbol{\Gamma}}_b = \mathbf{0} \; , \tag{4.24}$$

respectively. Equation (4.24) is substituted into (4.23) to give the generalized multiport adjoint equation

$$\hat{\bar{\mathbf{I}}}_b \triangleq \hat{\mathbf{I}}_b - \frac{\partial f}{\partial \mathbf{V}_b} = \mathbf{Y}_b^T \, \hat{\mathbf{V}}_b . \tag{4.25}$$

4.3.3 Adjoint Modeling of Source Branches

Based on the load and generator bus perturbed equations (4.15) and (4.16), the corresponding state and control variables are

$$x_\ell = V_\ell , \qquad u_\ell = [\,P_\ell \quad Q_\ell\,]^T, \tag{4.26}$$

$$x_g = [V_g^* \quad I_g]^T \quad \text{and} \quad u_g = [\,P_g \quad |V_g|\,]^T . \tag{4.27}$$

Using (4.15), (4.23) and (4.26), the adjoint load bus is

$$\hat{\hat{I}}_\ell \triangleq \hat{I}_\ell - \frac{\partial f}{\partial V_\ell} = -\frac{S_\ell}{V_\ell^2}\hat{V}_\ell^* . \tag{4.28}$$

The gth adjoint generator bus equation is obtained from (4.16), (4.23) and (4.27) as

$$\begin{bmatrix} \hat{\hat{I}}_g^* \\ \hat{\hat{V}}_g \end{bmatrix} \triangleq \begin{bmatrix} \hat{I}_g - \dfrac{\partial f}{\partial V_g} \\ \hat{V}_g^* + \dfrac{\partial f}{\partial I_g} \end{bmatrix} = \begin{bmatrix} 2j\dfrac{Q_g}{|V_g|^2} & \dfrac{V_g}{V_g^*} \\ \dfrac{V_g^*}{V_g} & 0 \end{bmatrix} \begin{bmatrix} \hat{V}_g^* \\ \hat{I}_g \end{bmatrix} . \tag{4.29}$$

4.3.4 Adjoint Modeling of Transmission Branches

The transmission line equation $I_t = Y_t V_t$, pertaining to the t-th element (El-Kady 1980), does not involve any conjugate terms. The corresponding adjoint equation is

$$\hat{\hat{I}}_t \triangleq \hat{I}_t - \frac{\partial f}{\partial V_t} = Y_t \hat{V}_t . \tag{4.30}$$

Using the terminal behaviour of control transformers, discussed in Section 2.2.5, the original transformer equations are

$$\begin{bmatrix} I_p \\ I_q \end{bmatrix} = \frac{1}{Z_t} \begin{bmatrix} \dfrac{1}{a_t^*} \\ -1 \end{bmatrix} \begin{bmatrix} \dfrac{1}{a_t} & -1 \end{bmatrix} \begin{bmatrix} V_p \\ V_q \end{bmatrix}, \tag{4.31}$$

where subscripts p and q denote the terminal buses (Fig. 2.5). The adjoint transformer equations are obtained from (4.23) and (4.31) as

$$\begin{bmatrix} \hat{\hat{I}}_p \\ \hat{\hat{I}}_q \end{bmatrix} \triangleq \begin{bmatrix} \hat{I}_p - \dfrac{\partial f}{\partial V_p} \\ \hat{I}_q - \dfrac{\partial f}{\partial V_q} \end{bmatrix} = \frac{1}{Z_t} \begin{bmatrix} \dfrac{1}{a_t} \\ -1 \end{bmatrix} \begin{bmatrix} \dfrac{1}{a_t^*} & -1 \end{bmatrix} \begin{bmatrix} \hat{V}_p \\ \hat{V}_q \end{bmatrix}. \tag{4.32}$$

4.3.5 Generalized Sensitivity Formula and its Applications

The mathematical treatment presented in Section 4.3.2 has been intentionally confined to the real control variables. The choice of real variables avoids the subsequent transformations (El- Kady 1980, Grewal 1983).

Substituting (4.23) together with its conjugate in (4.21), the expression for δf leads to the generalized sensitivity formula given by

$$\frac{df}{d\mathbf{u}_b} = \frac{\partial f}{\partial \mathbf{u}_b} + 2\,\mathrm{Re}\,\{\boldsymbol{\kappa}_b^T \hat{\mathbf{x}}_b\}. \tag{4.33}$$

The validity of (4.33) has been verified using a package called TTM1 (Bandler, El-Kady and Wojciechowski 1983) for different types of control variables, listed in Table 4.4. The TTM1 package readily handles the power transmission networks containing reciprocal elements. However, the networks containing phase-shifting transformers have also been successfully investigated by employing the XLF3 package in conjunction with the TTM1 package. The conceptual details for the pertinent computer program are shown in Fig. 4.2. Different call statements to the subroutines of the two packages are indicated in Fig. 4.3.

TABLE 4.4

SENSITIVITY FORMULAS PERTAINING TO THE TELLEGEN THEOREM METHOD

Control Variable Description	Indices	Formula for $\mathrm{Re}\{\boldsymbol{\kappa}_b^T \hat{\mathbf{x}}_b\}$
Bus real power P_i	$i = \ell, g$	$\mathrm{Re}\{\hat{V}_i / V_i^*\}$
Bus reactive power Q_i	$i = \ell$	$\mathrm{Im}\{\hat{V}_i / V_i^*\}$
Bus voltage magnitude $\lvert V_i \rvert$	$i = g, n$	$-\mathrm{Re}\{\hat{V}_i I_i + \hat{I}_i V_i\} / \lvert V_i \rvert$
Bus voltage angle δ_i	$i = n$	$-\mathrm{Im}\{\hat{V}_i I_i - \hat{I}_i V_i\}$
Input shunt conductance G_{si}	$p = 1, r = si$	
Line conductance G_t	$p = t, r = t$	$-\mathrm{Re}\left\{V_p\left(\hat{V}_p + 2\frac{\partial f}{\partial V_r}\right)\right\}$
Output shunt conductance G_{so}	$p = o, r = so$	
Input shunt susceptance B_{si}	$p = i, r = si$	
Line susceptance B_t	$p = t, r = t$	$\mathrm{Im}\left\{V_p\left(\hat{V}_p + 2\frac{\partial f}{\partial V_r}\right)\right\}$
Output shunt susceptance B_{so}	$p = o, r = so$	
Transformer resistance R_t		$\mathrm{Re}\left\{I_t\left(\hat{I}_t - 2\frac{\partial f}{\partial I_t}\right)\right\}$
Transformer reactance X_t		$-\mathrm{Im}\left\{I_t\left(\hat{I}_t - 2\frac{\partial f}{\partial I_t}\right)\right\}$
Turns ratio magnitude $\lvert a_t \rvert$		$-\mathrm{Re}\{V_p \hat{I}_p + \hat{\bar{\bar{V}}}_p I_p\}$ **
Turns ratio phase angle ϕ_t		$\mathrm{Im}\{V_p \hat{I}_p - I_p \hat{\bar{\bar{V}}}_p\}$ **

** subscript p refers the primary side of the t-th transformer.

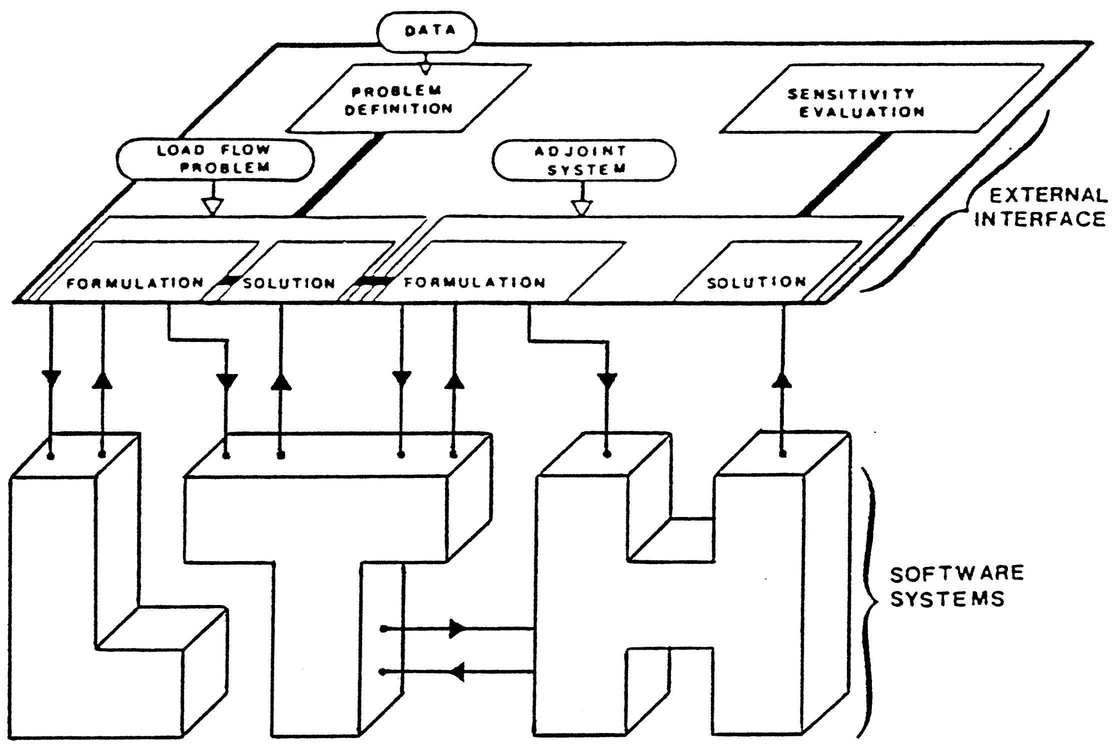

L - XLF3 package

T - TTM1 package

H - MA28 Harwell package

Fig. 4.2 Conceptual structure for the sensitivity evaluation of nonreciprocal power networks.

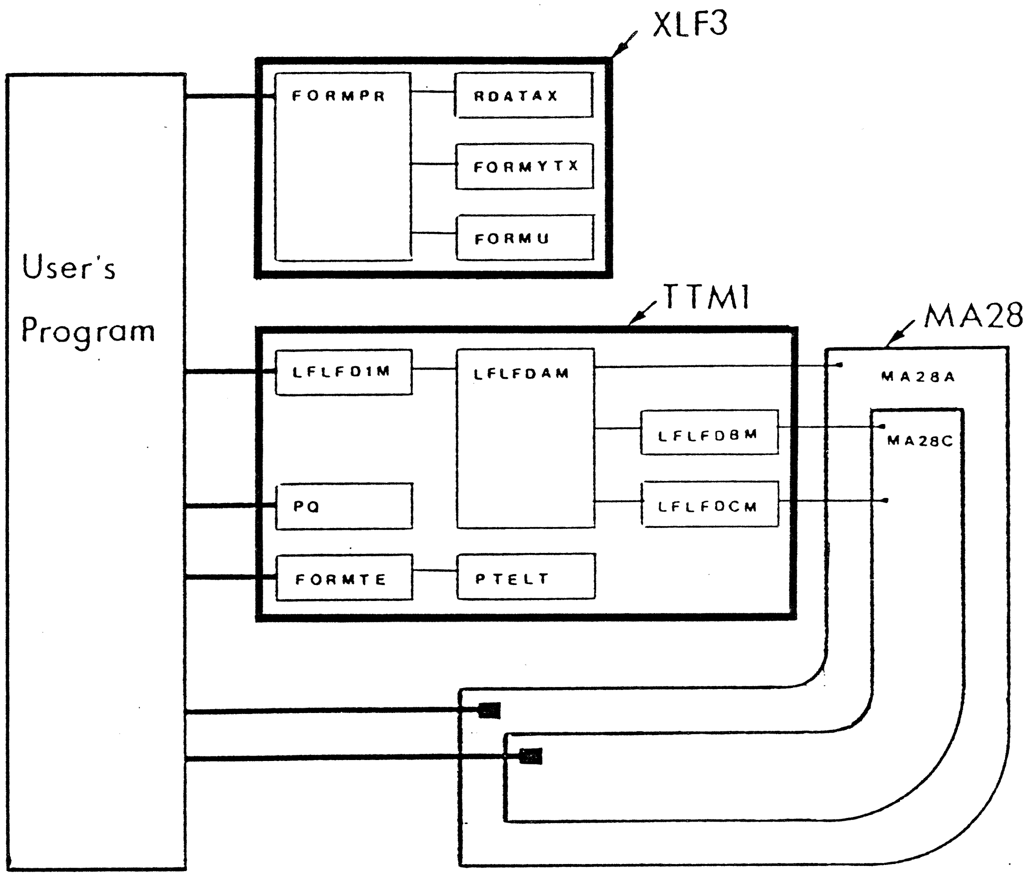

Fig. 4.3 An innovative combination of XLF3 and TTM1 packages.

4.4 Conclusion

In this chapter, a unified study for the class of adjoint power networks has been provided in the context of sensitivity evaluation. Generalized sensitivity formulas have been systematically derived and tabulated. The implementation of these formulas has been discussed with the help of illustrations from the existing software systems. The control variables associated with the source branches as well as a.c. transmission branches have been considered.

The analysis has been done in a manner deemed suitable for deriving the generalized adjoint formulation and the sensitivity expression. These results have been extended to achieve, verify, and establish the formulas for different types of power network elements. An innovative combination of some computer packages is also illustrated.

CHAPTER 5

SPECIAL PURPOSE TWO-PORT TRANSMISSION BRANCHES

5.1 Introduction

In order to provide satisfactory service to the customers, substantial effort is required to maintain the operation of an electrical power system within rather stringent constraints. Large investments and continuing advancements in the methods of dealing with the power flow control options have become mandatory as the load steadily increases from year to year (DyLiacco 1978; Elgerd 1982; Wildi 1981). Some of the requirements of a well-established power system are recognized by most customers. A constant voltage level at the customer's service entrance is of prime concern. This demand is furnished by installing regulating transformers in series with the transmission lines of interest (Flatabo et al. 1985; Fletcher and Stadlin 1983; Singh 1983).

In practice, every power transformer is equipped with taps for the turns ratio control. This type of control is incorporated at subtransmission- as well as distribution-levels (Dhar 1982; Weedy 1979). The transformers, exclusively used on the transmission levels are often characterized by quite limited megavoltampere ratings (Elgerd 1982; Han 1982). The primary function of these transformers is to monitor the voltage excursions in a particular system.

The expansion planning actively concentrates on the future new transmission lines. Recently, prime consideration is being given to the re-emergence of high-voltage d.c. (HVDC) transmission systems (Wildi 1979; Zorpette 1985). The HVDC transmission systems are capable of wheeling more power from electricity-rich areas over longer distances than a.c. lines of equivalent cost (Ellert and Hingorani 1976; Kimbark 1971). Certain advantages of the HVDC transmission have prompted the system planners to choose HVDC for lines not justified by the break-even distance. Of foremost importance is the linking of neighbouring asynchronous networks more economically and reliably.

In this chapter, the mathematical models pertaining to converters and control transformers are considered. The rectifier and inverter terminal equations being quite similar, only the rectifier model is investigated. An adjoint rectifier model is developed using the generalized adjoint equations derived in Chapter 4. Additionally, exact sensitivity relations pertaining to rectifier delay angle and commutation reactance are obtained.

Furthermore, a cascaded transformer model is discussed. The need of a variable impedance transformer model is emphasized, however, the analysis is confined to the conventional fixed impedance transformer model. The ideal transformer, and equivalent admittance of the cascaded model, are considered as separate branches. The hybrid complex notation is utilized to develop a topologically similar adjoint transformer model. Finally, the theoretical results are verified with the help of simple test cases.

5.2 Two-terminal AC-DC Converters

The operation of a modern HVDC transmission involves rectification at one end, and inversion at the other end (Kimbark 1971; Uhlmann 1975). A single circuit link is shown in Fig 5.1, indicating two conductors (Zorpette 1985). Both end converters are composed of tap-changing transformers, and groups of valves, called silicon-controlled rectifiers (SCR).

The terminal behaviour of the rectifier model, considered in Chapter 2, is rewritten in the form

$$\bar{V}_q = |V_p| \cos\alpha + \bar{I}_q\left(\frac{\pi}{6} X_c\right) \tag{5.1}$$

$$\bar{I}_q = -|I_p|, \tag{5.2}$$

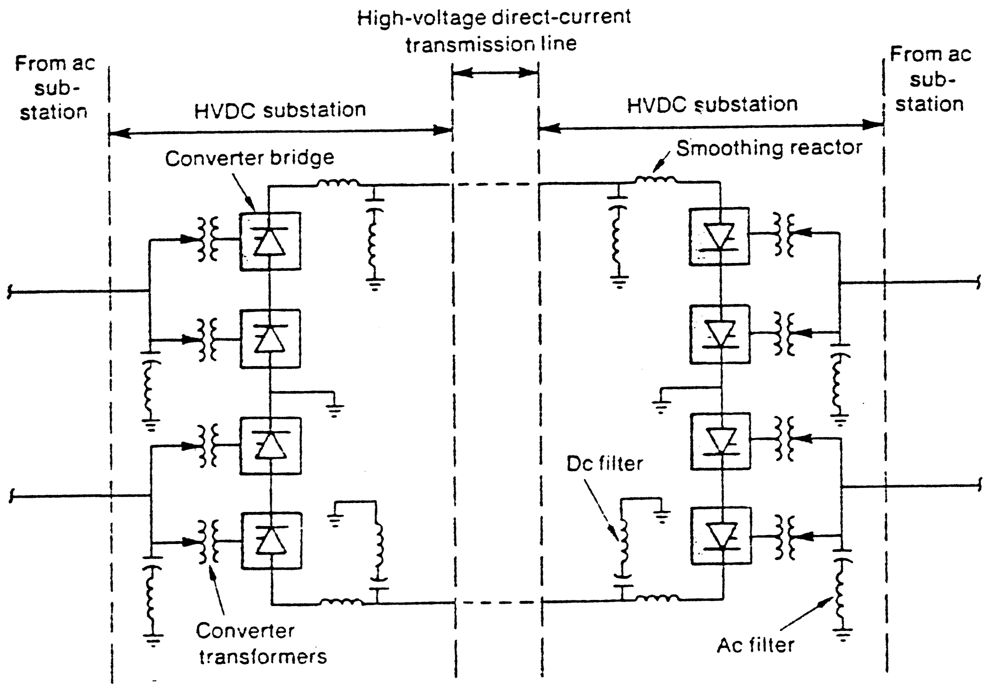

Fig. 5.1 Basic constituents of an HVDC link. (Zorpette 1985, p. 34)

where the a.c.-d.c. per-unit system (Appendix A) has been used. Alternatively, the rectifier equations are expressed as

$$\mathbf{h}_b = \begin{bmatrix} -\overline{V}_q \\ |I_p| \end{bmatrix} = -\begin{bmatrix} \frac{\pi}{6} X_c & \cos\alpha \\ 1 & 0 \end{bmatrix} \begin{bmatrix} \bar{I}_q \\ |V_p| \end{bmatrix}, \tag{5.3}$$

where the rectifier state vector is defined as $\mathbf{x}_b \triangleq [\bar{I}_q \; |V_p|]^T$. This gives the partial derivative $\boldsymbol{\Gamma}_b$ as

$$\boldsymbol{\Gamma}_b = -\begin{bmatrix} \frac{\pi}{6} X_c & \cos\alpha \\ 1 & 0 \end{bmatrix}, \tag{5.4}$$

and $\overline{\boldsymbol{\Gamma}}_b = \mathbf{0}$. Using (4.23) and (5.3), the adjoint rectifier equations are

$$\begin{bmatrix} -\hat{\bar{V}}_q \\ |\hat{\bar{I}}_p| \end{bmatrix} = -\begin{bmatrix} \frac{\pi}{6} X_c & 1 \\ \cos\alpha & 0 \end{bmatrix} \begin{bmatrix} \hat{I}_q \\ |\hat{V}_p| \end{bmatrix}. \quad (5.5)$$

Furthermore, the partial derivative $\mathbf{\kappa}_b$, associated with the rectifier control vector $\mathbf{u}_b = [\alpha \;\; X_c]^T$ is given by

$$\mathbf{\kappa}_b = -\begin{bmatrix} |V_p| \sin\alpha & \frac{\pi}{6} \bar{I}_q \\ 0 & 0 \end{bmatrix}. \quad (5.6)$$

Substituting (5.6) into (4.33), the sensitivity formulas for the specified control variables are obtained as

$$\frac{df}{d\mathbf{u}_b} = \frac{\partial f}{\partial \mathbf{u}_b} - 2 \begin{bmatrix} |V_p| \sin\alpha & 0 \\ \frac{\pi}{6} \bar{I}_q & 0 \end{bmatrix} \begin{bmatrix} \hat{I}_q \\ |\hat{V}_p| \end{bmatrix}. \quad (5.7)$$

The vector/matrix equation (5.7) has been verified in Section 5.5.1 for two different network functions.

5.3 Tap-changing-under-load Transformers

The off-load tap-changing and tap-changing-under-load transformers are shown in Figs. 5.2a and 5.2b, respectively. In the first case, a disconnection of the transformer is required when tap setting is to be changed. The transfer switches S_1 and S_2 are utilized in the case of on-load changers.

In power flow studies, the transformer models are assumed to exhibit constant leakage reactance with regard to their tap positions (Elgerd 1982; Stagg and El-Abiad 1968; Weedy 1979). However, variable impedance transformer models are being considered in the recent literature (Flatabo et al. 1985). These models are capable of providing more accurate voltage profile of a given system. Table 5.1 indicates the tap positions of a 380 kV/220 kV transformer, and the corresponding turns ratio, resistance and reactance are also mentioned. Such nonlinearities are detectable from the transformer name-plate data.

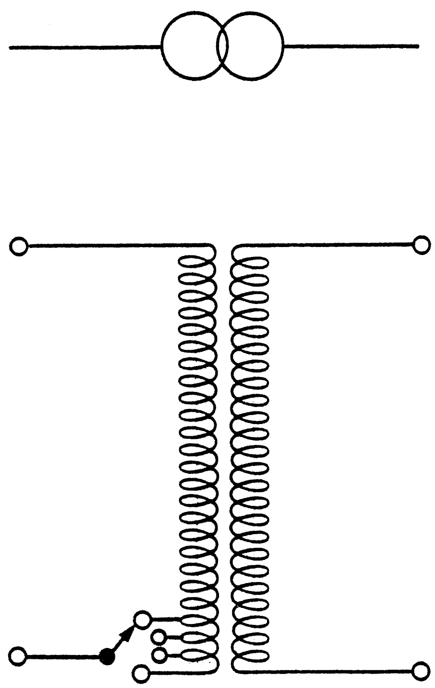

Fig. 5.2a Off-load tap-changing transformer

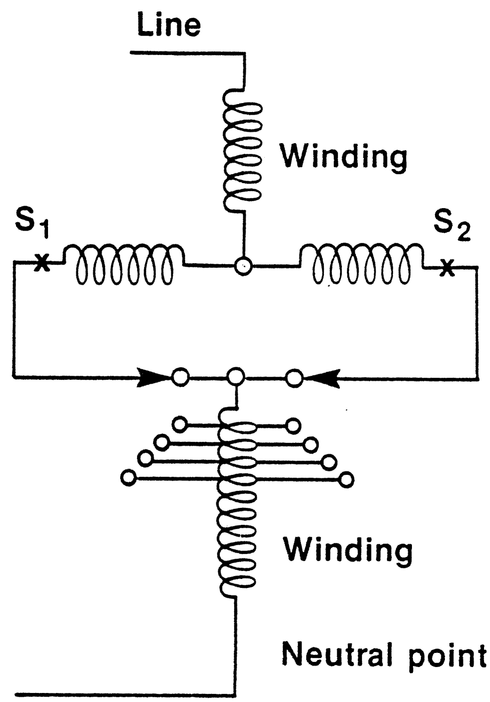

Fig. 5.2b Tap-changing-under-load transformer

TABLE 5.1

VARIABLE IMPEDANCE TRANSFORMER MODEL DATA

Tap position	Turns ratio	Resistance	Reactance
1	1.0517	0.0007	0.0327
6	1.0294	0.0006	0.0320
11	1.0052	0.0006	0.0314
16	0.9794	0.0005	0.0309
21	0.9794	0.0005	0.0304

5.4 Phase-shifting Transformers

This type of transformers is used in power systems to control the power flow, and to maintain a certain voltage profile in the system (Elgerd 1982; Han 1982; Wildi 1981). These transformers contain two main units to perform the two basic functions. The first unit is for phase shifting, which controls the routing of the real power in parallel path networks. The second unit is for voltage as well as reactive power flow control. The phase shifting is accomplished by generating a quadrature component of voltage to be added to the original voltage (Grewal 1983; Gross 1979). Using an on-load tap changer, the quadrature component is adjusted for a specific phase shift. Another set of tap changers is used for the second unit to adjust a voltage component generated in phase with the original voltage. Both generated voltage components are then added to the original voltage via a series transformer.

It has been common practice to represent the regulating (or control) transformers by a fixed impedance regardless of their respective tap positions. However, with the sophistication and increased accuracies of the power flow analysis, it has been recognized that the transformers should be modelled more accurately (Kilmer et al. 1983; Mukherjee and Fuerst 1984).

Consider a phase-shifting transformer model (Bandler, El-Kady and Grewal 1985b) depicted in Fig. 2.3. Let the transformer turns ratio a_t have its magnitude $|a_t|$ and phase-angle ϕ_t. The primary side quantities of the ideal transformer are $V_p = a_t V_s$ and $I_p = -I_s/a_t^*$, where V_s and I_s are the secondary voltage and current, respectively. Using a hybrid conjugate description, it is straightforward to express the transformer current-voltage relations in the matrix form

$$\begin{bmatrix} -V_p \\ I_s^* \end{bmatrix} = -a_t \begin{bmatrix} 0 & 1 \\ 1 & 0 \end{bmatrix} \begin{bmatrix} I_p \\ V_s^* \end{bmatrix}^* . \tag{5.8}$$

By selecting the transformer state vector $\mathbf{x}_t = [I_p \; V_s^*]^T$, we can recognize (5.8) as

$$\mathbf{h}_t = -a_t \begin{bmatrix} 0 & 1 \\ 1 & 0 \end{bmatrix} \mathbf{x}_t^*, \tag{5.9}$$

where $\mathbf{h}_t = [-V_p \; I_s^*]^T$. The transformer hybrid conjugate vector $\mathbf{h}_t$ of (5.9) is linearly dependent on $\mathbf{x}_t^*$ and is independent of $\mathbf{x}_t$.

The adjoint transformer equation corresponding to (5.9) is obtained from (4.23) as

$$\hat{\mathbf{h}}_t = -a_t^* \begin{bmatrix} 0 & 1 \\ 1 & 0 \end{bmatrix} \hat{\mathbf{x}}_t^*. \tag{5.10}$$

The comparison of (5.9) and (5.10) indicates that the adjoint transformer turns ratio is simply a_t^*. In other words, the adjoint turns ratio magnitude is same as that of the original, however, the phase-angle $\hat{\phi}_t$ is $-\phi_t$. The transformer control vector $\mathbf{u}_t$, constituting $|a_t|$ together with ϕ_t, has the 2x2 $\boldsymbol{\kappa}_t$ as

$$\boldsymbol{\kappa}_t = -\begin{bmatrix} V_p/|a_t| & j\,V_p \\ a_t I_p^*/|a_t| & j\,a_t I_p^* \end{bmatrix}. \tag{5.11}$$

Substituting (5.11) into (4.33), we get

$$\frac{df}{d\mathbf{u}_t} = \frac{\partial f}{\partial \mathbf{u}_t} - 2\,\mathrm{Re}\left\{ \begin{matrix} (V_p \hat{I}_p + a_t \hat{V}_s^* I_p^*)/|a_t| \\ j\,(V_p \hat{I}_p + a_t \hat{V}_s^* I_p^*) \end{matrix} \right\}. \tag{5.12}$$

Alternatively, we observe $\hat{\hat{V}}_p^* \triangleq \hat{V}_p^* + \partial f/\partial I_p^* = a_t \hat{V}_s^*$ involved in (5.10); to express (5.12) as

$$\frac{df}{d|a_t|} = \frac{\partial f}{\partial |a_t|} - \frac{2}{|a_t|}\,\mathrm{Re}\left\{ V_p \hat{I}_p + \hat{\hat{V}}_p^* I_p^* \right\} \tag{5.13}$$

and

$$\frac{df}{d\phi_t} = \frac{\partial f}{\partial \phi_t} + 2\,\mathrm{Im}\left\{ V_p \hat{I}_p + \hat{\hat{V}}_p^* I_p^* \right\}. \tag{5.14}$$

The sensitivity formulas (5.13) and (5.14) involve the transformer primary quantities associated with the original as well as adjoint models. Another way of deriving these formulas deals with the y-matrix description of the conventional transformer model (Bandler, El-Kady and Grewal 1985a; Grewal 1983). The transformer series impedance branch is also investigated with the help of the generalized equations (4.23) and (4.33).

5.5 Numerical Examples

First, a simple a.c.-d.c. power system is considered. Two different network functions of this system are investigated, and their corresponding adjoint networks are derived in an elegant manner. The phase-shifting transformer sensitivities are also verified by considering a large transformer phase angle of a 2-bus system.

5.5.1 Example 5.1

Consider a simple system shown in Fig. 5.3. Let the slack bus voltage V_2 be equal to 1.21 + j0. For a d.c. load $P_1 = 0.22$ p.u., we assume the rectifier firing angle as 7°. The d.c. voltage is

$$V_d = V_2 \cos a = 1.2009808 \ .$$

The converter terminal equations become

$$V_1 I_d = 0.22 \ ,$$

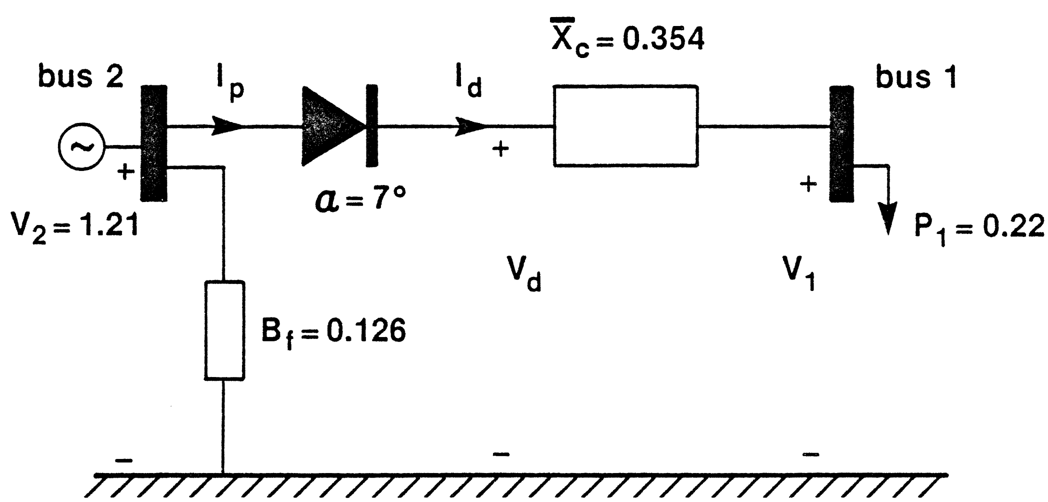

Fig. 5.3 A two-bus a.c.-d.c. power system.

and

$$V_d - V_1 = 0.354\, I_d .$$

After simple manipulations, these converter equations yield the unknown voltage V_1 and current I_d as

$$V_1 = 1.1322114 , \qquad I_d = -0.019431 .$$

Consider a network function $f_1 = -I_1$. Using the theoretical results developed in the previous chapter, the adjoint system associated with Fig. 5.3 and the function of interest, is obtained as shown in Fig. 5.4.

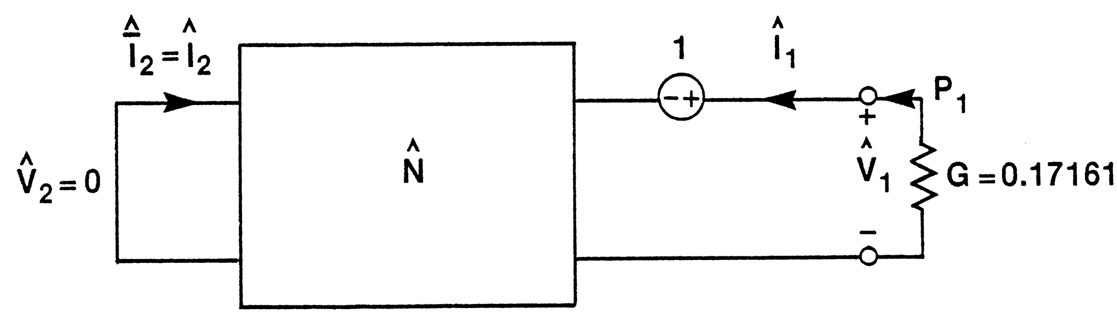

Fig. 5.4 An adjoint power system for $f_1 = -I_1$.

The adjoint solution gives $\hat{V}_1$ equal to 0.94277. Using (4.33), the sensitivities of $f_1 = -I_1$ with respect to $u_1 = \cos\alpha$ and $u_2 = \overline{X}_c$ are

$$\frac{df}{d\zeta} = \begin{bmatrix} -0.195738 \\ -0.003143 \end{bmatrix} ,$$

where $\zeta \triangleq [\cos\alpha \quad \overline{X}_c]^T$. These numerical values have been verified by small perturbations at the nominal point.

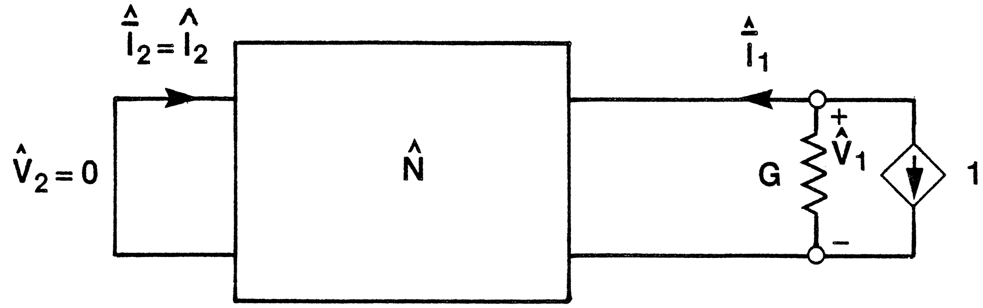

Fig. 5.5 An adjoint network associated with function $f_2 = V_1$.

Consider another network function, that is, $f_2 = V_1$. The corresponding adjoint network is as shown in Fig 5.5. The adjoint solution yields

$$\hat{V}_1 = 5.826857$$

$$\hat{I}_1 = 0.942721 .$$

Again, using (4.33), the sensitivities of $f_2 = V_1$ w.r.t. $\zeta = [\cos\alpha \quad \overline{X}_c]^T$ are

$$\frac{df}{d\zeta} = -[1.1406989 \quad -0.0183179]^T .$$

5.5.2 Example 5.2

A two-bus sample power system is shown in Fig. 5.6 (Bandler, El-Kady and Grewal 1985a). It contains a phase-shifting transformer in series with the line connecting the slack and load buses. A large transformer phase angle is deliberately chosen to verify the validity and accuracy of the sensitivity formulas associated with the complex turns ratio variables.

The nodal admittance matrix of the system is given by

$$Y_T = \begin{bmatrix} 6 - j18 & 7.2 + j19.6 \\ -16.8 + j12.4 & 6 - j17 \end{bmatrix} .$$

The load flow equation for the specified load bus complex power S_1, and the slack bus voltage V_2 is

$$(6 - j18)\, V_1 V_1^* + (7.2 + j19.6)\ V_1^* = -5 + j3 .$$

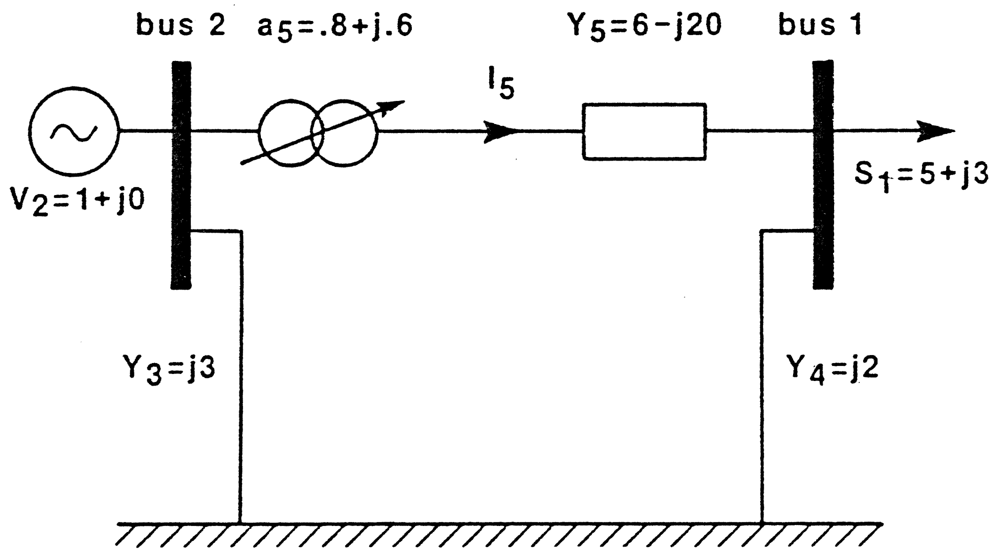

Fig.5.6 A slack-load bus power system (Bandler, El-Kady and Grewal 1985a, p. 1859)

Commencing with the flat voltage profile; i.e., $V_1 = 1.0+j0.0$, the solution is obtained in five exact Newton iterations for an accuracy of 1.E-06. The load bus voltage at the solution is

$$V_1 = 0.46573 - j\,0.60442\,.$$

The current I_5 flowing through the line admittance Y_5 is calculated as

$$I_5 = (V_2/a_5 - V_1)Y_5 = 2.09402 - j6.65888\ .$$

Consider a function $f = |V_1| = (V_1\, V_1^*)^{1/2}$, and observe that $\hat{\hat{V}}_1 = \hat{V}_1$ together with $\hat{\hat{V}}_2 = \hat{V}_2$, as the function is explicitly independent of the corresponding branch currents. The adjoint system of linear equations for the function is cast into the rectangular form

$$\begin{bmatrix} 13.17154 & 11.00949 \\ -24.99051 & -1.17154 \end{bmatrix} \begin{bmatrix} \hat{v}_{11} \\ \hat{v}_{12} \end{bmatrix} = - \begin{bmatrix} 0.30518 \\ 0.39608 \end{bmatrix},$$

where $\hat{V}_{11}$ and $\hat{V}_{12}$ are the real and imaginary parts of $\hat{V}_1$, respectively. The adjoint solution yields

$$\hat{V}_1 = 0.01817 - j\,0.04945\,.$$

Moreover, $\hat{V}_2 = 0$ for the function considered which leads to a simple expression for $\hat{I}_5$, that is

$$\hat{I}_5 = -\hat{V}_1\,Y_5 = 0.88 + j\,0.66\,,$$

and the adjoint transformer primary current $\hat{I}_2$ is given by

$$\hat{I}_2 = \hat{I}_5/a_5 = 1.1 + j0\,.$$

The sensitivities of $|V_1|$ w.r.t. various control parameters of the transformer model are obtained using $-\hat{I}_5\,I_5$ for the transformer impedance, and (5.13-5.14) for the complex turns ratio.

The sensitivity results are summarized as:

$$\frac{df}{d\zeta} = -[12.47520 \quad 8.94552 \quad 2.2 \quad 0]^T\,,$$

where $\zeta \triangleq [R_5 \quad X_5 \quad |a_5| \quad \phi_5]^T$.

5.6 Discussion

This chapter has primarily dealt with the two-port nonreciprocal power transmission element models with regard to their practical applications in controlling the flow in a given network. An a.c.-d.c. converter model, containing a voltage-controlled voltage source (VCVS), has been considered. Its definable branch relationships have been subscribed to the conventional matrix format with the help of hybrid parameter description. In addition, a phase-shifting transformer model has been investigated by considering the ideal transformer as a separate branch.

It is apparent from the contents of this chapter that the hybrid method of analysis is an extremely systematic procedure for writing the power network equations, commensurate with finding the pertinent unknown states. The procedure is straightforward and unambiguous, since it effectively reduces the network problem to the problem of expressing simple branch relationships for separate branches.

Furthermore, the sensitivity formulas are valid for different types of the control variables ranging from the load bus real power to converter delay angle. Most importantly, the methodical application of the hybrid method leads to a compact formulation and satisfying understanding of the two-port nonreciprocal adjoint modeling. This understanding is, certainly, essential in streamlining the invocation of realistic power network analysis involving procedural short-cuts that diminish or eliminate the computational tedium. Moreover, the method is capable of handling the cases where it is not possible (or convenient) to coalesce the controlled-source branches with the passive element branches.

The hybrid method is readily amenable to computer programming. The concept of the generalized adjoint modeling is finding applications in supplementing the traditional analytical methods. In particular, the adjoint transformer model developed by the hybrid method is in precise agreement with that evolved from the transformer y-matrix description. The topological similarities of the adjoint modeling can be further exploited to encompass the variable impedance transformer models.

CHAPTER 6

APPLICATIONS TO TEST POWER SYSTEMS

6.1 Introduction

Based on the decision time involved, the predominant power system problems are accordingly classified as illustrated in Fig. 6.1 (Talukdar and Wu 1981; Wollenberg 1976). The figure indicates one possible range of the decision time, where the number of years is commonly assigned to the planning programs. The degree of detail of such programs is primarily concerned with whether a complete a.c. solution be necessary or not, and it is often

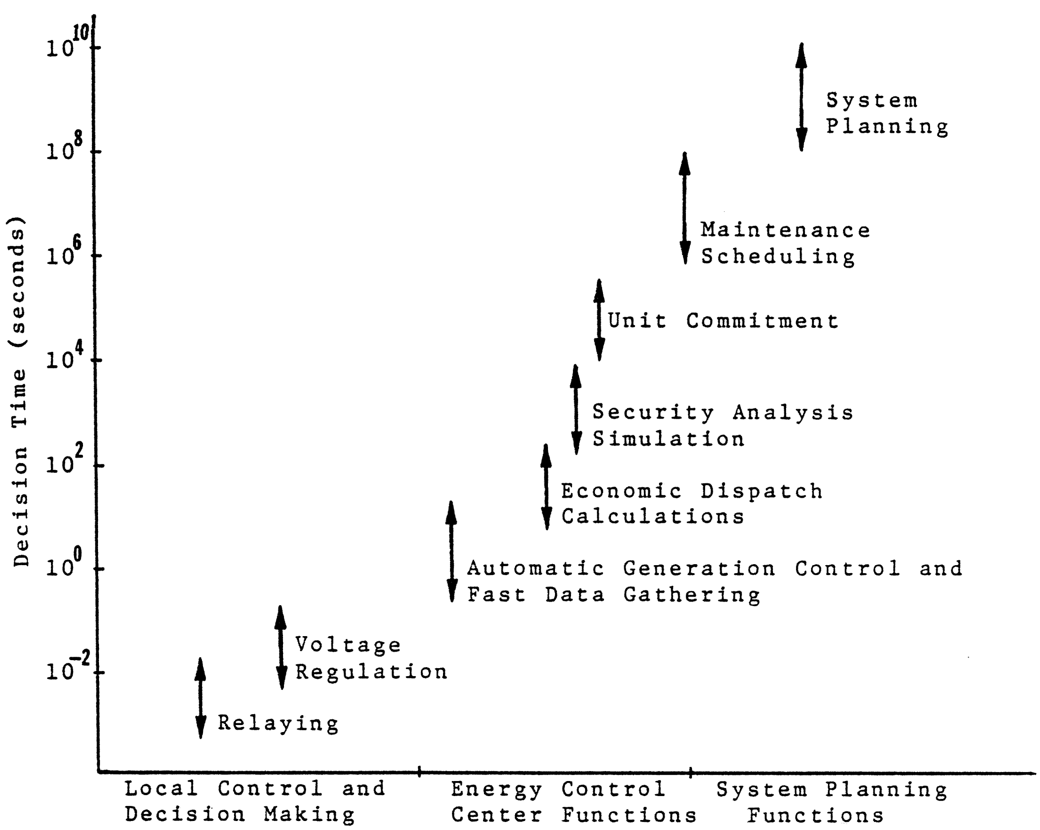

Fig. 6.1 Decision time involved in power system problems.

a determining factor in the selection of the type of model used for the load flow analysis as well as sensitivity evaluation (El-Kady 1980). For systems requiring voltage information, very fast a.c. solution methods are available (Arrillaga et al. 1983; Stott 1974; Wildi 1981). The d.c. load flow models can be solved much more rapidly, although they are capable of providing only a rough estimate of the actual real power loadings on the lines of a particular system (Dhar 1982; Stagg and El-Abiad 1968; Elgerd 1982).

As most of the power systems are sparsely interconnected, the nodal equations, and consequently, the associated Jacobian are exploited by using efficient sparsity techniques (Duff 1977, 1981). The sparse matrix algorithms have been devised in such a way that only nonzeros are processed. The irrelevant operations involving addition with, or multiplication by zero, are avoided by taking advantage of the previous knowledge of the positions of the nonzeros.

This chapter deals with some interesting test cases, which have been extensively used by researchers to investigate the performance of different algorithms (Alsac and Stott 1974; Sachdev and Ibrahim 1974; Burchett et al. 1982). Firstly, the 6-bus sample power system is discussed. The adjoint network formulation of this system is systematically described. A load bus voltage magnitude is investigated using the Tellegen's theorem method of sensitivity evaluation. The sensitivities of the function of interest with respect to several system control variables are reported in a tabular form.

Secondly, the IEEE 30-bus power system (Alsac and Stott 1974) is considered. An optimally structured one-line diagram of this system is included. A generator bus voltage angle is taken as the function of interest, and various sensitivities associated with this function are presented elegantly. Furthermore, the applications of the sensitivity evaluation in the domain of contingency assessment as well as transmission planning are highlighted.

Finally, the IEEE 118-bus system (Grewal 1983) is discussed. The sensitivities of the slack bus real power are calculated efficiently. For the sake of brevity, only significant and useful sensitivity results are mentioned. Additionally, the optimization results of the minimum-loss problem are included.

6.2 A 6-bus Sample System

This system has three load buses ($n_L = 3$), two generator buses ($n_G = 2$), and a slack bus ($n = 6$). The buses are interconnected with the help of eight transmission branches, shown in Fig. 3.1 (Bandler, El-Kady and Grewal 1985b). The transmission branch, connecting buses 1 and 4, contains a phase-shifting transformer. The transmission network data of the system is provided in Table 3.1. The transformer turns ratio phase angle ϕ_7 is deliberately chosen large in order to verify the validity of the adjoint formulation as well as the accuracy of the pertinent sensitivity formulas.

6.2.1 Formulation of the Nodal Admittance Matrix

The nodal admittance matrix of the 6-bus system, systematically provided in Tables 3.2a and 3.2b, is a 6 by 6 unsymmetric matrix. The number of nonzero elements of this matrix is equal to 22. The numerical values of Y_{14} and Y_{41} are unequal, owing to the presence of the phase-shifting transformer buses 1 and 4. The power flow solution of this system is provided in Table 6.1.

6.2.2 The Adjoint Network Formulation and Sensitivity Evaluation

The adjoint network of the 6-bus system is obtained by considering equation (3.29) of Chapter 3. As the network is nonreciprocal, proper care is observed to transpose the

TABLE 6.1

POWER FLOW SOLUTION OF THE 6-BUS SYSTEM

Bus Index i	Rectangular Coordinates V_{i1}	V_{i2}	Polar Coordinates $\|V_i\|$	δ_i
1	0.88812	−0.40719	0.97702	−0.42989
2	0.91190	−0.27668	0.95295	−0.29459
3	0.82475	−0.29829	0.87703	−0.034704
4	0.69671	−0.74498	1.02000	−0.81887
5	0.98821	−0.32411	1.04000	−0.31693
6	1.04000	0.	1.04000	0.

various matrices (Bandler, El-Kady and Grewal 1985b). The adjoint coefficient matrix of the system is provided in Table 6.2. Furthermore, the sparsity structure of the rearranged adjoint matrix is displayed in Fig. 6.2.

Consider a network function $f = |V_1|$. The adjoint right-hand side vector associated with this function is

$$\hat{I} = [\,-0.454505 \quad 0 \quad 0 \quad 0 \quad 0 \quad -0.208386 \quad 0 \quad 0 \quad 0 \quad 0\,]^T.$$

Upon solving the linear adjoint system for the function of interest, the adjoint solution yields

$$\hat{V} = \begin{bmatrix} 0.000878 - j0.037527 \\ 0.000234 + j0.013591 \\ 0.000567 + j0.025813 \\ 0.001652 + j0.001767 \\ 0.001010 + j0.003946 \\ 0 \end{bmatrix}.$$

TABLE 6.2

ADJOINT COEFFICIENT MATRIX FOR THE 6-BUS SYSTEM

1.8888	0	0	1.8818	−2.3529	12.2098	0	0	−4.4708	−9.4118
0	3.2932	−0.5882	−0.5882	−1.1764	0	20.4864	−2.3529	−2.3529	−4.7059
0	−0.5882	1.2828	−0.3922	0	0	−2.3529	8.4662	−1.5686	0
4.9362	2.0778	1.3852	−6.9228	0	−0.3441	1.3428	0.8954	−3.7512	0
10.0588	5.0322	0	0	−13.9231	0.7253	0.3626	0	0	−1.9718
−16.0118	0	0	4.4708	9.4118	5.1697	0	0	1.8818	−2.3529
0	−23.4286	2.3529	2.3529	4.7059	0	7.6866	−0.5882	−0.5882	−1.1764
0	2.3529	−11.9288	1.5686	0	0	−0.5882	3.8149	−0.3922	0
0	0	0	−0.7450	0	0	0	0	0.6967	0
0	0	0	0	−0.3241	0	0	0	0	0.9882

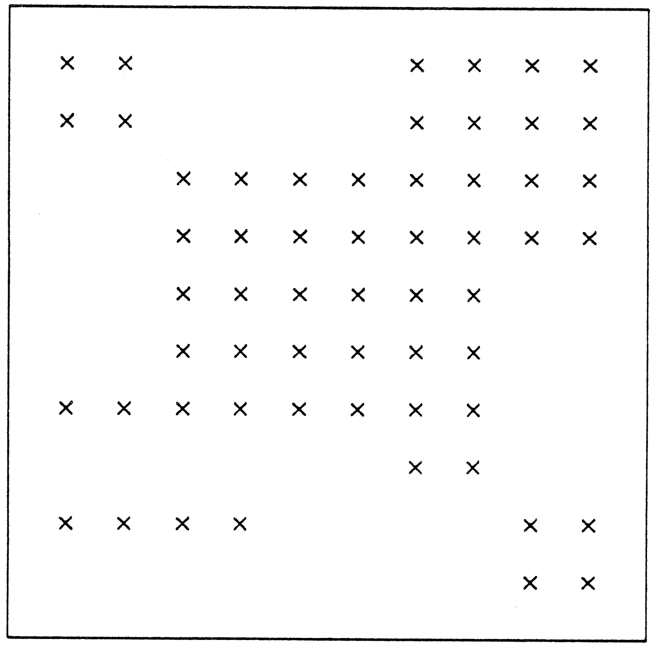

Fig. 6.2 Structural details of the 6-bus adjoint coefficient matrix.

The sensitivity formulas of Table 4.5 are used to give the results as summarized in Table 6.3. These values accurately agree with those obtained by using the complex Lagrangian method (Grewal 1983).

TABLE 6.3

SENSITIVITIES OF $|V_1|$ OF THE 6-BUS SYSTEM

-- Load Bus Quantities

Bus	Real Power	Reactive Power	Shunt Conductance	Shunt Susceptance
1	.030383	.070579	−.029003	.067373
2	.000012	−.000317	−.000011	−.000288
3	−.000889	−.000647	.000684	−.000497

-- Generator Bus Quantities

Bus	Real Power	Voltage Magnitude	Shunt Conductance	Shunt Susceptance
4	−.004743	.370314	.004935	0.000000
5	.002579	.713495	−.002790	0.000000

-- Line Quantities

Line Index	Element	Line Conductance	Line Susceptance
2	1,5	−.006597	−.007071
3	2,3	−.000045	.000059
4	2,4	.000789	.002293
5	2,5	−.000240	−.000031
6	2,6	.000092	.000009

-- Phase-shifting Transformer Quantities

Element	Turns Ratio Magnitude	Turns Ratio Phase Angle	Internal Resistance	Internal Reactance
1,4	.332271	−.011565	−.459281	−.008697

6.3 The IEEE 30-bus Power System

6.3.1 System Configuration

The transmission network details of the IEEE 30-bus system is shown in Fig. 6.3. The system contains two three-winding transformers, three two-winding transformers together with thirty six transmission lines. The total number of source branches is

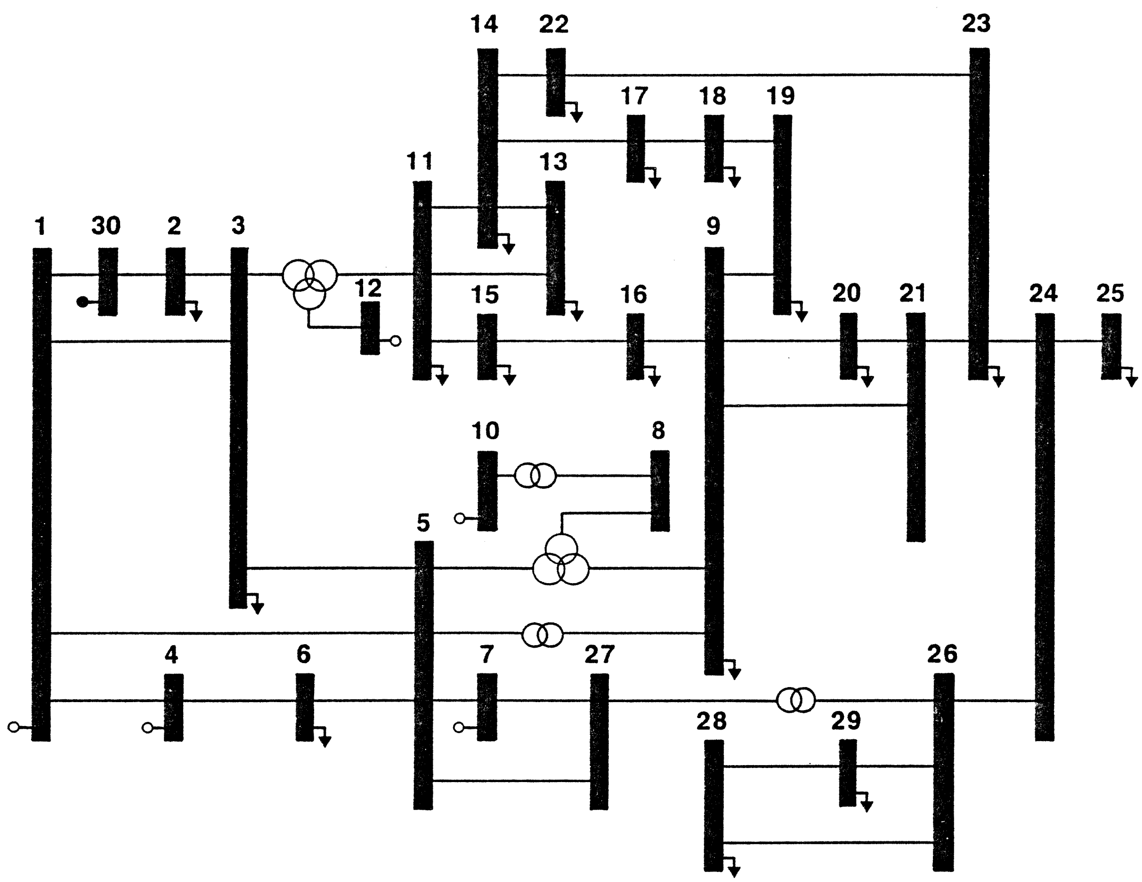

Fig. 6.3 One-line diagram of the IEEE 30-bus power system.

$n = n_L + n_G + 1 = 30$, where $n_L = 23$ and $n_G = 6$. The buses characterized by zero demand are considered as the load buses having $P_\ell = Q_\ell = 0$. These buses, called dummy buses, are installed to provide an intermediate point between important buses (Wildi 1981). The system data is provided in the Appendix B.1.

6.3.2. The Nodal Admittance Matrix and its Sparsity

The nodal admittance matrix structure of the IEEE 30-bus system is depicted in Fig. 6.4. The matrix has nonzero elements $NZ = 30 + 2*41 = 112$. The storage scheme of these nonzero elements is efficiently done as illustrated in Table 6.4.

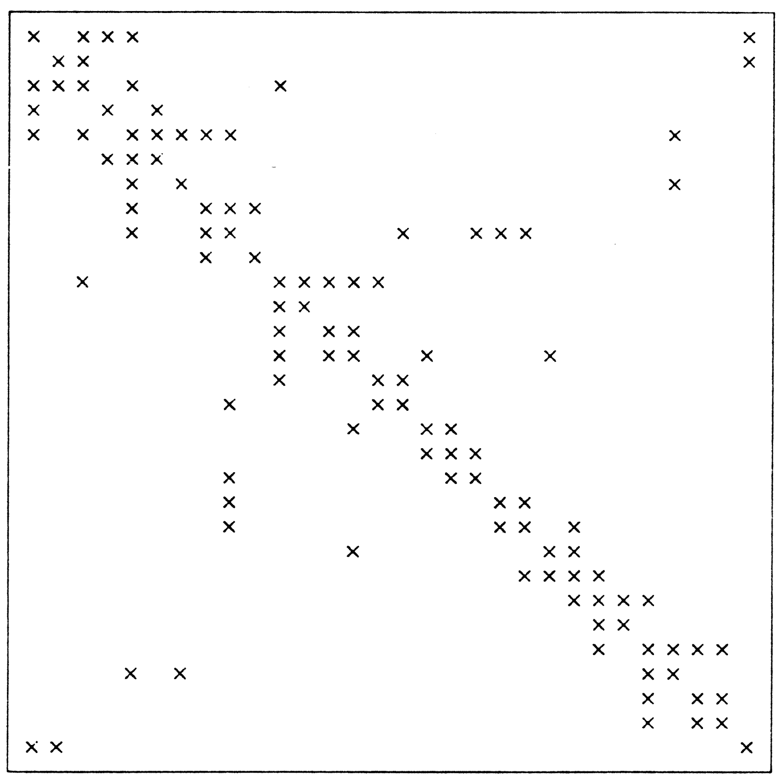

Fig. 6.4 Structure of the IEEE 30-bus nodal admittance matrix.

TABLE 6.4

STORAGE OF THE IEEE 30-BUS NODAL ADMITTANCE MATRIX

I	JRYT(I)	ICYT(I)	Real (YT)	Imaginary (YT)
1	1	1	9.752282	-30.690863
2	6	30	-5.224646	15.646727
3	9	3	-1.705530	5.197379
4	14	4	-1.135961	4.772479
5	17	5	-1.686145	5.116477
6	25	2	9.439186	-28.614594
7	28	30	-1.243737	5.096021
8	31	3	-8.195449	23.530873
9	35	3	16.314103	-54.932155
10	42	1	-1.705530	5.197379
11	44	2	-8.195449	23.530873
12	50	5	-6.413124	22.311204
13	52	11	0.000000	3.856120
14	55	4	4.089981	-12.206197
15	60	1	-1.135961	4.772479
16	63	6	-2.954020	7.449268
17	66	5	22.341631	-82.514849
18	69	1	-1.686145	5.116477
19	72	3	-6.413124	22.311204
20	75	6	-3.590210	11.026114
21	78	7	-6.289308	22.012579
22	82	8	0.000000	4.736643
23	85	9	0.000000	1.867665
24	89	27	-4.362844	15.463572
25	93	6	6.544230	-18.466032
26	95	4	-2.954020	7.449268
27	100	5	-3.590210	11.026114
28	104	7	7.733287	-26.540443
29	107	5	-6.289308	22.012579
30	110	27	-1.443979	4.540815
31	113	8	0.000000	-18.565244
32		5	0.000000	4.736643
33		10	0.000000	4.807692
34		9	0.000000	9.090909
35		9	13.462043	-41.714623
36		5	0.000000	1.867665
37		8	0.000000	9.090909
38		19	-1.784830	3.985358

TABLE 6.4 (continued)

STORAGE OF THE IEEE 30-BUS NODAL ADMITTANCE MATRIX

I	JRYT(I)	ICYT(I)	Real (YT)	Imaginary (YT)
39		16	-3.956039	10.317448
40		20	-5.101854	10.980714
41		21	-2.619320	5.400770
42		10	0.000000	-4.617692
43		8	0.000000	4.807692
44		11	6.573962	-24.324552
45		3	0.000000	3.856120
46		12	0.000000	7.142857
47		13	-1.526568	3.173425
48		14	-3.095396	6.097276
49		15	-1.951998	4.104359
50		12	0.000000	-7.142857
51		11	0.000000	7.142857
52		13	4.017520	-5.424299
53		11	-1.526568	3.173425
54		14	-2.490952	2.250874
55		14	9.362397	-16.015639
56		11	-3.095396	6.097276
57		13	-2.490952	2.250874
58		17	-1.807700	3.691424
59		22	-1.968349	3.976065
60		15	3.819801	-8.483723
61		11	-1.951998	4.104359
62		16	-1.867803	4.379363
63		16	5.823842	-14.696811
64		15	-1.867803	4.379363
65		9	-3.956039	10.317448
66		17	4.883386	-9.910183
67		14	-1.807700	3.691424
68		18	-3.075686	6.218759
69		18	8.958039	-17.983465
70		17	-3.075686	6.218759
71		19	-5.882353	11.764706
72		19	7.667183	-15.750064
73		18	-5.882353	11.764706
74		9	-1.784830	3.985358
75		20	21.876495	-45.108433
76		9	-5.101854	10.980714
77		21	-16.774641	34.127719
78		21	21.934499	-43.482892

TABLE 6.4 (continued)

STORAGE OF THE IEEE 30-BUS NODAL ADMITTANCE MATRIX

I	JRYT(I)	ICYT(I)	Real (YT)	Imaginary (YT)
79		9	-2.619320	5.400770
80		20	-16.774641	34.127719
81		23	-2.540538	3.954403
82		22	3.429755	-6.965304
83		14	-1.968349	3.976065
84		23	-1.461406	2.989239
85		23	5.311837	-9.231264
86		21	-2.540538	3.954403
87		22	-1.461406	2.989239
88		24	-1.309893	2.287622
89		24	4.495715	-7.821979
90		23	-1.309893	2.287622
91		25	-1.216530	1.817144
92		26	-1.969292	3.760213
93		25	1.216530	-1.817144
94		24	-1.216530	1.817144
95		26	3.652281	-9.686717
96		24	-1.969292	3.760213
97		27	0.000000	2.635963
98		28	-.995534	1.881006
99		29	-.687456	1.293971
100		27	5.806823	-22.515689
101		26	0.000000	2.635963
102		7	-1.443979	4.540815
103		5	-4.362844	15.463572
104		28	1.907587	-3.604364
105		26	-.995534	1.881006
106		29	-.912053	1.723359
107		29	1.599509	-3.017330
108		26	-.687456	1.293971
109		28	-.912053	1.723359
110		30	6.468383	-20.719348
111		1	-5.224646	15.646727
112		2	-1.243737	5.096021

6.3.3 The Power Flow Solution

Using the flat voltage profile as a starting point, the power flow solution of this system is obtained in five Newton iterations. A summary of the analysis is provided in Table 6.5.

TABLE 6.5

POWER FLOW SOLUTION OF THE IEEE 30-BUS SYSTEM

Bus Index	Rectangular Coordinates		Polar Coordinates	
i	V_{i1}	V_{i2}	$\lvert V_i \rvert$	δ_i
1	1.032613	-.049520	1.033800	-.047919
2	1.024293	-.083488	1.027690	-.081328
3	1.017570	-.099593	1.022432	-.097563
4	.993387	-.157530	1.005800	-.157269
5	1.013359	-.114595	1.019818	-.112606
6	.996028	-.140362	1.005870	-.140000
7	1.016473	-.115376	1.023000	-.113022
8	1.025941	-.145573	1.036218	-.140951
9	.993393	-.175390	1.008758	-.174755
10	1.084946	-.117594	1.091300	-.107966
11	1.027622	-.174660	1.042360	-.168356
12	1.076485	-.159927	1.088300	-.147485
13	1.006547	-.187510	1.023863	-.184179
14	.998791	-.186162	1.015992	-.184273
15	1.005133	-.178546	1.020867	-.175801
16	.990873	-.179127	1.006934	-.178845
17	.982114	-.192608	1.000822	-.193658
18	.976047	-.193515	.995046	-.195726
19	.979346	-.189835	.997575	-.191464
20	.978707	-.181554	.995404	-.183419
21	.979124	-.181473	.995799	-.183263
22	.979537	-.188423	.997495	-.190038
23	.963527	-.186755	.981459	-.191451
24	.957778	-.185600	.975595	-.191410
25	.938167	-.189577	.957130	-.199387
26	.956285	-.175729	.972297	-.181735
27	1.011116	-.121766	1.018422	-.119850
28	.931267	-.194177	.951295	-.205563
29	.915955	-.207450	.939153	-.222727
30	1.050000	0.000000	1.050000	0.000000

6.3.4 Sensitivity Calculations for a Voltage Phase Angle

Consider a network function $f = \delta_2$. This function represents the voltage phase angle at the load bus $\ell = 2$. Alternatively, this function is expressed in its more useful form as

$$f = \tan^{-1} \frac{j(V_2^* - V_2)}{V_2^* + V_2} .$$

The partial differentiation of f gives the nonzero element of vector $\partial f/\partial \mathbf{V}_M$ as

$$\frac{\partial f}{\partial V_2} = -j \frac{0.5}{V_2} .$$

This information is supplied to the DERIVX subroutine of the XLF3 package, as indicated in Appendix C.1. The sensitivities of δ_2 with respect to various control variables are obtained straightforwardly, and are listed in Table 6.6.

TABLE 6.6

SENSITIVITIES OF δ_2 OF THE IEEE 30-BUS SYSTEM

-- Generator Bus Quantities

Bus	Real Power	Voltage Magnitude	Shunt Conductance	Shunt Susceptance
1	.029702	-.002854	-.031744	0.000000
4	.048161	.003874	-.048721	0.000000
7	.064233	-.075500	-.067221	0.000000
10	.064881	-.005771	-.077269	0.000000
12	.068083	-.022052	-.080638	0.000000

TABLE 6.6 (continued)

SENSITIVITIES OF δ_2 OF THE IEEE 30-BUS SYSTEM

-- Load Bus Quantities

Bus	Real Power	Reactive Power	Shunt Conductance	Shunt Susceptance
2	.089425	-.013340	-.094445	-.014089
3	.072267	-.006708	-.075545	-.007012
5	.063455	-.002592	-.065994	-.002696
6	.057512	-.001784	-.058189	-.001805
8	.064843	-.001158	-.069625	-.001243
9	.065554	-.001109	-.066707	-.001128
11	.068022	-.002961	-.073906	-.003217
13	.068653	-.002576	-.071969	-.002700
14	.068614	-.001961	-.070827	-.002025
15	.067414	-.001895	-.070257	-.001975
16	.066385	-.001151	-.067308	-.001167
17	.068491	-.001313	-.068604	-.001315
18	.068155	-.000991	-.067482	-.000981
19	.067549	-.000974	-.067221	-.000969
20	.066334	-.000704	-.065726	-.000698
21	.066333	-.000739	-.065776	-.000733
22	.068396	-.001207	-.068054	-.001201
23	.067522	-.000466	-.065042	-.000449
24	.066231	-.000605	-.063038	-.000576
25	.067519	.000256	-.061854	.000234
26	.064891	-.000500	-.061345	-.000473
27	.064021	-.001860	-.066401	-.001929
28	.066838	.000055	-.060486	.000050
29	.068195	.000284	-.060148	.000250

-- Transformer Quantities

Element	Turns Ratio	Internal Resistance	Internal Reactance
8, 5	.006858	-.002256	-.000946
9, 5	.002564	-.001534	-.000342
11, 3	.016167	-.009506	.004813
26,27	.003554	-.002166	-.000415

TABLE 6.6 (continued)

SENSITIVITIES OF δ_2 OF THE IEEE 30-BUS SYSTEM

-- Transmission Line Quantities

Line Index	Element	Line Conductance	Line Susceptance
1	30, 1	.000460	-.001544
2	30, 2	.002901	-.007581
3	1, 3	.000710	-.002163
4	2, 3	-.000230	.000254
5	1, 4	.000013	-.002095
6	1, 5	.000447	-.002269
7	3, 5	-.000105	.000126
8	4, 6	-.000048	.000163
9	5, 6	-.000165	.000153
10	5, 7	-.000004	.000008
13	10, 8	-.000236	.000067
14	8, 9	-.000109	-.000029
16	11,12	-.000110	.000143
17	11,13	-.000036	-.000020
18	11,14	-.000067	-.000039
19	11,15	-.000057	-.000020
20	13,14	-.000005	-.000005
21	15,16	-.000031	-.000008
22	14,17	-.000030	-.000009
23	17,18	-.000005	-.000001
24	18,19	-.000000	-.000003
25	9,19	-.000007	-.000035
26	9,16	.000000	-.000003
27	9,20	-.000010	-.000012
28	9,21	-.000009	-.000012
29	20,21	-.000000	-.000000
30	14,22	-.000034	-.000013
31	21,23	-.000003	-.000014
32	22,23	-.000032	-.000011
33	23,24	-.000010	.000001
34	24,25	-.000010	-.000025
35	24,26	-.000010	-.000013
37	26,28	-.000037	-.000054
38	26,29	-.000100	-.000149
39	28,29	-.000016	-.000023
40	7,27	.000008	.000010
41	5,27	-.000008	-.000005

6.3.5 Applications in Contingency Assessment

The first-order sensitivity calculations find extensive applications in estimating the effects of transmission network contingencies, and ranking them accordingly (Ejebe and Wollenberg 1976; Sachdev and Ibrahim 1974). The generator outages, device malfunctioning, and other defects, resulting in subsequent service deterioration are also investigated in practice. The distribution factor technique (Srinivasan et al. 1985) is quite popular in analyzing the contingency problem, however, in this section, the utilization of exact theoretical results is illustrated.

Consider a network function represented by the voltage phase angle δ_2. At the nominal point, the value of this function is -0.081328 as indicated in Table 6.5. The 50% loss of generation at $i=12$; that is, $P_{12} = 0.08455$, yields $\Delta\delta_2 = -0.005756$. The corresponding exact change in δ_2, obtained by pre- and post-contingency power flow solutions, is -0.005768. Similarly, the effect of partial outage of the transmission line connecting buses 1 and 3 results in $\Delta\delta_2 = 0.014352$, which agrees with the value obtained by the power flow solutions.

The case of multiple contingency is also investigated using the sensitivity formulas developed in this thesis. Using the total change formula together with the control variable vector $\mathbf{u} = [P_{12}\ Q_2\ |V_{30}|]$, the change in voltage phase angle is δ_2 is equal to 0.01205. The corresponding exact value obtained by the power flow solution is 0.01365. The small discrepancy indicates the effect of neglecting the higher-order terms in the chain formula.

6.3.6 Applications in Transmission Planning

The transmission planning is another important aspect of the power system design. It includes the sensitivity-based knowledge of future expansion plans, and is primarily concerned with the overload alleviation of the transmission lines. In addition, corridor selection as well as enhancement of the existing network is considered. Both, the voltage magnitude at important buses and the magnitude of line current in lines, are investigated. The effect of future reinforcements is determined in advance.

Consider a double circuit between the buses 1 and 3 of the system shown in Fig. 6.3. The new load flow indicates a reduction in the current flowing in the line connecting buses 2 and 3. The current at the nominal point is 0.189103, and reduces to 0.14868 due to the reinforcement. The new voltages at the neighbouring buses are:

$$V_1 = 1.033800$$

$$V_2 = 1.029237$$

$$V_3 = 1.024308.$$

These voltages have been verified by using the sensitivity results for the function under consideration. The sensitivities of this function with respect to line variables of interest are summarized as:

Line Index	Terminal Buses	Conductance	Susceptance
1	30 , 1	−0.002110	0.007077
2	30 , 2	0.008994	−0.036600
3	1 , 3	−0.001868	0.010697
4	2 , 3	−0.004321	0.012900
6	1 , 5	−0.001387	0.010865
13	10 , 8	0.001344	0.000082

The gradient information of pertinent cost functions is required by the optimal power flow. A minimum-loss problem associated with the IEEE 118-bus system is discussed in the following section.

6.4 The IEEE 118-bus Power System

The IEEE 118-bus system (Bandler, El-Kady and Grewal 1986; Grewal 1983) is a standard, average size test power network. It has been extensively used in a variety of steady-state analysis and planning studies (Sachdev and Ibrahim 1974). The transmission network of the system contains lines, tap-changing-under-load transformers and phase-shifting transformers. At some of the nodes, the static load is specified. The static load is usually used to manipulate the reactive power flow in the network (Weedy 1979; Wildi 1981).

6.4.1 Network Description

An optimally structured one-line diagram of the system is provided in Fig. 6.5. The diagram indicates load as well as generator buses, and their interconnections through different transmission elements. The diagram is very useful for investigating expansion plans, fault and/or contingency analysis, and real-time operations. The generator bus with widest P, Q limits is generally recommended to be considered as the slack bus of the system. In the present analysis, the last numbered bus is assumed as the slack bus. The sparsity structure of the nodal admittance matrix is illustrated in Fig. 6.6.

6.4.2 The Power Flow Solution

The power flow problem of the system is formulated in the complex mode (Bandler, El-Kady, Grewal and Wojciechowski 1983). The base-case solution is provided in Table 6.7.

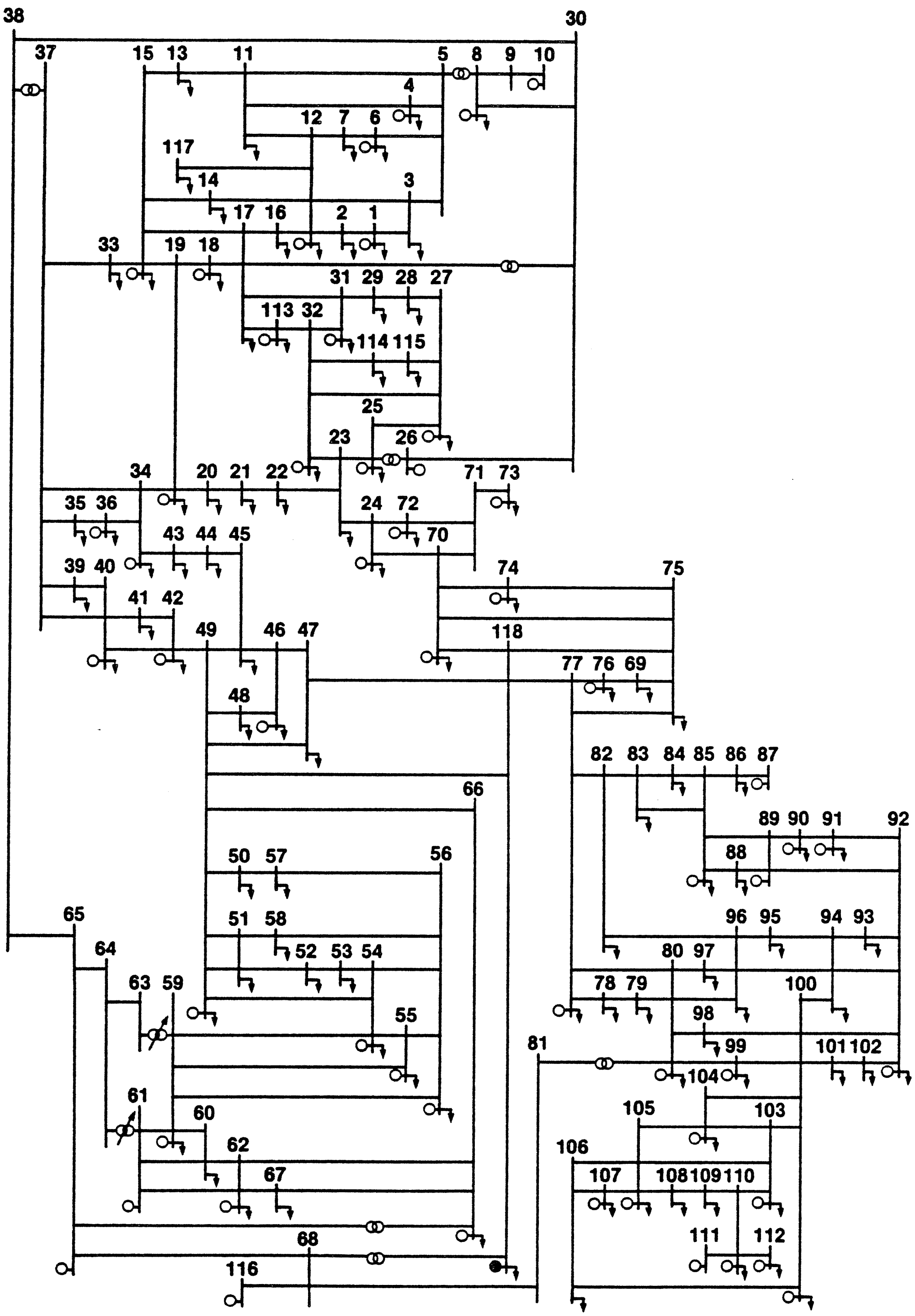

Fig. 6.5 One-line diagram of the IEEE 118-bus system. (Bandler, El-Kady and Grewal 1986, p. 87).

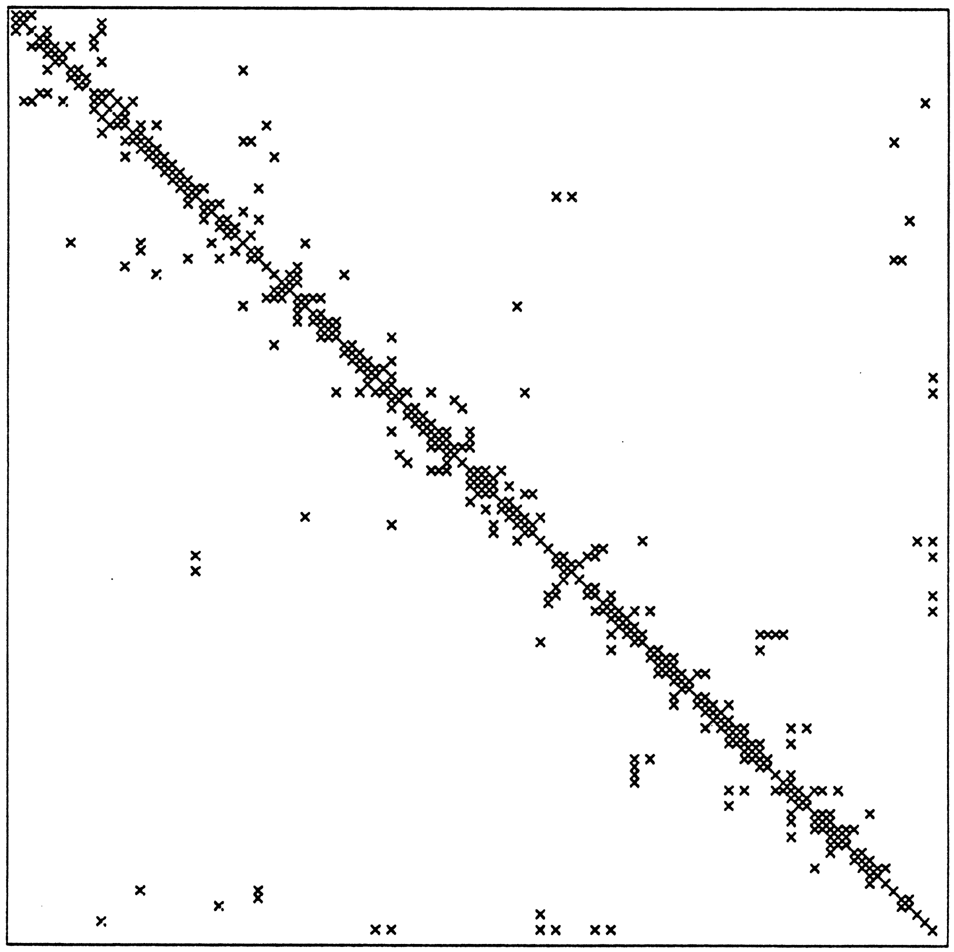

Fig. 6.6 Sparsity structure of the IEEE 118-bus nodal admittance matrix.

TABLE 6.7

POWER FLOW SOLUTION OF THE IEEE 118-BUS SYSTEM

Bus Index	Rectangular Coordinates		Polar Coordinates	
i	V_{i1}	V_{i2}	$\|V_i\|$	δ_i
1	1.131244	-.206849	1.150000	-.180853
2	1.070512	-.172068	1.084252	-.159371
3	1.099422	-.174081	1.113118	-.157035
4	1.089881	-.148860	1.100000	-.135744
5	1.072844	-.082936	1.076045	-.077151
6	1.044973	-.121388	1.052000	-.115645
7	1.042799	-.131234	1.051024	-.125189
8	1.089986	.005511	1.090000	.005056
9	1.087659	.129896	1.095388	.118864
10	1.043179	.259618	1.075000	.243917
11	1.044416	-.141351	1.053938	-.134523
12	1.041421	-.141571	1.051000	-.135112
13	1.010503	-.154866	1.022301	-.152073
14	1.017973	-.147428	1.028593	-.143825
15	.960389	-.136208	.970000	-.140886
16	1.024364	-.136802	1.033459	-.132763
17	.976660	-.098182	.981583	-.100192
18	.961167	-.130608	.970000	-.135057
19	.950337	-.135865	.960000	-.142002
20	.926309	-.125566	.934781	-.134734
21	.915221	-.102601	.920955	-.111639
22	.913521	-.064137	.915770	-.070093
23	.919534	.014842	.919654	.016139
24	.909999	-.001423	.910000	-.001564
25	.957763	.153589	.970000	.159008
26	.992151	.189039	1.010000	.188277
27	.821024	-.056990	.823000	-.069303
28	.654166	-.037646	.655249	-.057485
29	.710519	-.062692	.713280	-.088006
30	1.048195	-.013344	1.048280	-.012729
31	.778874	-.080279	.783000	-.102708
32	.868666	-.076177	.872000	-.087470
33	.949110	-.144188	.960000	-.150766
34	.948541	-.141246	.959000	-.147822
35	.951288	-.145636	.962371	-.151914
36	.951739	-.146837	.963000	-.153076
37	.959499	-.125073	.967617	-.129621
38	1.038953	-.044492	1.039906	-.042798
39	.942714	-.188108	.961298	-.196953

TABLE 6.7 (continued)

POWER FLOW SOLUTION OF THE IEEE 118-BUS SYSTEM

Bus Index	Rectangular Coordinates		Polar Coordinates	
i	V_{i1}	V_{i2}	$\|V_i\|$	δ_i
79	1.004228	.063909	1.006259	.063554
80	1.032444	.125140	1.040000	.120619
81	.997925	.110048	1.003975	.109833
82	.983303	.110623	.989506	.112030
83	.974321	.144195	.984933	.146929
84	.960312	.208333	.982651	.213632
85	.958865	.246330	.990000	.251460
86	.960119	.238422	.989279	.243402
87	.972812	.271547	1.010000	.272207
88	.939349	.300807	.986337	.309911
89	.927210	.374542	1.000000	.383902
90	.954174	.263917	.990000	.269845
91	.943916	.263482	.980000	.272208
92	.952882	.275828	.992000	.281765
93	.963270	.210163	.985930	.214811
94	.976858	.162440	.990272	.164780
95	.970930	.135210	.980300	.138368
96	.984363	.122238	.991923	.123548
97	1.004268	.117035	1.011064	.116014
98	1.017749	.117120	1.024465	.114573
99	1.000749	.136388	1.010000	.135452
100	1.006788	.163637	1.020000	.161125
101	.974315	.194368	.993513	.196907
102	.959756	.246767	.990972	.251663
103	1.003706	.112584	1.010000	.111702
104	.967397	.071015	.970000	.073277
105	.963539	.053082	.965000	.055035
106	.960581	.044726	.961622	.046527
107	.950000	.000200	.950000	.000210
108	.965624	.036196	.966303	.037467
109	.966648	.029922	.967111	.030945
110	.972810	.019247	.973000	.019782
111	.978848	.047506	.980000	.048494
112	.979363	-.035335	.980000	-.036063
113	.984466	-.104530	.990000	-.105783
114	.852662	-.078830	.856299	-.092189
115	.829344	-.078732	.833072	-.094649
116	.998125	.061206	1.000000	.061245
117	1.024321	-.164517	1.037448	-.159250
118	1.030000	0.000000	1.030000	0.000000

TABLE 6.7 (continued)

POWER FLOW SOLUTION OF THE IEEE 118-BUS SYSTEM

Bus Index	Rectangular Coordinates		Polar Coordinates	
i	V_{i1}	V_{i2}	$\|V_i\|$	δ_i
40	.946719	-.211244	.970000	-.219537
41	.969475	-.233493	.997196	-.236344
42	1.069621	-.256730	1.100000	-.235563
43	.945642	-.150891	.957605	-.158231
44	.965470	-.123569	.973346	-.127296
45	.973483	-.097446	.978348	-.099768
46	.998283	-.058571	1.000000	-.058605
47	1.013063	-.033433	1.013615	-.032989
48	1.015091	-.026405	1.015435	-.026007
49	1.019979	-.006589	1.020000	-.006460
50	.996619	-.029862	.997066	-.029954
51	.962489	-.054652	.964039	-.056721
52	.952104	-.063381	.954211	-.066471
53	.940110	-.060522	.942056	-.064288
54	.949454	-.032194	.950000	-.033894
55	.948494	-.053464	.950000	-.056308
56	.948575	-.052011	.950000	-.054776
57	.965709	-.049500	.966977	-.051213
58	.953949	-.058387	.955734	-.061130
59	.989973	-.007276	.990000	-.007349
60	.990423	.030062	.990879	.030343
61	.997638	.068694	1.000000	.068748
62	.998746	.050074	1.000000	.050095
63	1.019159	.045168	1.020159	.044290
64	1.014108	.070944	1.016587	.069843
65	.993778	.111377	1.000000	.111609
66	1.044664	.115230	1.051000	.109859
67	1.018927	.070194	1.021342	.068782
68	1.019396	.047426	1.020499	.046490
69	.949185	-.054920	.950772	-.057796
70	.979036	-.043468	.980000	-.044369
71	.983319	-.047274	.984454	-.048039
72	.978877	-.046902	.980000	-.047877
73	.988662	-.051459	.990000	-.052003
74	.957892	-.063589	.960000	-.066287
75	.967855	-.048574	.969074	-.050146
76	.944337	-.035402	.945000	-.037471
77	1.008204	.060203	1.010000	.059642
78	.998461	.051868	.999807	.051902

6.4.3 Sensitivity Calculations for the Slack Bus Real Power

The function, representing the slack bus real power, is conveniently expressed as

$$f = P_n = \frac{S_n + S_n^*}{2},$$

where S_n is the complex power injected at the slack bus. The complex power S_n is given by

$$S_n = V_n \sum_{k=1}^{n} (Y_{nk}^* V_k^*).$$

Further, the nonzero elements of the right-hand side vector $\partial f/\partial V_M$ are

$$\frac{\partial f}{\partial V_k} = 0.5\,[Y_{nk} V_n^* + \delta_{kn} \sum_{k=1}^{n} Y_{nk}^* V_k^*],$$

where

$$\delta_{kn} = \begin{cases} 0 \text{ for } k \neq n \\ 1 \text{ for } k = n \end{cases}.$$

The XLF3 package is utilized to evaluate various sensitivities of this function. The corresponding computer program is provided in Appendix C.2. The sensitivity results from the program are recapitulated in Table 6.8.

6.4.4 Formulation and Solution of the Minimum-loss Problem

The minimum-loss problem associated with a particular power system is a constrained minimization problem. The cost function (performance index or objective function) of this problem reflects the total transmission active power loss in the system (Sasson 1968; Grewal 1983). The problem is formulated for the IEEE 118-bus system as

$$\text{Minimize } f = \sum_{i=1}^{n} P_n$$

subject to

$$\mathbf{h}(\mathbf{x},\mathbf{u}) = \mathbf{0} \quad \text{-- power flow equations}$$

and

$$\mathbf{g}(\mathbf{x},\mathbf{u}) \geq \mathbf{0} \quad \text{-- generator constraints.}$$

TABLE 6.8

SENSITIVITIES OF THE IEEE 118-BUS SLACK REAL POWER

-- Load Bus Quantities

Bus	Real Power	Reactive Power	Shunt Conductance	Shunt Susceptance
2	-1.039480	-.001776	1.222015	-.002087
3	-1.036504	-.005536	1.284263	-.006860
5	-.995079	-.007493	1.152184	-.008676
7	-1.018347	-.000194	1.124920	-.000214
9	-.977067	.000778	1.172358	.000933
11	-1.027684	-.003698	1.141535	-.004108
13	-1.039668	-.007191	1.086555	-.007516
14	-1.030295	.000799	1.090055	.000845
16	-1.026259	-.007931	1.096103	-.008471
17	-1.005144	.002108	.968617	.002032
20	-1.033789	-.004819	.903283	-.004211
21	-1.028398	-.008006	.872155	-.006790
22	-1.014626	-.007771	.850805	-.006516
23	-.983963	-.001731	.832173	-.001464
28	-1.039391	-.148142	.446264	-.063605
29	-1.038307	-.072010	.528257	-.036636
30	-.998461	-.000823	1.097824	-.000904
33	-1.031377	-.005461	.952281	-.005042
35	-1.029373	-.001356	.953935	-.001257
37	-1.012143	-.005472	.951330	-.005143
38	-1.004240	-.002092	1.088326	-.002267
39	-1.061038	-.005893	.981905	-.005454
41	-1.090438	-.001984	1.084327	-.001973
43	-1.053792	-.002668	.966027	-.002446
44	-1.058629	-.003158	1.002369	-.002990
45	-1.052171	-.005841	1.006600	-.005588
47	-1.010749	.000872	1.038441	.000896
48	-1.005823	.001667	1.037093	.001719
50	-1.008318	-.001080	1.002412	-.001074
51	-1.025980	-.006817	.953519	-.006336
52	-1.031752	-.008662	.939432	-.007887
53	-1.025027	-.007288	.909682	-.006468
57	-1.020321	-.000690	.954047	-.000645
58	-1.027549	-.004319	.938594	-.003945
60	-.987745	.000007	.969808	.000007
63	-.978277	.001177	1.018111	.001225
64	-.969480	.000824	1.001903	.000852

TABLE 6.8 (continued)

SENSITIVITIES OF THE IEEE 118-BUS SLACK REAL POWER

-- Load Bus Quantities

Bus	Real Power	Reactive Power	Shunt Conductance	Shunt Susceptance
67	-.970500	-.001316	1.012369	-.001372
68	-.996487	.011340	1.037755	.011810
69	-1.045342	.007383	.944950	.006674
71	-1.027714	.000585	.996009	.000567
75	-1.037294	.001418	.974123	.001331
78	-.982543	-.007871	.982164	-.007868
79	-.975549	-.007183	.987800	-.007273
81	-.952472	.001083	.960059	.001091
82	-.947823	-.005311	.928035	-.005200
83	-.927885	-.004839	.900134	-.004694
84	-.885244	-.005147	.854794	-.004970
86	-.863121	-.001071	.844713	-.001048
88	-.844329	-.002407	.821415	-.002341
93	-.895657	-.007314	.870630	-.007110
94	-.921829	-.008117	.903981	-.007960
95	-.937759	-.012071	.901174	-.011600
96	-.943976	-.006223	.928789	-.006123
97	-.947014	-.004244	.968086	-.004339
98	-.944671	-.001492	.991460	-.001566
101	-.901381	-.005396	.889725	-.005326
102	-.874498	-.002702	.858778	-.002654
106	-.977820	-.003407	.904207	-.003150
108	-.982431	-.000472	.917336	-.000441
109	-.985982	-.000648	.922193	-.000606
114	-1.026927	-.003365	.752992	-.002468
115	-1.027243	.002406	.712915	.001669
117	-1.037589	-.003583	1.116755	-.003856

TABLE 6.8 (continued)

SENSITIVITIES OF THE IEEE 118-BUS SLACK REAL POWER

-- Generator Bus Quantities

Bus	Real Power	Voltage Magnitude	Shunt Conductance	Shunt Susceptance
1	-1.050857	.882783	1.389758	0.000000
4	-1.032740	.726316	1.249615	0.000000
6	-1.013095	-.311308	1.121196	0.000000
8	-.994774	-.167660	1.181891	0.000000
10	-.957590	-.165486	1.106614	0.000000
12	-1.024958	-.571404	1.132170	0.000000
15	-1.029115	-.164177	.968294	0.000000
18	-1.024733	.081266	.964171	0.000000
19	-1.030086	-.162855	.949328	0.000000
24	-.995664	-.377848	.824509	0.000000
25	-.940147	.297842	.884584	0.000000
26	-.947080	-.220668	.966117	0.000000
27	-1.016621	-1.020986	.688587	0.000000
31	-1.024528	-1.433695	.628127	0.000000
32	-1.023842	.515771	.778513	0.000000
34	-1.033093	-.198182	.950116	0.000000
36	-1.031219	-.001704	.956321	0.000000
40	-1.077351	-.769418	1.013680	0.000000
42	-1.092801	1.205544	1.322289	0.000000
46	-1.026242	-.034182	1.026242	0.000000
49	-.992892	-.107537	1.033005	0.000000
54	-1.006052	-.459040	.907961	0.000000
55	-1.018023	-.034121	.918766	0.000000
56	-1.020272	-.256278	.920796	0.000000
59	-.987729	.229232	.968073	0.000000
61	-.965655	-.071162	.965655	0.000000
62	-.976510	-.071795	.976510	0.000000
65	-.959474	-.587420	.959474	0.000000
66	-.954143	.177197	1.053948	0.000000
70	-1.026790	-.014542	.986129	0.000000
72	-1.023735	.184778	.983195	0.000000
73	-1.029367	.064730	1.008883	0.000000
74	-1.046155	-.091067	.964137	0.000000
76	-1.018810	-.456361	.909822	0.000000
77	-.975753	-.110255	.995366	0.000000
80	-.945021	.463286	1.022135	0.000000
85	-.858860	-.313478	.841768	0.000000

TABLE 6.8 (continued)

SENSITIVITIES OF THE IEEE 118-BUS SLACK REAL POWER

-- Generator Bus Quantities

Bus	Real Power	Voltage Magnitude	Shunt Conductance	Shunt Susceptance
87	-.856185	.013011	.873394	0.000000
89	-.822792	-.390672	.822792	0.000000
90	-.870385	.138436	.853065	0.000000
91	-.867543	-.096896	.833189	0.000000
92	-.860097	-.422372	.846391	0.000000
99	-.935353	-.084126	.954153	0.000000
100	-.919584	.230646	.956735	0.000000
103	-.945492	.251899	.964496	0.000000
104	-.962487	-.167148	.905604	0.000000
105	-.972445	-.234093	.905565	0.000000
107	-1.003723	-.021297	.905860	0.000000
110	-.990648	-.291774	.937876	0.000000
111	-.974205	-.011202	.935626	0.000000
112	-1.034338	.282971	.993378	0.000000
113	-1.012186	.595070	.992044	0.000000
116	-.989912	-.101326	.989912	0.000000

-- Transformer Quantities

Element	Turns Ratio	Internal Resistance	Internal Reactance
8, 5	.316354	11.930163	-.084332
26,25	-.004820	.529850	-.131223
30,17	-.058476	5.266261	.337658
38,37	.094365	5.157105	.443463
63,59	.039796	1.860750	.312149
64,61	.029692	.000229	-.009722
66,65	-.000316	9.261379	-.008021
118,68	-1.670888	-13.543352	-36.080895
81,80	.037468	.371101	.078608

The following allowable range for the generator real power P_g, and voltage magnitude $|V_g|$, for $g = n_L + 1, ..., n_L + n_G$, are considered:

$$0 \leq P_g \leq P_{max}$$

$$0.95 \leq |V_g| \leq 1.05.$$

Using the optimization package MINOS Version 4 (Murtagh and Saunders 1980), the losses are reduced from 1.874029 to 0.898881 as indicated in Table 6.9 (Grewal 1983).

TABLE 6.9

RESULTS OF THE MINIMUM-LOSS PROBLEM

Iteration	Objective Function	Iteration	Objective Function
1	1.874029	31	1.113729
2	1.791540	32	1.106405
3	1.788261	33	1.099119
4	1.742582	34	1.098632
5	1.728534	35	1.097584
6	1.675286	36	1.077108
7	1.650821	37	1.069434
8	1.646664	38	1.058328
9	1.602012	39	1.057547
10	1.532712	40	1.039549
11	1.474493	41	1.026739
12	1.438996	42	1.012004
13	1.430586	43	1.001770
14	1.426693	44	0.998249
15	1.417182	45	0.993113
16	1.392310	46	0.991415
17	1.354504	47	0.990480
18	1.339082	48	0.984823
19	1.321483	49	0.971396
20	1.305068	50	0.969115
21	1.265463	51	0.962826
22	1.265322	52	0.941750
23	1.257992	53	0.935488
24	1.253278	54	0.931943
25	1.252076	55	0.927768
26	1.249091	56	0.922292
27	1.199212	57	0.914366
28	1.163750	58	0.910232
29	1.156131	59	0.902772
30	1.134962	60	0.898881

CHAPTER 7

CONCLUSIONS AND RECOMMENDATIONS FOR FURTHER RESEARCH

The material contained in this thesis is predicated on a recently developed methodology involving adjoint network modeling in the context of sensitivity evaluation of electrical power systems. A novel hybrid vector/matrix formulation is successfully developed in conjunction with the complex conjugate notation. In particular, the mathematical models of power system components ranging from a phase-shifting transformer to an a.c.–d.c converter have been investigated in a rather systematic manner.

The theoretical results are capable of handling multiport, nonreciprocal, a.c. as well as integrated a.c.–d.c. bulk transmission networks. Further, applications of the generalized sensitivity formulas to high voltage d.c. links and special-purpose transformers have been presented. The functions encountered in steady-state security assessment have also been considered, and investigated in applications to IEEE test power systems.

The bus frame of reference has been used throughout the analysis. Moreover, the phase symmetry of three-phase generation and transmission has been assumed, and thereby, the whole text has concerned itself with single-phase modeling. The load buses, also called non-voltage controlled buses, have been invariably considered as the buses at which both the real and reactive powers are specified. The current and voltage at these buses are determined by solving the ubiquitous power flow problem.

The generator buses have been assumed to exhibit the characteristics of synchronous machines installed with normal control actions. Consequently, the generator real power and voltage magnitude have been taken as the control variables of interest. Initially, the special case of two-port networks has been emphasized, since many concepts germane to the multiport case are logical extension of their two-port counterparts. The transmission line model with lumped parameter representation has been used. A cascaded model of power system control transformers has been investigated.

The high-voltage direct current transmission has been given adequate attention, since it has been recognized to be capable of wheeling more power from electricity-rich areas. A fairly simple converter model has been developed from the intrinsic branch relationships that generate observable terminal voltages and currents. In addition, some examples of the existing d.c. links have been reported.

Chapter 3 has dealt with the exact a.c. power flow problem. For brevity, emphasis has been laid on the Newton-Raphson method and its important variants. Many inducements for using the fast-decoupled method have been mentioned together with the adaptability of the method to real-time power system problems. The Tellegen theorem method for solving the power flow problem has also been discussed. The chapter basically reinforces the need for an understanding of the power network equations, and to gauge the effort involved in the sensitivity evaluation.

The concept of the adjoint network has been successfully utilized in efficient computation of the power network sensitivities. The flexibility of modeling various adjoint power network components has been enhanced via the hybrid vector/matrix notation, which encompasses the analysis of multiport, nonreciprocal networks. Additional benefit realized by the adjoint method is that all computations are amenable to efficient utilization of a digital computer. This assertion derives from the fact that the adjoint technique obviates the need to evaluate the partial derivatives implicit in the definition of the elements of the sensitivity matrix. The sensitivity evaluation by this method mandates two circuit analyses: one analysis is executed on the original network to obtain all branch variables, while the other analysis addresses the adjoint configuration. The requirements of topological identity between the two network branches, together with homologous excitation branches, uniquely define the adjoint structure.

Exact sensitivity formulas for various transmission elements have been derived and verified numerically for two-bus power systems. Additionally, some test cases have been discussed. These test cases are, namely, a six-bus system, the IEEE 30-bus system, and the IEEE 118-bus system. The information regarding their data, nodal admittance matrices, power flow solution and interconnection has been included. The network functions used to reflect the objective of optimal power flow problems have been considered, and their sensitivities with respect to several different control variables have been tabulated.

The elegance and simplicity of the numerical examples as well as the compactness of the theoretical manipulations have been emphasized in this thesis. The sensitivity expressions are general and have been successfully applied to networks containing a.c.–d.c. converters, phase shifting transformers, and static loads. However, the validity of the theoretical results has been confined only to fairly simple power network models.

For the power flow algorithms, the transformer models have been assumed to exhibit rather constant leakage reactance. But, in actual practice, some inherent nonlinearities are involved, and it has been recognized to consider variable impedance transformer model. The theoretical results of Chapter 5 can be applied to new transformer models, and their adjoint models can be readily developed. The modeling and sensitivity evaluation of untransposed three-phase transmission lines can be investigated with the help of the generalized hybrid formulation addressed in this thesis.

APPENDIX A

THE AC PER-UNIT SYSTEM AND AC-DC PER-UNIT SYSTEM

The impedances, currents, voltages and powers are usually preferred in the per-unit (p.u.) values rather than in ohms, amperes, kilovolts, and megavars or megawatts. There are several advantages in using the per-unit system, namely, the data representation yields valuable relative magnitude information, circuit analysis of the systems containing transformers of different transformation ratios is greatly simplified, and the circuit parameters tend to fall in relatively narrow numerical ranges.

For a system link, transmitting complex power S, let the corresponding voltage and current be V and I, respectively. Consider two base values V_{base} and I_{base}, expressed in rms voltage and current, respectively. Then the per-unit voltage and current of the system are given by

$$V_{pu} = \frac{V}{V_{base}} \quad \text{p.u. volts}$$

$$I_{pu} = \frac{I}{I_{base}} \quad \text{p.u. amps}$$

The base values of power and impedance in terms of already chosen V_{base} and I_{base} are obtained as

$$S_{base} = V_{base}\, I_{base} \quad \text{VA}$$

$$Z_{base} = \frac{V_{base}}{I_{base}} \quad \text{ohm}$$

The complex power S and an impedance Z pertaining to a system are expressed in the dimensionless per-unit values, according to

$$S_{pu} = \frac{S}{S_{base}} = \frac{P+jQ}{S_{base}} = \frac{P}{S_{base}} + j\,\frac{Q}{S_{base}} = P_{pu} + j\,Q_{pu}$$

$$Z_{pu} = \frac{Z}{Z_{base}} = \frac{R+jX}{Z_{base}} = R_{pu} + j\,X_{pu}\ .$$

In practice, the a.c. system base quantities are

$$(VA)_{a.c.-base} = VA_{3-phase}$$

$$(VA)_{a.c.-base} = V_{LL}$$

$$I_{ac-base} = \frac{(VA)_{ac-base}}{\sqrt{3}\ VA_{ac-phase}}$$

$$Z_{ac-base} = \frac{V_{ac-base}}{\sqrt{3}\ I_{ac-phase}} = \frac{(V_{ac-base})^2}{VA_{ac-phase}}\ ,$$

where V_{LL} represents the a.c. line-to-line voltage, and the symbol $VA_{3\text{-}phase}$ represents the three-phase voltampere rating chosen. Considering the terminal relationships described in Section 5.2 together with the converter equation obtained by assuming identical real power on the two sides of a converter, it is straightforward to arrive at the following relationships:

$$P_{dc\text{-}base} = VA_{ac\text{-}base}$$

$$I_{dc\text{-}base} = I_{ac\text{-}base}.$$

It should be noticed that while the ideal a.c. power transformer is a linear device, the a.c.-d.c. transformation characteristics of a bridge converter are nonlinear. The effective turns ratio of the converter changes as the current through the device changes. Subsequently, no one a.c.-d.c. per-unit system can be chosen which may allow the converter replacement by a simple circuit node, as in the case of power transformers. The selection of the a.c.-d.c. per-unit system is arbitrary (Tylavsky 1984). For convenience, it is equally justified to force the per-unit current and power on both sides of the converter to be identical.

APPENDIX B.1

THE IEEE 30-BUS SYSTEM - Transmission Network Data

Terminal Buses		Series Resistance	Series Reactance	Shunt Conductance	Shunt Susceptance	Turns Ratio Magnitude	Angle
30	1	.019	.058	0.000	.013	1.000	0.00
30	2	.045	.185	0.000	.010	1.000	0.00
1	3	.057	.174	0.000	.009	1.000	0.00
2	3	.013	.038	0.000	.002	1.000	0.00
1	4	.047	.198	0.000	.010	1.000	0.00
1	5	.058	.176	0.000	.009	1.000	0.00
3	5	.012	.041	0.000	.002	1.000	0.00
4	6	.046	.116	0.000	.005	1.000	0.00
5	6	.027	.082	0.000	.004	1.000	0.00
5	7	.012	.042	0.000	.002	1.000	0.00
8	5	0.000	.208	0.000	0.000	1.015	0.00
9	5	0.000	.556	0.000	0.000	.963	0.00
10	8	0.000	.208	0.000	0.000	1.000	0.00
8	9	0.000	.110	0.000	0.000	1.000	0.00
11	3	0.000	.256	0.000	0.000	1.013	0.00
11	12	0.000	.140	0.000	0.000	1.000	0.00
11	13	.123	.256	0.000	0.000	1.000	0.00
11	14	.066	.130	0.000	0.000	1.000	0.00
11	15	.095	.199	0.000	0.000	1.000	0.00
13	14	.221	.200	0.000	0.000	1.000	0.00
15	16	.082	.193	0.000	0.000	1.000	0.00
14	17	.107	.219	0.000	0.000	1.000	0.00
17	18	.064	.129	0.000	0.000	1.000	0.00
18	19	.034	.068	0.000	0.000	1.000	0.00
9	19	.094	.209	0.000	0.000	1.000	0.00
9	16	.032	.085	0.000	0.000	1.000	0.00
9	20	.035	.075	0.000	0.000	1.000	0.00
9	21	.073	.150	0.000	0.000	1.000	0.00
20	21	.012	.024	0.000	0.000	1.000	0.00
14	22	.100	.202	0.000	0.000	1.000	0.00
21	23	.115	.179	0.000	0.000	1.000	0.00
22	23	.132	.270	0.000	0.000	1.000	0.00
23	24	.189	.329	0.000	0.000	1.000	0.00

APPENDIX B.1 (continued)

THE IEEE 30-BUS SYSTEM - Transmission Network Data

Terminal Buses		Series Resistance	Series Reactance	Shunt Conductance	Shunt Susceptance	Turns Ratio Magnitude	Angle
24	25	.254	.380	0.000	0.000	1.000	0.00
24	26	.109	.209	0.000	0.000	1.000	0.00
26	27	0.000	.396	0.000	0.000	.958	0.00
26	28	.220	.415	0.000	0.000	1.000	0.00
26	29	.320	.603	0.000	0.000	1.000	0.00
28	29	.240	.453	0.000	0.000	1.000	0.00
7	27	.064	.200	0.000	.011	1.000	0.00
5	27	.017	.060	0.000	.003	1.000	0.00

APPENDIX B.1 (continued)

THE IEEE 30-BUS SYSTEM - Bus Data at the Base-case

Bus Index	Bus Type	Bus Voltage (Polar Coordinates)		Generated Real Power	Load Real Power	Load Reactive Power	Static Load
1	1	1.03380	0.00000	.576	.217	.127	0.00
2	0	1.00000	0.00000	0.000	.024	.012	0.00
3	0	1.00000	0.00000	0.000	.076	.016	0.00
4	1	1.00580	0.00000	.246	.942	.190	0.00
5	0	1.00000	0.00000	0.000	0.000	0.000	0.00
6	0	1.00000	0.00000	0.000	.228	.109	0.00
7	1	1.02300	0.00000	.350	.300	.300	0.00
8	0	1.00000	0.00000	0.000	0.000	0.000	0.00
9	0	1.00000	0.00000	0.000	.058	.020	0.00
10	1	1.09130	0.00000	.179	0.000	0.000	.19
11	0	1.00000	0.00000	0.000	.112	.075	0.00
12	1	1.08830	0.00000	.169	0.000	0.000	0.00
13	0	1.00000	0.00000	0.000	.062	.016	0.00
14	0	1.00000	0.00000	0.000	.082	.025	0.00
15	0	1.00000	0.00000	0.000	.035	.018	0.00
16	0	1.00000	0.00000	0.000	.090	.058	0.00
17	0	1.00000	0.00000	0.000	.032	.009	0.00
18	0	1.00000	0.00000	0.000	.095	.034	0.00
19	0	1.00000	0.00000	0.000	.022	.009	0.00
20	0	1.00000	0.00000	0.000	.175	.112	0.00
21	0	1.00000	0.00000	0.000	0.000	0.000	0.00
22	0	1.00000	0.00000	0.000	.032	.016	0.00
23	0	1.00000	0.00000	0.000	.087	.067	0.00
24	0	1.00000	0.00000	0.000	0.000	0.000	.04
25	0	1.00000	0.00000	0.000	.035	.023	0.00
26	0	1.00000	0.00000	0.000	0.000	0.000	0.00
27	0	1.00000	0.00000	0.000	0.000	0.000	0.00
28	0	1.00000	0.00000	0.000	.024	.009	0.00
29	0	1.00000	0.00000	0.000	.106	.019	0.00
30	2	1.05000	0.00000	0.000	0.000	0.000	0.00

APPENDIX B.2

THE IEEE 118-BUS SYSTEM - Transmission Network Data

Terminal Buses		Series Resistance	Series Reactance	Shunt Conductance	Shunt Susceptance	Turns Ratio Magnitude	Angle
1	2	.030	.099	0.000	.013	1.000	0.00
1	3	.013	.042	0.000	.005	1.000	0.00
4	5	.022	.058	0.000	.001	1.000	0.00
3	5	.024	.108	0.000	.014	1.000	0.00
5	6	.012	.054	0.000	.007	1.000	0.00
6	7	.005	.021	0.000	.003	1.000	0.00
8	9	.002	.031	0.000	.581	1.000	0.00
8	5	0.000	.027	0.000	0.000	1.020	0.00
9	10	.003	.032	0.000	.615	1.000	0.00
4	11	.021	.069	0.000	.009	1.000	0.00
5	11	.020	.068	0.000	.009	1.000	0.00
11	12	.006	.020	0.000	.003	1.000	0.00
2	12	.019	.062	0.000	.008	1.000	0.00
3	12	.048	.160	0.000	.020	1.000	0.00
7	12	.009	.034	0.000	.004	1.000	0.00
11	13	.022	.073	0.000	.009	1.000	0.00
12	14	.022	.071	0.000	.009	1.000	0.00
13	15	.074	.244	0.000	.031	1.000	0.00
14	15	.060	.195	0.000	.025	1.000	0.00
12	16	.021	.038	0.000	.011	1.000	0.00
15	17	.013	.044	0.000	.022	1.000	0.00
16	17	.045	.180	0.000	.023	1.000	0.00
17	18	.012	.051	0.000	.007	1.000	0.00
18	19	.012	.049	0.000	.006	1.000	0.00
19	20	.025	.117	0.000	.015	1.000	0.00
15	19	.012	.039	0.000	.005	1.000	0.00
20	21	.018	.085	0.000	.011	1.000	0.00
21	22	.021	.097	0.000	.012	1.000	0.00
22	23	.034	.159	0.000	.020	1.000	0.00
23	24	.014	.049	0.000	.025	1.000	0.00
23	25	.016	.080	0.000	.043	1.000	0.00
26	25	0.000	.038	0.000	0.000	1.040	0.00
25	27	.032	.163	0.000	.088	1.000	0.00
27	28	.019	.086	0.000	.011	1.000	0.00

APPENDIX B.2 (continued)

THE IEEE 118-BUS SYSTEM - Transmission Network Data

Terminal Buses		Series Resistance	Series Reactance	Shunt Conductance	Shunt Susceptance	Turns Ratio Magnitude	Angle
28	29	.027	.094	0.000	.012	1.000	0.00
30	17	0.000	.039	0.000	0.000	1.040	0.00
8	30	.004	.050	0.000	.257	1.000	0.00
26	30	.008	.086	0.000	.454	1.000	0.00
17	31	.047	.156	0.000	.020	1.000	0.00
29	31	.011	.033	0.000	.004	1.000	0.00
23	32	.032	.115	0.000	.059	1.000	0.00
31	32	.030	.096	0.000	.013	1.000	0.00
27	32	.023	.076	0.000	.010	1.000	0.00
15	33	.038	.124	0.000	.016	1.000	0.00
19	34	.075	.247	0.000	.032	1.000	0.00
35	36	.002	.010	0.000	.001	1.000	0.00
35	37	.011	.050	0.000	.007	1.000	0.00
33	37	.042	.142	0.000	.018	1.000	0.00
34	36	.009	.027	0.000	.003	1.000	0.00
34	37	.011	.029	0.000	.005	1.000	0.00
38	37	0.000	.038	0.000	0.000	1.070	0.00
37	39	.032	.106	0.000	.014	1.000	0.00
37	40	.059	.168	0.000	.021	1.000	0.00
30	38	.005	.054	0.000	.211	1.000	0.00
39	40	.018	.061	0.000	.008	1.000	0.00
40	41	.015	.048	0.000	.006	1.000	0.00
40	42	.056	.183	0.000	.023	1.000	0.00
41	42	.041	.135	0.000	.017	1.000	0.00
43	44	.061	.245	0.000	.030	1.000	0.00
34	43	.041	.168	0.000	.021	1.000	0.00
44	45	.022	.090	0.000	.011	1.000	0.00
45	46	.040	.136	0.000	.012	1.000	0.00
46	47	.038	.127	0.000	.016	1.000	0.00
46	48	.060	.189	0.000	.024	1.000	0.00
47	49	.019	.063	0.000	.008	1.000	0.00
42	49	.036	.162	0.000	.086	1.000	0.00
76	69	.061	.054	0.000	.043	1.000	0.00
45	49	.068	.186	0.000	.022	1.000	0.00
48	49	.018	.051	0.000	.006	1.000	0.00
49	50	.027	.075	0.000	.009	1.000	0.00
49	51	.049	.137	0.000	.017	1.000	0.00

APPENDIX B.2 (continued)

THE IEEE 118-BUS SYSTEM - Transmission Network Data

Terminal Buses		Series Resistance	Series Reactance	Shunt Conductance	Shunt Susceptance	Turns Ratio Magnitude	Turns Ratio Angle
75	69	.015	.048	0.000	.037	1.000	0.00
54	55	.017	.071	0.000	.010	1.000	0.00
54	56	.023	.060	0.000	.004	1.000	0.00
55	56	.025	.055	0.000	.002	1.000	0.00
56	57	.034	.097	0.000	.012	1.000	0.00
50	57	.047	.134	0.000	.017	1.000	0.00
56	58	.034	.097	0.000	.012	1.000	0.00
51	58	.026	.072	0.000	.009	1.000	0.00
54	59	.050	.229	0.000	.030	1.000	0.00
56	59	.041	.122	0.000	.055	1.000	0.00
12	117	.033	.140	0.000	.027	1.000	0.00
55	59	.047	.216	0.000	.028	1.000	0.00
59	60	.032	.145	0.000	.019	1.000	0.00
59	61	.033	.150	0.000	.019	1.000	0.00
60	61	.023	.054	0.000	.007	1.000	0.00
60	62	.012	.056	0.000	.007	1.000	0.00
61	62	.008	.038	0.000	.005	1.000	0.00
63	59	0.000	.039	0.000	0.000	1.040	0.00
63	64	.002	.020	0.000	.108	1.000	0.00
64	61	0.000	.027	0.000	0.000	1.020	0.00
38	65	.009	.099	0.000	.523	1.000	0.00
64	65	.003	.030	0.000	.190	1.000	0.00
49	66	.009	.046	0.000	.025	1.000	0.00
68	116	.020	.054	0.000	.012	1.000	0.00
62	66	.048	.218	0.000	.029	1.000	0.00
62	67	.026	.117	0.000	.016	1.000	0.00
66	65	0.000	.037	0.000	0.000	.940	0.00
66	67	.022	.102	0.000	.013	1.000	0.00
65	68	.021	.056	0.000	.319	1.000	0.00
47	118	.084	.278	0.000	.035	1.000	0.00
49	118	.099	.324	0.000	.041	1.000	0.00
118	68	0.000	.037	0.000	0.000	.990	0.00
118	70	.030	.127	0.000	.061	1.000	0.00
24	70	.102	.412	0.000	.051	1.000	0.00
70	71	.009	.036	0.000	.004	1.000	0.00

APPENDIX B.2 (continued)

THE IEEE 118-BUS SYSTEM - Transmission Network Data

Terminal Buses		Series Resistance	Series Reactance	Shunt Conductance	Shunt Susceptance	Turns Ratio Magnitude	Angle
24	72	.049	.196	0.000	.024	1.000	0.00
71	72	.045	.180	0.000	.022	1.000	0.00
71	73	.009	.045	0.000	.006	1.000	0.00
70	74	.040	.132	0.000	.017	1.000	0.00
70	75	.043	.141	0.000	.018	1.000	0.00
118	75	.041	.122	0.000	.062	1.000	0.00
74	75	.012	.041	0.000	.005	1.000	0.00
76	77	.044	.148	0.000	.018	1.000	0.00
118	77	.031	.101	0.000	.052	1.000	0.00
75	77	.060	.200	0.000	.025	1.000	0.00
77	78	.024	.052	0.000	.006	1.000	0.00
78	79	.006	.024	0.000	.003	1.000	0.00
77	80	.011	.033	0.000	.035	1.000	0.00
114	115	.002	.104	0.000	.011	1.000	0.00
79	80	.016	.070	0.000	.009	1.000	0.00
68	81	.002	.202	0.000	.404	1.000	0.00
81	80	0.000	.037	0.000	0.000	.950	0.00
77	82	.030	.085	0.000	.049	1.000	0.00
82	83	.011	.037	0.000	.019	1.000	0.00
83	84	.063	.132	0.000	.013	1.000	0.00
83	85	.043	.148	0.000	.017	1.000	0.00
84	85	.030	.064	0.000	.006	1.000	0.00
85	86	.035	.123	0.000	.014	1.000	0.00
86	87	.028	.207	0.000	.022	1.000	0.00
85	88	.020	.102	0.000	.014	1.000	0.00
85	89	.024	.173	0.000	.024	1.000	0.00
88	89	.014	.071	0.000	.010	1.000	0.00
89	90	.016	.065	0.000	.079	1.000	0.00
27	115	.016	.074	0.000	.053	1.000	0.00
90	91	.025	.084	0.000	.011	1.000	0.00
89	92	.008	.038	0.000	.048	1.000	0.00
32	114	.014	.061	0.000	.021	1.000	0.00
91	92	.039	.127	0.000	.016	1.000	0.00
92	93	.026	.085	0.000	.011	1.000	0.00
92	94	.048	.158	0.000	.020	1.000	0.00
93	94	.022	.073	0.000	.009	1.000	0.00
94	95	.013	.043	0.000	.006	1.000	0.00

APPENDIX B.2 (continued)

THE IEEE 118-BUS SYSTEM - Transmission Network Data

Terminal Buses		Series Resistance	Series Reactance	Shunt Conductance	Shunt Susceptance	Turns Ratio Magnitude	Turns Ratio Angle
80	96	.036	.182	0.000	.025	1.000	0.00
82	96	.016	.053	0.000	.027	1.000	0.00
94	96	.027	.087	0.000	.012	1.000	0.00
80	97	.018	.093	0.000	.013	1.000	0.00
80	98	.024	.108	0.000	.014	1.000	0.00
80	99	.045	.206	0.000	.027	1.000	0.00
92	100	.065	.295	0.000	.039	1.000	0.00
94	100	.018	.058	0.000	.030	1.000	0.00
95	96	.017	.055	0.000	.007	1.000	0.00
96	97	.017	.089	0.000	.012	1.000	0.00
98	100	.040	.179	0.000	.024	1.000	0.00
99	100	.018	.058	0.000	.011	1.000	0.00
100	101	.028	.126	0.000	.016	1.000	0.00
92	102	.012	.056	0.000	.007	1.000	0.00
101	102	.025	.112	0.000	.015	1.000	0.00
100	103	.016	.053	0.000	.027	1.000	0.00
100	104	.042	.204	0.000	.027	1.000	0.00
103	104	.047	.158	0.000	.020	1.000	0.00
103	105	.054	.163	0.000	.020	1.000	0.00
100	106	.061	.229	0.000	.031	1.000	0.00
104	105	.010	.038	0.000	.005	1.000	0.00
105	106	.014	.055	0.000	.007	1.000	0.00
105	107	.053	.183	0.000	.024	1.000	0.00
105	108	.026	.070	0.000	.009	1.000	0.00
106	107	.053	.183	0.000	.024	1.000	0.00
108	109	.011	.029	0.000	.004	1.000	0.00
103	110	.039	.181	0.000	.023	1.000	0.00
109	110	.028	.076	0.000	.010	1.000	0.00
110	111	.022	.076	0.000	.010	1.000	0.00
110	112	.025	.064	0.000	.031	1.000	0.00
17	113	.009	.030	0.000	.004	1.000	0.00
32	113	.062	.203	0.000	.026	1.000	0.00
51	52	.020	.059	0.000	.007	1.000	0.00
52	53	.041	.164	0.000	.020	1.000	0.00
53	54	.026	.122	0.000	.016	1.000	0.00
49	54	.040	.145	0.000	.073	1.000	0.00

APPENDIX B.2 (continued)

THE IEEE 118-BUS SYSTEM - Bus Data at the Base-case Solution

Bus Index	Bus Type	Bus Voltage (Polar Coordinates)		Generated Real Power	Load Real Power	Load Reactive Power	Static Load
1	1	1.15000	-.18129	.100	.510	.270	0.00
2	0	1.08425	-.15983	0.000	.200	.090	0.00
3	0	1.11312	-.15747	0.000	.390	.100	0.00
4	1	1.10000	-.13616	.200	.900	.120	0.00
5	0	1.07605	-.07754	0.000	0.000	0.000	-.40
6	1	1.05200	-.11607	.150	.520	.220	0.00
7	0	1.05102	-.12563	0.000	.190	.020	0.00
8	1	1.09000	.00473	.100	.500	0.000	0.00
9	0	1.09539	.11854	0.000	0.000	0.000	0.00
10	1	1.07500	.24359	4.500	0.000	0.000	0.00
11	0	1.05394	-.13498	0.000	.700	.230	0.00
12	1	1.05100	-.13558	.850	.370	.100	0.00
13	0	1.02230	-.15260	0.000	.340	.160	0.00
14	0	1.02859	-.14437	0.000	.140	.010	0.00
15	1	.97000	-.14168	.120	.900	.300	0.00
16	0	1.03347	-.13326	0.000	.250	.100	0.00
17	0	.98166	-.10082	0.000	.110	.030	0.00
18	1	.97000	-.13613	.100	.600	.340	0.00
19	1	.96000	-.14353	.200	.450	.250	0.00
20	0	.93475	-.13601	0.000	.180	.030	0.00
21	0	.92091	-.11272	0.000	.140	.080	0.00
22	0	.91572	-.07095	0.000	.100	.050	0.00
23	0	.91964	.01566	0.000	.070	.030	0.00
24	1	.91000	-.00197	.150	.300	2.000	0.00
25	1	.97000	.15860	2.200	0.000	2.000	0.00
26	1	1.01000	.18792	3.140	0.000	0.000	0.00
27	1	.82300	-.06980	.120	.820	.130	0.00
28	0	.65525	-.05800	0.000	.170	1.660	0.00
29	0	.71328	-.08854	0.000	.240	.990	0.00
30	0	1.04858	-.01295	0.000	0.000	0.000	0.00
31	1	.78300	-.10325	.100	.430	.990	0.00
32	1	.87200	-.08799	.200	.590	.230	0.00
33	0	.96089	-.15044	0.000	.230	.090	0.00
34	1	.95900	-.15684	.150	.590	.260	.14
35	0	.96266	-.15617	0.000	.330	.090	0.00
36	1	.96300	-.15854	.100	.310	.170	0.00
37	0	.96949	-.12807	0.000	0.000	0.000	-.25
38	0	1.04102	-.04228	0.000	0.000	0.000	0.00
39	0	.96199	-.19528	0.000	.270	.110	0.00

APPENDIX B.2 (continued)

THE IEEE 118-BUS SYSTEM - Bus Data at the Base-case Solution

Bus Index	Bus Type	Bus Voltage (Polar Coordinates)		Generated Real Power	Load Real Power	Load Reactive Power	Static Load
40	1	.97000	-.21788	.100	.760	.230	0.00
41	0	.99719	-.23488	0.000	.370	.100	0.00
42	1	1.10000	-.23458	.120	1.100	.230	0.00
43	0	.95745	-.16478	0.000	.180	.070	0.00
44	0	.97307	-.13027	0.000	.160	.080	.10
45	0	.97810	-.10145	0.000	.530	.220	.10
46	1	1.00000	-.05945	.200	.280	.100	.10
47	0	1.01361	-.03335	0.000	.340	0.000	0.00
48	0	1.01543	-.02634	0.000	.200	.110	.15
49	1	1.02000	-.00666	2.040	.870	.300	0.00
50	0	.99707	-.03013	0.000	.170	.040	0.00
51	0	.96404	-.05688	0.000	.170	.080	0.00
52	0	.95421	-.06662	0.000	.180	.050	0.00
53	0	.94206	-.06442	0.000	.230	.110	0.00
54	1	.95000	-.03402	.480	.130	.320	0.00
55	1	.95000	-.05642	.100	.630	.220	0.00
56	1	.95000	-.05489	.120	.840	.180	0.00
57	0	.96698	-.05136	0.000	.120	.030	0.00
58	0	.95574	-.06127	0.000	.120	.030	0.00
59	1	.99000	-.00740	1.550	2.770	1.130	0.00
60	0	.99088	.03031	0.000	.780	.030	0.00
61	1	1.00000	.06872	1.600	0.000	0.000	0.00
62	1	1.00000	.05006	.150	.770	.140	0.00
63	0	1.02016	.04427	0.000	0.000	0.000	0.00
64	0	1.01658	.06983	0.000	0.000	0.000	0.00
65	1	1.00000	.11164	3.910	0.000	0.000	0.00
66	1	1.05100	.10979	3.920	.390	.180	0.00
67	0	1.02134	.06873	0.000	.280	.070	0.00
68	0	1.02050	.04650	0.000	0.000	0.000	0.00
69	0	.95077	-.05784	0.000	.330	.150	0.00
70	1	.98000	-.04447	.500	.660	.200	0.00
71	0	.98445	-.04816	0.000	0.000	0.000	0.00
72	1	.98000	-.04813	.200	.320	0.000	0.00
73	1	.99000	-.05212	.150	.210	0.000	0.00
74	1	.96000	-.06634	.100	.680	.270	.12
75	0	.96907	-.05019	0.000	.470	.110	0.00
76	1	.94500	-.03750	.100	.680	.360	0.00
77	1	1.01000	.05963	.120	.610	.280	0.00
78	0	.99981	.05189	0.000	.710	.260	0.00
79	0	1.00626	.06354	0.000	.390	.320	.20

APPENDIX B.2 (continued)

THE IEEE 118-BUS SYSTEM - Bus Data at the Base-case Solution

Bus Index	Bus Type	Bus Voltage (Polar Coordinates)		Generated Real Power	Load Real Power	Load Reactive Power	Static Load
80	1	1.04000	.12061	4.770	1.300	.260	0.00
81	0	1.00398	.10982	0.000	0.000	0.000	0.00
82	0	.98951	.11202	0.000	.540	.270	.20
83	0	.98493	.14691	0.000	.200	.100	.10
84	0	.98265	.21362	0.000	.110	.070	0.00
85	1	.99000	.25145	.200	.240	.150	0.00
86	0	.98928	.24339	0.000	.210	.100	0.00
87	1	1.01000	.27219	.150	0.000	0.000	0.00
88	0	.98634	.30990	0.000	.480	.100	0.00
89	1	1.00000	.38389	6.070	0.000	0.000	0.00
90	1	.99000	.26983	.100	1.730	.420	0.00
91	1	.98000	.27219	.120	.220	0.000	0.00
92	1	.99200	.28175	.500	.650	.100	0.00
93	0	.98593	.21480	0.000	.120	.070	0.00
94	0	.99027	.16477	0.000	.300	.160	0.00
95	0	.98030	.13835	0.000	.420	.310	0.00
96	0	.99192	.12353	0.000	.380	.150	0.00
97	0	1.01106	.11600	0.000	.150	.090	0.00
98	0	1.02447	.11456	0.000	.340	.080	0.00
99	1	1.01000	.13544	.200	.620	0.000	0.00
100	1	1.02000	.16111	2.520	.370	.180	0.00
101	0	.99351	.19689	0.000	.220	.150	0.00
102	0	.99097	.25165	0.000	.050	.030	0.00
103	1	1.01000	.11169	.500	.230	.160	0.00
104	1	.97000	.07326	.100	.380	.250	0.00
105	1	.96500	.05502	.100	.310	.260	.20
106	0	.96162	.04651	0.000	.430	.160	0.00
107	1	.95000	.00020	.120	.620	.120	.06
108	0	.96630	.03745	0.000	.020	.010	0.00
109	0	.96711	.03093	0.000	.080	.030	0.00
110	1	.97300	.01977	.120	.390	.300	.06
111	1	.98000	.04848	.360	0.000	0.000	0.00
112	1	.98000	-.03608	.120	.800	.130	0.00
113	1	.99000	-.10638	.120	.120	0.000	0.00
114	0	.85630	-.09270	0.000	.080	.030	0.00
115	0	.83307	-.09515	0.000	.220	.070	0.00
116	1	1.00000	.06125	.120	0.000	0.000	0.00
117	0	1.03745	-.15972	0.000	.200	.080	0.00
118	2	1.03000	0.00000	2.278	3.000	0.000	0.00

APPENDIX C.1

SENSITIVITY EVALUATION OF THE IEEE 30-BUS SYSTEM

```
      PROGRAM XLFSD2 (B30,OUTPUT,TAPE4=B30,TAPE6=OUTPUT)
*
*           THIS IS THE MAIN  PROGRAM  FOR LOAD FLOW AND
*           SENSITIVITY  EVALUATION  OF  DELTA 2  OF THE
*           IEEE 30-BUS POWER SYSTEM USING PACKAGE XLF3
*
      INTEGER BTYP(30),JRYT(31),ICYT(200),LBINP(41),LBOUT(41),BNR(30),   &
     +OTPT
      REAL BCV(60),LINPG(41),LINPB(41),LG(41),LB(41),LOUTG(41),LOUTB(41)&
     +,BVMOD(30),BVARG(30),BGP(30),BLP(30),WS(6000),BLQ(30),BSTL(30),DR1&
     +(29),DR2(29),DS1(29),DS2(29)
      COMPLEX YT(112),V(30),LTAP(41),DSX(60),DLX(29)
      COMMON /XLF3ID/ ITEL,TIMEL,VEPS,IDER,ILOAD,IADJ
      REWIND 4
      INPT=4
      OTPT=6
      LWS=6000
      NB=30
      NTL=41
      NYT=NB+NTL+NTL
      IFLAG=0
      IDER=1
      IP=0
      IWRITE=1
      ITEL=20
      TIMEL=5
*
*            SUBROUTINE RDATAX READS THE INPUT FILE AND
*            CONCURRENTLY PREPROCESSES IT
*
      CALL RDATAX(LBINP,LBOUT,LINPG,LINPB,LG,LB,LOUTG,LOUTB,LTAP,BNR,BTY&
     +P,BVMOD,BVARG,BGP,BLP,BLQ,BSTL,JRYT,NB,NTL,NLB,INPT,OTPT,IWRITE)
*
*            SUBROUTINE FORMYTX FORMULATES THE NODAL ADMITTANCE
*            MATRIX OF THE SYSTEM AND STORES IT IN A SPARSE FORM
*
      CALL FORMYTX(LBINP,LBOUT,LINPG,LINPB,LG,LB,LOUTG,LOUTB,LTAP,BSTL, &
     +JRYT,ICYT,YT,NB,NTL,NYT,OTPT,IWRITE)
*
*            SUBROUTINE FORMU CONSTRUCTS THE VECTOR OF
*            BUS CONTROL VARIABLES OF THE GIVEN SYSTEM
*
      CALL FORMU(BTYP,BVMOD,BVARG,BGP,BLP,BLQ,BCV,NB,OTPT,IWRITE)
*
```

APPENDIX C.1 (continued)

SENSITIVITY EVALUATION OF THE IEEE 30-BUS SYSTEM

```
      DO 10 I=1,NB
      R1=BVMOD(I)
      R2=BVARG(I)
      V(I)=CMPLX(R1*COS(R2),R1*SIN(R2))
   10 CONTINUE
      MODE=1
*
*             SUBROUTINE LFNCM SOLVES THE LOAD FLOW EQUATIONS
*             USING THE COMPLEX NEWTON METHOD
*
      CALL LFNCM (NB,NLB,NYT,JRYT,ICYT,BTYP,YT,V,BCV,WS,LWS,DSX,MODE,IFL&
     +AG,OTPT,IWRITE)
      WRITE(OTPT,130) IFLAG
      IF(IFLAG.LT.0) GO TO 120
      N=NB-1
      WRITE(OTPT,140) NB
      DO 20 I=1,N
      J=2*I-1
      DLX(I)=DSX(J)
   20 CONTINUE
      DO 30 I=1,N
      DR1(I)=0.
      DR2(I)=0.
      DS1(I)=0.
      DS2(I)=0.
   30 CONTINUE
*
*             SENSITIVITIES OF DELTA 2  WITH RESPECT TO
*             BUS-TYPE CONTROL VARIABLES
*
      ICODE=1
      DO 40 I=1,N
      CALL DERIVX(LBINP,LBOUT,LG,LB,LTAP,BTYP,V,NB,I,L2,DLX,NTL,ICODE    &
     +,DF1,DF2)
      DR1(I)=DF1
      DR2(I)=DF2
   40 CONTINUE
*
      ICODE=2
      DO 50 I=1,N
      CALL DERIVX (LBINP,LBOUT,LG,LB,LTAP,BTYP,V,NB,I,L2,DLX,NTL,ICODE,D
     +F1,DF2)
      DS1(I)=DF1
      DS2(I)=DF2
```

APPENDIX C.1 (continued)

SENSITIVITY EVALUATION OF THE IEEE 30-BUS SYSTEM

```
   50 CONTINUE
      WRITE(OTPT,150)
      WRITE(OTPT,160)
      DO 60 I=1,N
      IF(BTYP(I).NE.0) GO TO 60
      WRITE(OTPT,170) I,DR1(I),DR2(I),DS1(I),DS2(I)
   60 CONTINUE
      WRITE(OTPT,180)
      WRITE(OTPT,190)
      DO 70 I=1,N
      IF(BTYP(I).NE.1) GO TO 70
      WRITE(OTPT,170) I, DR1(I),DR2(I),DS1(I),DS2(I)
   70 CONTINUE
*
*             SENSITIVITIES OF DELTA 2   WITH RESPECT TO
*             LINE CONTROL VARIABLES
*
      WRITE(OTPT,180)
      WRITE(OTPT,200)
      ICODE=3
      DO 80 I=1,NTL
      TAP1=REAL(LTAP(I))
      IF(TAP1.NE.1) GO TO 80
      L1=LBINP(I)
      L2=LBOUT(I)
      CALL DERIVX(LBINP,LBOUT,LG,LB,LTAP,BTYP,V,NB,L1,L2,DLX,NTL,ICODE,
     +DF1,DF2)
      WRITE(OTPT,210) I,LBINP(I),LBOUT(I),DF1,DF2
   80 CONTINUE
*
*             SENSITIVITIES OF DELTA 2  WITH RESPECT TO
*             TRANSFORMER CONTROL VARIABLES
*
      WRITE(OTPT,180)
      WRITE(OTPT,220)
      DO 110 I=1,NTL
      TAP1=REAL(LTAP(I))
      IF(TAP1.EQ.1) GO TO 110
      ITN=0
      ICODE=6
      L1=LBINP(I)
      L2=LBOUT(I)
   90 CALL DERIVX(LBINP,LBOUT,LG,LB,LTAP,BTYP,V,NB,L1,L2,DLX,NTL,ICODE,
     +DF1,DF2)
```

APPENDIX C.1 (continued)

SENSITIVITY EVALUATION OF THE IEEE 30-BUS SYSTEM

```
      IF(ITN.EQ.1) GO TO 100
      DA=DF1
      ICODE=7
      ITN=ITN+1
      GO TO 90
  100 DR=DF1
      DX=DF2
      WRITE(OTPT,230)LBINP(I),LBOUT(I),DA,DR,DX
  110 CONTINUE
      WRITE(OTPT,150)
*
  120 STOP
  130 FORMAT(//,30X,"RETURN FLAG FROM LFNCM:",I3)
  140 FORMAT("1",16X,I3,"-BUS SYSTEM: SENSITIVITIES OF DELTA 2")
  150 FORMAT(/,1X,68("-"),/)
  160 FORMAT(1X,"LOAD BUS QUANTITIES - TOTAL DERIVATIVES",// 5X,64("-")
     +,//,5X,"BUS",7X,"REAL",9X,"REACTIVE",9X,"SHUNT",10X,"SHUNT",/,15X,
     +"POWER",9X,"POWER",8X,"CONDUCTANCE",4X,"SUSCEPTANCE",//,5X,64("-")
     +,/,1X)
  170 FORMAT(5X,I3,F13.6,3F15.6)
  180 FORMAT(/,5X,64("-"),/)
  190 FORMAT(1X,"GENERATOR BUS QUANTITIES - TOTAL DERIVATIVES",//5X,64(
     +"-"),//,5X,"BUS",7X,"REAL",10X,"VOLTAGE",9X,"SHUNT",10X,"SHUNT",/,
     +15X,"POWER",8X,"MAGNITUDE",5X,"CONDUCTANCE",4X,"SUSCEPTANCE",//,5X
     +,64("-"),/,1X)
  200 FORMAT(1X,"LINE QUANTITIES - TOTAL DERIVATIVES",//,5X,64("-"),//,
     +5X,"LINE",5X,"ELEMENT",8X,"LINE",9X,"LINE",/,5X,"INDEX",15X,
     +"CONDUCTANCE",3X,"SUSCEPTANCE",//,5X,64("-"),/,1X)
  210 FORMAT(5X,I3,6X,I3,",",I2,4X,F10.6,4X,F10.6)
  220 FORMAT(1X,"TRANSFORMER QUANTITIES - TOTAL DERIVATIVES",//,5X
     +,64("-"),//,5X,"ELEMENT",5X,"TURNS RATIO",9X,"INTERNAL",11X,
     +"INTERNAL",/,36X,"RESISTANCE",9X,"REACTANCE",//,5X,64("-"),/,1X)
  230 FORMAT(5X,I3,",",I2,3(F15.6,3X))
      END
*
```

APPENDIX C.1 (continued)

SENSITIVITY EVALUATION OF THE IEEE 30-BUS SYSTEM

```
*
      SUBROUTINE FORMMU(V,AI,NB,DS,DSL,IDER,YT,JRYT,ICYT,BTYP,NYT,OTPT)
      COMPLEX V(1),AI(1),DS(1),YT(1),DSL,AV1
      INTEGER JRYT(1),ICYT(1),BTYP(1),IDER,OTPT
      N=NB-1
      DO 10 I=1,N
      DS(I)=(0.,0.)
      DS(N+I)=(0.,0.)
   10 CONTINUE
      AV1=-.5/V(2)
      A1=REAL(AV1)
      A2=AIMAG(AV1)
      DS(3)=CMPLX(-A2,A1)
      DS(4)=CONJG(DS(3))
      DSL=(0.,0.)
      RETURN
      END
```

APPENDIX C.2

SENSITIVITY EVALUATION OF THE IEEE 118-BUS SYSTEM

```
      PROGRAM XLFSPN (B118,OUTPUT,TAPE4=B118,TAPE6=OUTPUT)
*
*           THIS IS THE MAIN  PROGRAM  FOR LOAD FLOW AND
*          SENSITIVITY EVALUATION OF SLACK BUS REAL POWER
*        OF THE IEEE 118-BUS POWER SYSTEM USING PACKAGE XLF3
*
      INTEGER BTYP(118),JRYT(120),ICYT(1200),LBINP(179),LBOUT(179),BNR(1&
     +18),OTPT
      REAL BCV(236),LINPG(179),LINPB(179),LG(179),LB(179),LOUTG(179),LOU&
     +TB(179),BVMOD(118),BVARG(118),BGP(118),BLP(118),WS(30000),BLQ(118)&
     +,BSTL(118),DR1(117),DR2(117),DS1(117),DS2(117)
      COMPLEX YT(1200),V(118),LTAP(179),DSX(236),DLX(117)
      COMMON /XLF3ID/ ITEL,TIMEL,VEPS,IDER,ILOAD,IADJ
      REWIND 4
      INPT=4
      OTPT=6
      LWS=30000
      NB=118
      NTL=179
      NYT=NB+NTL+NTL
      IFLAG=0
      IDER=1
      IP=0
      IWRITE=0
*
*            SUBROUTINE RDATAX READS THE INPUT FILE AND
*            CONCURRENTLY PREPROCESSES IT
*
      CALL RDATAX(LBINP,LBOUT,LINPG,LINPB,LG,LB,LOUTG,LOUTB,LTAP,BNR,BTY&
     +P,BVMOD,BVARG,BGP,BLP,BLQ,BSTL,JRYT,NB,NTL,NLB,INPT,OTPT,IWRITE)
*
*            SUBROUTINE FORMYTX FORMULATES THE NODAL ADMITTANCE
*            MATRIX OF THE SYSTEM AND STORES IT IN A SPARSE FORM
*
      CALL FORMYTX(LBINP,LBOUT,LINPG,LINPB,LG,LB,LOUTG,LOUTB,LTAP,BSTL, &
     +JRYT,ICYT,YT,NB,NTL,NYT,OTPT,IWRITE)
*
*            SUBROUTINE FORMU CONSTRUCTS THE VECTOR OF
*            BUS CONTROL VARIABLES OF THE GIVEN SYSTEM
*
      CALL FORMU(BTYP,BVMOD,BVARG,BGP,BLP,BLQ,BCV,NB,OTPT,IWRITE)
*
```

APPENDIX C.2 (continued)

SENSITIVITY EVALUATION OF THE IEEE 118-BUS SYSTEM

```
      DO 10 I=1,NB
      R1=BVMOD(I)
      R2=BVARG(I)
      V(I)=CMPLX(R1*COS(R2),R1*SIN(R2))
   10 CONTINUE
      MODE=1
*
*            SUBROUTINE LFNCM SOLVES THE LOAD FLOW EQUATIONS
*            USING THE COMPLEX NEWTON METHOD
*
      CALL LFNCM (NB,NLB,NYT,JRYT,ICYT,BTYP,YT,V,BCV,WS,LWS,DSX,MODE,IFL&
     +AG,OTPT,IWRITE)
      WRITE(OTPT,130) IFLAG
      IF(IFLAG.LT.0) GO TO 120
      N=NB-1
      WRITE(OTPT,140) NB
      DO 20 I=1,N
      J=2*I-1
      DLX(I)=DSX(J)
   20 CONTINUE
      DO 30 I=1,N
      DR1(I)=0.
      DR2(I)=0.
      DS1(I)=0.
      DS2(I)=0.
   30 CONTINUE
*
*            SENSITIVITIES OF P(SLACK)  WITH RESPECT TO
*            BUS-TYPE CONTROL VARIABLES
*
      ICODE=1
      DO 40 I=1,N
      CALL DERIVX(LBINP,LBOUT,LG,LB,LTAP,BTYP,V,NB,I,L2,DLX,NTL,ICODE    &
     +,DF1,DF2)
      DR1(I)=DF1
      DR2(I)=DF2
   40 CONTINUE
*
      ICODE=2
      DO 50 I=1,N
      CALL DERIVX (LBINP,LBOUT,LG,LB,LTAP,BTYP,V,NB,I,L2,DLX,NTL,ICODE,D
     +F1,DF2)
```

APPENDIX C.2 (continued)

SENSITIVITY EVALUATION OF THE IEEE 118-BUS SYSTEM

```
      DS1(I)=DF1
      DS2(I)=DF2
   50 CONTINUE
      WRITE(OTPT,150)
      WRITE(OTPT,160)
      DO 60 I=1,N
      IF(BTYP(I).NE.0) GO TO 60
      WRITE(OTPT,170) I,DR1(I),DR2(I),DS1(I),DS2(I)
   60 CONTINUE
      WRITE(OTPT,180)
      WRITE(OTPT,190)
      DO 70 I=1,N
      IF(BTYP(I).NE.1) GO TO 70
      WRITE(OTPT,170) I, DR1(I),DR2(I),DS1(I),DS2(I)
   70 CONTINUE
*
*             SENSITIVITIES OF P(SLACK)   WITH RESPECT TO
*             LINE CONTROL VARIABLES
*
      WRITE(OTPT,180)
      WRITE(OTPT,200)
      ICODE=3
      DO 80 I=1,NTL
      TAP1=REAL(LTAP(I))
      IF(TAP1.NE.1) GO TO 80
      L1=LBINP(I)
      L2=LBOUT(I)
      CALL DERIVX(LBINP,LBOUT,LG,LB,LTAP,BTYP,V,NB,L1,L2,DLX,NTL,ICODE,
     +DF1,DF2)
      WRITE(OTPT,210) I,LBINP(I),LBOUT(I),DF1,DF2
   80 CONTINUE
*
*             SENSITIVITIES OF P(SLACK)  WITH RESPECT TO
*             TRANSFORMER CONTROL VARIABLES
*
      WRITE(OTPT,180)
      WRITE(OTPT,220)
      DO 110 I=1,NTL
      TAP1=REAL(LTAP(I))
      IF(TAP1.EQ.1) GO TO 110
      ITN=0
      ICODE=6
      L1=LBINP(I)
      L2=LBOUT(I)
```

APPENDIX C.2 (continued)

SENSITIVITY EVALUATION OF THE IEEE 118-BUS SYSTEM

```
 90 CALL DERIVX(LBINP,LBOUT,LG,LB,LTAP,BTYP,V,NB,L1,L2,DLX,NTL,ICODE,
   +DF1,DF2)
    IF(ITN.EQ.1) GO TO 100
    DA=DF1
    ICODE=7
    ITN=ITN+1
    GO TO 90
100 DR=DF1
    DX=DF2
    WRITE(OTPT,230)LBINP(I),LBOUT(I),DA,DR,DX
110 CONTINUE
    WRITE(OTPT,150)
*
120 STOP
130 FORMAT(//,30X,"RETURN FLAG FROM LFNCM:",I3)
140 FORMAT("1",16X,I3,"-BUS SYSTEM: SENSITIVITIES OF P(SLACK)")
150 FORMAT(/,1X,68("-"),/)
160 FORMAT(1X,"LOAD BUS QUANTITIES - TOTAL DERIVATIVES",// 5X,64("-")
   +,//,5X,"BUS",7X,"REAL",9X,"REACTIVE",9X,"SHUNT",10X,"SHUNT",/,15X,
   +"POWER",9X,"POWER",8X,"CONDUCTANCE",4X,"SUSCEPTANCE",//,5X,64("-")
   +,/,1X)
170 FORMAT(5X,I3,F13.6,3F15.6)
180 FORMAT(/,5X,64("-"),/)
190 FORMAT(1X,"GENERATOR BUS QUANTITIES - TOTAL DERIVATIVES",//5X,64(
   +"-"),//,5X,"BUS",7X,"REAL",10X,"VOLTAGE",9X,"SHUNT",10X,"SHUNT",/,
   +15X,"POWER",8X,"MAGNITUDE",5X,"CONDUCTANCE",4X,"SUSCEPTANCE",//,5X
   +,64("-"),/,1X)
200 FORMAT(1X,"LINE QUANTITIES - TOTAL DERIVATIVES",//,5X,64("-"),//,
   +5X,"LINE",5X,"ELEMENT",8X,"LINE",9X,"LINE",/,5X,"INDEX",15X,
   +"CONDUCTANCE",3X,"SUSCEPTANCE",//,5X,64("-"),/,1X)
210 FORMAT(5X,I3,6X,I3,",",I2,4X,F10.6,4X,F10.6)
220 FORMAT(1X,"TRANSFORMER QUANTITIES - TOTAL DERIVATIVES",//,5X
   +,64("-"),//,5X,"ELEMENT",5X,"TURNS RATIO",9X,"INTERNAL",11X,
   +"INTERNAL",/,36X,"RESISTANCE",9X,"REACTANCE",//,5X,64("-"),/,1X)
230 FORMAT(5X,I3,",",I2,3(F15.6,3X))
    END
*
*
```

APPENDIX C.2 (continued)

SENSITIVITY EVALUATION OF THE IEEE 118-BUS SYSTEM

```
      SUBROUTINE FORMMU(V,AI,NB,DS,DSL,IDER,YT,JRYT,ICYT,BTYP,NYT,OTPT)
*
*             SUBROUTIONE FORMMU EVALUATES THE PARTIAL DERIVATIVES
*             OF REAL SLACK BUS POWER W.R.T. COMPLEX BUS VOLTAGES
*             AS WELL AS THEIR COMPLEX CONJUGATES
*
      COMPLEX V(1),AI(1),DF(118),DS(1),YT(1),DSL,AV1,AV2
      INTEGER JRYT(1),ICYT(1),BTYP(1),IDER,OTPT
      N=NB-1
      DO 10 I=1,N
      DS(I)=(0.,0.)
      DF(I)=(0.,0.)
      DS(N+I)=(0.,0.)
   10 CONTINUE
      DF(NB)=(0.,0.)
*
      DO 30 I=1,NB
      IF(I.NE.NB) GO TO 30
      KK=JRYT(I+1)-JRYT(I)
      DO 20 J=1,KK
      KJ=JRYT(I)+J-1
      KA=ICYT(KJ)
      AV1=YT(KJ)*CONJG(V(I))
      DF(KA)=DF(KA)+0.5*AV1
      AV2=CONJG(YT(KJ)*V(ICYT(KJ)))
      DF(I)=DF(I)+0.5*AV2
   20 CONTINUE
   30 CONTINUE
      DSL=(0.,0.)
      DO 40 I=1,N
      J=2*I-1
      K=J+1
      DS(J)=DF(I)
      DS(K)=CONJG(DF(I))
   40 CONTINUE
      RETURN
      END
```

REFERENCES

C. Adamson and N.G. Hingorani (1960), High Voltage Direct Current Power Transmission. London: Garraway Ltd.

L.V. Ahlfors (1966), Complex Analysis. New York: McGraw-Hill.

O. Alsac and B. Stott (1974), "Optimal load flow with steady-state security", IEEE Trans. Power Apparatus and Systems, vol. PAS-93, pp. 745-751.

F.L. Alvarado (1978), "Penalty factors from Newton's method", ibid., vol. PAS-97, pp. 2031-2040.

J. Arrillaga, C.P. Arnold and B.J. Harker (1983), Computer Modelling of Electrical Power Systems. New York: Wiley.

J.W. Bandler (1973), "Computer-aided circuit optimization", G.C. Temes and S.K. Mitra (Ed.), Modern Filter Theory and Design. New York: Wiley-Interscience.

J.W. Bandler and M.A. El-Kady (1981), "Power network sensitivity analysis and formulation simplified", IEEE Trans. Automatic Control, vol. AC-26, pp. 773-775.

J.W. Bandler and M.A. El-Kady (1982a), "Exact power network sensitivities via generalized complex branch modelling", Proc. IEEE ISCAS (Rome, Italy), pp. 313-316.

J.W. Bandler and M.A. El-Kady (1982b), "A new method for computerized solution of power flow equations", IEEE Trans. Power Apparatus and Systems, vol. PAS-101, pp. 1-9.

J.W. Bandler and M.A. El-Kady (1982c), "A complex Lagrangian approach with applications to power network sensitivity analysis", IEEE Trans. Circuits and Systems, vol. CAS-29, pp. 1-6.

J.W. Bandler and M.A. El-Kady (1984), "A generalized complex adjoint approach to power network sensitivities", Int. J. Circuit Theory and Applications, vol. 12, pp. 194-222.

J.W. Bandler, M.A. El-Kady, H.K. Grewal and J. Wojciechowski (1983), "XLF3 - A Fortran implementation of the complex Lagrangian method to power system analysis and design", Department of Electrical and Computer Engineering, McMaster University, Hamilton, Canada, Report SOS-83-18-U.

J.W. Bandler, M.A. El-Kady and H.K. Grewal (1983), "Sensitivity evaluation and optimization of the IEEE 118-bus power system", Department of Electrical and Computer Engineering, McMaster University, Hamilton, Canada, Report SOS-83-19-R.

J.W. Bandler, M.A. El-Kady and H.K. Grewal (1985a), "Exact sensitivities for nonreciprocal two-port power elements", Proc. IEEE, vol. 73, pp. 1858-1859.

J.W. Bandler, M.A. El-Kady and H.K. Grewal (1985b), "An application of complex branch modeling to nonreciprocal power transmission elements", IEEE Trans. Circuits and Systems, vol. CAS-32, pp. 1292-1295.

J.W. Bandler, M.A. El-Kady and H.K. Grewal (1986), "Sensitivity evaluation of phase-shifting transformers using the complex Lagrangian method", Int. J. Circuit Theory and Applications, vol. 14, pp.83-87.

J.W. Bandler, M.A. El-Kady and J. Wojciechowski (1983), "TTM1 - a Fortran implementation of the Tellegen theorem method to power system simulation and design", Department of Electrical and Computer Engineering, McMaster University, Hamilton, Canada, Report SOS-83-7 U.

N.N. Bengiamin (1985), "Regulating transformer model for use in load flow analysis", IEEE Trans. Power Apparatus and Systems, vol. PAS-104, pp. 1102-1108.

F.H. Branin, Jr. (1973), "Network sensitivity and noise analysis simplified", IEEE Trans. Circuit Theory, vol. CT-20, pp. 285-288.

R.C. Burchett, H.H. Happ and K.A. Wirgau (1982), "Large scale optimal power flow", IEEE Trans. Power Apparatus and Systems, vol. PAS-101, pp. 3722-3732.

J. Carpentier (1979), "Optimal power flows", Int. J. Electrical Power and Energy Systems, vol. 1, pp. 3-15.

J. Carpentier and A. Merlin (1982), "Optimization methods in planning and operation", ibid., vol. 4, pp.11-18.

M.S. Chen and W.E. Dillon (1974), "Power system modeling", Proc. IEEE, vol. 62, pp. 901-915.

J. Choma, Jr. (1985), Electrical Networks. New York: Wiley.

L.O. Chua and P. Lin (1975), Computer-Aided Analysis of Electronic Circuits: Algorithms and Computational Techniques. Englewood Cliffs, NJ: Prentice-Hall.

P.L. Dandeno (1982), "General overview of steady-state (small signal) stability in bulk electricity systems - A North American perspective", Int. J. Electrical Power and Energy Systems, vol. 4, pp. 253-264.

C.A. Desoer and E.S. Kuh (1969), Basic Circuit Theory. New York: McGraw-Hill.

R.N. Dhar (1982), Computer Aided Power System Operation and Analysis. New York: McGraw-Hill.

S.W. Director (1975), Circuit Theory -- A Computational Approach. New York: Wiley.

S.W. Director and R.A. Rohrer (1969), "Generalized adjoint network and network sensitivities", IEEE Trans. Circuit Theory, vol. CT-16, pp. 318-323.

H.W. Dommel and W.F. Tinney (1968), "Optimal power flow solutions", IEEE Trans. Power Apparatus and Systems, vol. PAS-87, pp. 1866-1876

I.S. Duff (1977), "A survey of sparse matrix research", Proc. IEEE, vol. 65, pp. 530-535.

I.S. Duff (1981), Sparse Matrices and Their Uses. New York: Academic Press.

T.E. DyLiacco (1978), "System security: the computer's role", IEEE Spectrum (June), pp. 43-50.

O.I. Elgerd (1982), Electric Energy Systems Theory. New York: McGraw- Hill.

M.A. El-Kady (1980), "A unified approach to generalized network sensitivities with applications to power system analysis and planning", Ph.D. Thesis, Department of Electrical and Computer Engineering, McMaster University, Hamilton, Canada.

M.E. El-Hawary and G.S. Christensen (1979), Optimal Economic Operation of Electric Power Systems. New York: Academic Press.

F.J. Ellert and N.G. Hingorani (1976), "HVDC for the long run", IEEE Spectrum (August), pp. 37-42.

V.V. Ershovich, A.G. Kreis and L.F. Krivoshkin (1982), "Some results of development and introduction of quadrature voltage regulation in 750-330 kV networks", Electric Technology USSR, no. 1, pp. 76-83.

R. Fischl and W.R. Puntel (1972), "Computer aided design of electric power transmission networks", IEEE Winter Power Meeting, Paper No. C72-168-8.

R. Fischl and R.G. Wasley (1978), "Efficient computation of optimal load flow sensitivities", IEE Canadian Communications and Power Conference, Cat. No. 78 CH1373-0 REG7, pp. 401-404.

N. Flatabo, J.A. Foosnaes and T.O. Berntsen (1985), "Transformer tap setting in optimal load flow", IEEE Trans. Power Apparatus and Systems, vol. PAS-104, pp. 1356-1362.

D.L. Fletcher and W.O. Stadlin (1983), "Transformer tap position estimation", IEEE Trans. Power Apparatus and Systems, vol. PAS-102, pp. 3680-3686.

P.M. Frank (1978), Introduction to System Sensitivity Theory. New York: Academic Press.

H.K. Grewal (1983), "Sensitivity evaluation and optimization of electrical power systems with emphasis on nonreciprocal elements", M.Eng. Thesis, Department of Electrical and Computer Engineering, McMaster University, Hamilton, Canada.

C.A. Gross (1979), Power System Analysis. New York: Wiley.

Z.X. Han (1982), "Phase shifter and power flow control", IEEE Trans. Power Apparatus and Systems, vol. PAS-101, pp. 3790-3795.

H.H. Happ (1973), "Power pools and superpools", IEEE Spectrum (March), pp. 54-61.

H.H. Happ and N.E. Nour (1975), "Interconnection modelling of power systems", IEEE Trans. Power Apparatus and Systems, vol. PAS-94, pp. 884-893.

H.H. Happ (1976), "An overview of short and long range operation planning functions in power systems", S.C. Savulescu (Ed.), Computerized Operation of Power Systems, New York: Elsevier.

H.H. Happ (1977), "Optimal power dispatch -- A comprehensive survey", IEEE Trans. Power Apparatus and Systems, vol. PAS-96, pp. 841-854.

C.S. Indulkar, P. Kumar and D.P. Kothari (1982), "Sensitivity study of an untransposed overhead transmission line", Int. J. Electrical Power and Energy Systems, vol. 4, pp. 265-269.

G. Irisarri, A.M. Sasson and S.F. Hodges (1978), "An optimal ordering algorithm for sparse matrix applications", IEEE Trans. Power Apparatus and Systems, vol. PAS-97, pp. 2253-2261.

R. Kilmer, D. Karloski, F.J. Arriola and V. Echave (1983), "Variable impedance transformer models for use in real-time security analysis functions", ibid., vol. PAS-102, pp. 3558-3563.

E.W. Kimbark (1971), Direct Current Transmission Vol.I. New York: Wiley.

W.J. Lyman (1930), "Controlling power flow with phase-shifting equipment", AIEE Trans. Power Apparatus and Systems, vol. 49, pp. 825-831.

W.J. Lyman and J.R. North (1938), "Application of large phase-shifting transformer on an interconnected system loop", ibid., vol. 57, pp. 3733-3741.

A.P. Meliopoulos, R.P. Webb, R.J. Bennon and J.A. Juves (1982), "Optimal long range transmission planning with ac load flow", IEEE Trans. Power Apparatus and Systems, vol. PAS-101, pp. 4156-4163.

B.K. Mukherjee and G.R. Fuerst (1984), "Transformer tap position estimation -- field experience", ibid., vol. PAS-103, pp. 1454-1458.

B.A. Murtagh and M.A. Saunders (1980), "MINOS/AUGNMENTED user's manual", Department of Operations Research, Stanford, California, Technical Report SOL 80-14.

K. Najaf-Zadeh and S.W. Anderson (1978), "Sensitivity analysis in optimal simultaneous power interchange", IEEE Trans. Power Apparatus and Systems, vol. PAS-97, pp. 2405- 2415.

P. Penfield, Jr., R. Spence and S. Duinker (1970), "A generalized form of Tellegen's theorem", IEEE Trans. Circuit Theory, vol. CT-17, pp. 302-305.

J. Peschon, D.W. Bree and L.P. Hajdu (1972), "Optimal power flow solutions for power system planning", Proc. IEEE, vol. 60, pp. 64-70.

J. Peschon, D.S. Piercy, W.F. Tinney and O.J. Tveit (1968), "Sensitivity in power systems", IEEE Trans. Power Apparatus and Systems, vol. PAS-87, pp. 1687-1696.

C.A. Powel (1955), Principles of Electric Utility Engineering. New York: Wiley.

H.B. Puttgen and R.L. Sullivan (1978), "A novel comprehensive approach to power systems sensitivity analysis", IEEE Summer Power Meeting, Paper No. A78-525-8.

A.M.H. Rashed and D.H. Kelly (1974), "Optimal load flow solution using Lagrangian multipliers and the Hessian matrix", IEEE Trans. Power Apparatus and Systems, vol. PAS-93, pp. 1292-1297.

M.S. Sachdev and S.A. Ibrahim (1974), "A fast approximate technique for outage studies in power system planning and operation", ibid., vol. PAS-93, pp. 1133-1142.

M.S. Sachdev and S.A. Ibrahim,(1975), "A simulation technique for studying real and reactive power flow patterns", ibid., vol. PAS-94, pp.2092-2100.

A.M. Sasson (1969), "Nonlinear programming solutions for load-flow, minimum-loss, and economic dispatching problems", ibid., vol. PAS-88, pp. 399-409.

A.M. Sasson and H.M. Merrill (1974), "Some applications of optimization techniques to power systems problems", Proc. IEEE, vol. 62, pp. 959-972.

L.P. Singh (1983), Advanced Power System Analysis and Dynamics. New York: Wiley.

N. Srinivasan, K.S.P. Rao, C.S. Indulkar and S.S. Venkata (1985), "On-line computation of phase shifter distribution factors and lineload alleviation", IEEE Trans. Power Apparatus and Systems, vol. PAS-104, pp. 1656-1662.

G.W. Stagg and A.H. El-Abiad (1968), Computer Methods in Power System Analysis. New York: McGraw-Hill.

B. Stott (1972), "Decoupled Newton load flow", IEEE Trans. Power Apparatus and Systems, vol. PAS-91, pp. 1955-1959.

B. Stott (1974), "Review of load-flow calculation methods", Proc. IEEE, vol.62, pp. 916-929.

B. Stott and O. Alsac (1974), "Fast decoupled load flow", IEEE Trans. Power Apparatus and Systems, vol. PAS-93, pp. 859-869.

B. Stott and E. Hobson (1978), "Power system security control calculations using linear programming, part I and part II", ibid., vol. PAS-97, pp. 1713-1720 and 1721-1731.

S.N. Talukdar and F.F. Wu (1981), "Computer-aided dispatch of electric power", Proc. IEEE, vol. 69, pp. 1212-1231.

W.F. Tinney and C.E. Hart (1967), "Power flow solution by Newton's method", IEEE Trans. Power Apparatus and Systems, vol. PAS-86, pp. 1449-1460.

W.F. Tinney and J.W. Walker (1967), "Direct solutions of sparse network equations by optimally ordered triangular factorization", Proc. IEEE, vol. 55, pp. 1801-1809.

R. Tomovic and M. Vukobratovic (1972), General Sensitivity Theory. New York: Elsevier.

D.J. Tylavsky (1984), "A simple approach to the solution of the ac-dc power flow problems", IEEE Trans. Education, vol. E-27, pp. 31-40.

E. Uhlmann (1975), Power Transmission by Direct Current. Berlin: Springer-Verlag.

J.E. Van Ness and J.H. Griffin (1961), "Elimination methods for load flow studies", AIEE Trans. Power Apparatus and Systems, vol. 80, pp. 299-302.

B.M. Weedy (1979), Electric Power Systems (Third edition). New York: Wiley.

T. Wildi (1981), Electrical Power Technology. New York: Wiley.

B.F. Wollenberg (1976), "Power system simulation in an operating environment", S.C. Savulescu (Ed.), Computerized Operation of Power Systems. New York: Elsevier.

F.F. Wu and R.L. Sullivan (1976), "Nonlinear resistive circuit models for power system steady-state analysis", Proc. 14th Allerton Conf. Circuit and System Theory (Urbana, IL), pp. 261-268.

G. Zorpette (1985), "HVDC: wheeling lots of power", IEEE Spectrum (June), pp. 30-36.

AUTHOR INDEX